BIOOXIDATION OF A GOLD BEARING ARSENOPYRITE/PYRITE CONCENTRATE

by

D.M. MILLER
B. Sc. Eng (UNIVERSITY OF THE WITWATERSRAND) 1984

Submitted to the University of Cape Town in fulfilment of the requirements for the degree of Masters of Science in Engineering

February 1990

ABSTRACT

Biooxidation of gold bearing refractory sulphide concentrates is emerging as a viable alternative to roasting and pressure oxidation as the procedure where by gold liberation is achieved. Agitated, aerated bioreactors are required for rapid oxidation; hence the need for the development of a kinetic model where by results obtained by batch and small scale testwork are interpreted and the performance of biooxidation reactors can be predicted and which facilitates reactor design and scale-up

Many models have been proposed to describe biooxidation, predicting either bacterial growth in the system, or the rate of sulphide mineral oxidation. Of these, only one, incorporating the empirical logistic equation to describe the rate of sulphide oxidation, (Pinches *et al.*, 1987), was found to include rate parameters useful for design and scale-up purposes.

The literature survey also indicated that interpretation of rate data, with respect to total solid surface area, varied either by fineness of the concentrate or by solid concentration, was useful (Pinches, 1972; Drossou, 1986; Drossou and Hansford, 1987; Chapman, Hansford and Pinches, 1989).

The objectives of this project have been to characterise the biooxidation of an auriferous pyrite/arsenopyrite flotation concentrate, and to interpret laboratory batch and continuous pilot plant data in the light of the logistic model. Furthermore, the possibility of predicting continuous biooxidation plant performance from batch data was considered.

The batch testing was carried out on five narrowly sized fractions of Fairview concentrate, as well as on the bulk concentrate. Extents of removal of iron, arsenic and sulphide-sulphur were described by the logistic equation and values of the kinetic parameters obtained. Maximum rates of removal of these components, predicted by the logistic parameters, correlated well with experimentally determined rates of removal obtained from the linear portions of the fractional removal versus time curves. Values obtained for the bulk concentrate are shown in the following table.

COMPONENT	RATE OF OXIDATION			
	Predicted		Experimental	
	kg m^{-3} d^{-1}	mol m^{-3} d^{-1}	kg m^{-3} d^{-1}	mol m^{-3} d^{-1}
Sulphide-sulphur	4,66	145,3	3,89	121,5
Iron	4,00	71,7	3,98	71,2
Arsenic	0,99	13,2	0,95	12,7

The rates obtained directly from these curves were termed specific rates of removal (d^{-1}), and their dependance on total surface area tended to be linear. Absolute rates of removal (mol m^{-3} d^{-1}), were found to increase linearly with initial increase in total surface area, (for low surface areas), and then to remain constant despite further increases in surface area.

As the five size fractions were produced by screening of a single sample, separation of the sulphide minerals was not even, these tended to report preferentially to the intermediate fractions, rather than to the finest and coarsest fractions. In order to compensate for this difference in composition, the dependance of the rate of arsenic removal on arsenopyrite surface area and of pyrite removal on pyrite surface area were investigated. Again, absolute rates of removal increased linearly with initial increase in mineral surface area and then levelled off to a constant value in spite of further increases in the mineral surface areas. This was in agreement with literature findings for arsenic removal, but not for pyrite removal, which was found to have a linear dependance on pyrite surface area (Pinches, 1972). During the linear phase of rate dependance on mineral surface area, surface area rates were found for arsenic based on arsenopyrite surface area (0,83 g m^{-2} d^{-1}), and for sulphide-sulphur (1,31 g m^{-2} d^{-1}), and iron (1,18 m^{-2} d^{-1}) based on pyrite surface area.

The removal of pyrite and arsenopyrite with time indicated preferential biooxidation of the arsenopyrite prior to pyrite oxidation, and not more rapid oxidation of the arsenopyrite. Gold dissolution was linearly dependant on arsenopyrite removal, and showed a rapid increase with initial sulphide-sulphur removal. Further improvement in gold dissolution required much greater sulphide-

sulphur removal. This dependance of gold liberation on removal of the different sulphide minerals confirms the findings of Swash (1988), that the gold in this concentrate is associated with the arsenopyrite.

Continuous pilot plant data from the GENMIN Process Research report by Ming and Olën (1986), was analysed for periods of stable operation. Sulphide-sulphur removal during these periods was fitted by the logistic equation, and the value of k, the logistic rate constant, for the primary tanks was 1,35 d^{-1}. This is significantly higher than the value of 0,68 d^{-1} obtained for batch biooxidation of the bulk concentrate. A similar discrepancy between continuous and batch logistic rate constants was found for the biooxidation of an arsenopyrite/pyrite concentrate (Pinches *et al.*, 1987).

The performance of various configurations of a five reactor continuous biooxidation cascade were investigated using values obtained for the logistic rate constant from the pilot plant data. Total sulphide-sulphur oxidation through the entire cascade for each configuration was compared, and it was in fact confirmed that a multiple primary stage, followed by a number of stages in series, was the optimum configuration

ACKNOWLEDGEMENTS

I would like to express my grateful thanks to GENMIN Process Research for providing the opportunity to carry out this research project, for the laboratory and analytical facilities, and for the financial support.

Special thanks to my supervisor Professor G.S. Hansford of the Department of Chemical Engineering, University of Cape Town, for his supervision and advice.

I also gratefully acknowledge the interest and assistance received from the following people:

Mr Reckson Ngobeni for his invaluable assistance with the experimental work, Mrs Gerty Moolman for her help with the typing, Ms Dot Poss for the hours spent proof reading, and all at GENMIN Process Research for their assistance.

Special thanks to my family and friends, especially Eike, for their moral support, encouragement and assistance.

Thank All Mighty God.

TABLE OF CONTENTS

LIST OF TABLES

LIST OF FIGURES

NOMENCLATURE

C_i	concentration of mineral or element in slurry	[kg m^{-3}]
d	diameter of particles	[micron]
d_c	characteristic diameter of solid particles in a particular size interval	[micron]
f	mass fraction of solids in a particular size interval	
d_s	specific gravity of solids	
k	logistic rate constant	[d^{-1}]
M	Concentration of solids in the slurry	[kg m^{-3}]
N	bacterial cell numbers	[bacterial cells ml^{-1}]
N_m	maximum population size	[bacterial cells ml^{-1}]
N_0	initial population size	[bacterial cells ml^{-1}]
t	time	[d]
T_i	retention time in the *i*th tank in a cascade of reactors	[d]
r_i	rate of removal of component of slurry in reactor *i*	[kg m^{-3} d^{-1}]
Q	volumetric flowrate of slurry	[m^3 d^{-1}]
V	volume of reactor	[m^3]
X	fractional removal of constituent (pyrite, arsenopyrite, S^{2-}, Fe)	
Y	constant of proportionality in relationship between fractional removal of sulphide-sulphur and bacterial cell numbers	
Z	fraction of component present in solid	

CHAPTER 1

INTRODUCTION

In recent years biooxidation has emerged as an alternative process for the treatment of refractory gold bearing sulphide ores and concentrates. These sulphides, while containing high gold values, are not amenable to direct cyanidation, and, with the depletion of deposits of free milling gold, economically viable processes for the recovery of these alternative refractory sources are being sought. While roasting and pressure oxidation have become the more accepted methods of liberating the finely disseminated gold particles from within the sulphide crystal lattice, it has been shown that biooxidation has the potential to be economically competitive (Haines, 1986; Bruynesteyn *et al.*, 1986; Livesey-Goldblatt *et al.*, 1983).

Treatment of large quantities of high value gold-bearing sulphides requires a more sophisticated, highly efficient, low retention time process in contrast to the heap and *in situ* bacterial oxidation systems which have been utilised for copper extraction. These processes have become widely used, 10 - 20% of copper being produced in the USA by means of bacterially aided oxidation of low grade ores (Olson and Kelly, 1986) and use of *in situ* leaching for uranium recovery (Lakshmanan, 1986). Agitated, aerated bioreactors are required for rapid biooxidation.

The effect of factors influencing biooxidation have been studied to a large extent (Hutchins *et al.*, 1986; Karavaiko, 1985; Kelly *et al.*, 1979; Lundgren and Silver, 1980; Torma, 1977), nevertheless their interactions are not clearly understood and process engineers are called to deal with relatively uncharacterised systems (Olson and Kelly, 1986).

In spite of the proposal of several models describing various aspects of biooxidation, no established procedure has arisen for the determination of kinetic parameters on which to base the design of biooxidation reactors. Modelling of continuous biooxidation of both metal sulphides and the pyrite content of coal have been based on the heterogeneous fermentation model proposed by Erickson *et al.* (1970). These models have dealt mainly with the attachment of bacteria and hence the affect of the adsorbed population on biooxidation rates (Gormeley *et al.*, 1975; Chang and Myerson, 1982; Sanmugasunderam *et al.*, 1985). Other models incorporating mechanisms such as a shrinking particle (Blancarte-Zurita *et al.*,

1985; Chaudhury *et al.*, 1985) and propagating pores (Hansford and Drossou, 1987) have been presented. These models deal with the extent of mineral extraction with time rather than directly with bacterial action. Subsequently the use of a simple empirical relationship, the logistic equation, has been shown to adequately describe both batch and continuous biooxidation in terms of extent of mineral extraction (Pinches *et al.*, 1987; Chapman, 1989).

The purpose of this study has been the characterisation of the biooxidation of an auriferous pyrite/arsenopyrite flotation concentrate to maximise gold recovery. In order to achieve this, batch biooxidation tests were run using both the bulk concentrate as well as five narrowly sized fractions of the concentrate. The usefulness of the logistic equation in describing the course of the biooxidation was assessed and used to generate rate parameters which are compared to experimentally determined rates. In addition, the dependance of biooxidation rates on surface area concentrations of concentrate are assessed.

Large scale pilot plant testing of this concentrate has been conducted and extensive sets of data have been generated which are a valuable basis for the testing of models. Analysis of this existing pilot plant data in order to determine rate constants which could provide an engineering basis for sound reactor design will be carried out.

CHAPTER 2

LITERATURE SURVEY

2.1 Introduction

The empirical, logistic equation was used to interpret the kinetics of the bio-oxidation of narrowly sized fractions of a pyrite/arsenopyrite concentrate in order to assess the suitability of the model in characterizing continuous biooxidation systems. It was also used to describe the kinetic rate during continuous operation and to ascertain the relationship between rate and surface area concentrations.

The literature which is available on kinetics and modelling of biooxidation will be analysed in some detail, while in a more general manner the background to biooxidation, the microorganisms involved, the minerals oxidised and the chemistry by which this occurs will be presented.

2.2 Iron and Sulphur Oxidising Bacteria

Applications of biooxidation in the mining industry began centuries ago albeit without understanding or recognition of the contribution of microorganisms. The earliest report on the biooxidation of metal sulphides was published in 1922 (Torma, 1977) though *Thiobacillus ferrooxidans* was only isolated in 1947 by Colmer and Hinkle (1947). Subsequent to this the field has been extensively reviewed (Torma, 1977; Kelly *et al.*, 1979; Lundgren and Silver, 1980; Brierley, 1984; Harrison, 1984; Hutchins *et al.*, 1986; Olson and Kelly, 1986).

Interest in biooxidation has occurred owing to the potential commercial use of these sulphide and iron oxidising microorganisms in the mining industry. Commercial applications of biooxidation include heap, dump and *in situ* biooxidation for the treatment of low grade ores, while development of viable treatment methods for high grade concentrates in agitated reactors continues (Kelly *et al.*, 1979; Karavaiko, 1985).

These organisms have been identified as the biological catalysts involved in the solubilisation of metal sulphides, whether by indirect or direct attack. These two

terms have been introduced to differentiate between indirect acid and ferric attack of the mineral sulphides resulting in solubilisation, where the major contribution by the bacterial population is in regeneration of ferric iron and acid production and direct oxidation. Direct attachment of the bacteria to the mineral surface has been shown to occur, as has solubilisation of iron-free sulphides, giving evidence to support the theory of direct biooxidation. Both mechanisms are thought to occur simultaneously (Kelly *et al.*, 1979; Hutchins *et al.*, 1986).

The bacteria contributing towards mineral solubilisation have been isolated from natural mineral sulphide deposits, as well as from mineral sulphide and coal waste dumps (Lundgren *et al.*, 1986; Hutchins *et al.*, 1986), where the natural phenomenon of acid leaching of the sulphides and the occurrence of acid mine drainage has increased with the exposure of these minerals during mining operations.

Several microorganisms are directly involved in the biooxidation of mineral sulphides and include *Thiobacillus ferrooxidans, Thiobacillus thiooxidans, Leptospirillum ferrooxidans*, a group of thiobacillus like moderate thermophiles and the extremely thermophilic *Sulfolobus* species (Brierley, 1984; Olson and Kelly, 1986). A comprehensive review covering the thiobacilli and bacteria sharing their habitat, including cultivation and isolation techniques, has also been published (Harrison, 1984).

The characteristics of the organisms of major importance in biooxidation may be summarised as follows (Torma, 1977; Brierley, 1984; Kelly *et al.*, 1979; Hutchins *et al.*, 1986).

> *Thiobacillus ferrooxidans* is a motile, non spore-forming, gram negative, rod-shaped (0,1 x 0,5 micron) flagellate. It is aerobic, mesophilic, acidophilic and autotrophic, obtaining energy via the oxidation of reduced iron and sulphur compounds.
>
> *Thiobacillus thiooxidans* is very similar to *Th. ferrooxidans* with the exception of utilising only reduced sulphur compounds.
>
> *Leptospirillum ferrooxidans* is a highly motile curved rod shaped bacterium capable of forming spirals of joined cells and is also gram negative. As with the thiobacilli, it is aerobic, mesophilic, acidophilic and autotrophic, but oxidises ferrous iron and no sulphur compounds.

Most mineral sulphide oxidation studies have utilised pure cultures of, in general, *Thiobacillus ferrooxidans* (Gormeley *et al.*, 1975; Sanmugasunderam *et al.*, 1985; Chang and Myerson, 1982). More relevant to the industrial process is the recognition that the most practical situation involves the use of mixed cultures of both thiobacilli and leptospirillum where *Thiobacillus ferrooxidans* contributes to the total breakdown of the sulphide lattice, utilising both iron and sulphur, *Thiobacillus thiooxidans* utilising sulphide-sulphur, elemental-sulphur and any other intermediate sulphur compounds and *Leptospirillum ferrooxidans* aiding in the oxidation of ferrous to ferric iron (Kelly *et al.*, 1979; Brierley, 1984; Hutchins *et al.*, 1986; Helle and Onken, 1988).

During batch biooxidation of a pyrite flotation concentrate no significant contribution by leptospirillum like bacteria in a mixed culture was noted (Helle and Onken, 1988). During continuous biooxidation these microorganisms were found to displace the thiobacilli and iron oxidation rates achieved by leptospirillum rich cultures were significantly higher than those including only the thiobacilli. These findings emphasise the importance of mixed cultures for industrial applications.

The microorganisms mentioned above generally operate in the optimum temperature range for mesophilic growth which has been found to vary from 25 - 45 ^{o}C depending on the culture strain used (Torma, 1977). There is, however, a growing interest in, and reports of, successful applications of the use of thermophilic bacteria capable of biooxidation at elevated temperatures, a significant benefit being reduced cooling costs (Brierley, 1984; Hutchins *et al.*, 1986; Groudeva *et al.*, 1985; Norris and Parrot, 1985).

2.3 Biooxidation Reactions

The iron and sulphur oxidising bacteria which populate a biooxidation system obtain their energy from the transfer of electrons from reduced iron and sulphur species. This is shown in a very simplified manner by the following reactions (Torma, 1977).

$$S^{2-} = S^{6+} + 8e^{-}$$

$$Fe^{2+} = Fe^{3+} + e^{-}$$

The microbially catalysed oxidation of ferrous iron to ferric, and of elemental-sulphur to sulphuric acid, are generally expressed as

$$4FeSO_4 + O_2 + 2H_2SO_4 = 2Fe_2(SO_4)_3 + 2H_2O$$

$$2S^0 + 3O_2 + 2H_2O = 2H_2SO_4$$

Energy derived from the sulphur metabolism (642 kJ/mol S) is far greater than from the ferrous iron metabolism (102,5 kJ/mol Fe^{2+}).

The mechanism of pyrite oxidation may be expressed as follows:

$$4FeS_2 + 15O_2 + 2H_2O = 2Fe_2(SO_4)_3 + 2H_2SO_4 \qquad \text{(Bacteria)}$$

This is the overall reaction which is thought to consist of a number of intermediate reactions as shown below (Lundgren *et al.*, 1986).

$$2FeS_2 + 7O_2 + 2H_2O = 2FeSO_4 + 2H_2SO_4 \qquad \text{(Bacteria)}$$

$$FeS_2 + Fe_2(SO_4)_3 = 3FeSO_4 + 2S \qquad \text{(Chemical)}$$

$$4FeSO_4 + O_2 + 2H_2SO_4 = 2Fe_2(SO_4)_3 + 2H_2O \qquad \text{(Bacteria)}$$

$$2S + 3O_2 + 2H_2O = 2H_2SO_4 \qquad \text{(Bacteria)}$$

The above reactions indicate both the direct attack by the bacteria as well as ferric oxidation of the sulphide followed by bacterial regeneration of the ferric sulphate. Also evident is the removal of the elemental-sulphur which often forms an impermeable layer coating particles and causing oxidation to cease in purely chemical systems (Natarajan and Iwasaki, 1985).

It has also been claimed (Karavaiko, 1985, p9, p185) that the biooxidation rate of pyrite proceeds 20 - 1000 times faster than purely chemical oxidation.

The oxidation of arsenopyrite can be summarised as follows (Livesey-Goldblatt *et al.*, 1983; Bruynesteyn *et al.*, 1986).

$$4FeAsS + 11O_2 + 6H_2O = 4H_3AsO_3 + 4FeSO_4$$

$$2FeAsS + Fe_2(SO_4)_3 + 6O_2 + 4H_2O = 2H_3AsO_4 + 4FeSO_4 + H_2SO_4$$

$$2H_3AsO_3 + O_2 = 2H_3AsO_4$$

Precipitation of ferric arsenate occurs both during biooxidation and during later neutralisation of the liquors.

$$2H_3AsO_4 + Fe_2(SO_4)_3 = 2FeAsO_4 + 3H_2SO_4$$

Other precipitation reactions which occur involve the precipitation of jarosite in the presence of monovalent cations (H^+, K^+, NH_4^+). The precipitation of gypsum occurs with the addition of either lime or limestone, added for neutralisation purposes.

$$3Fe_2(SO_4)_3 + 14H_2O = 2H_3O\,Fe_3(SO_4)_2(OH)_6 + 5H_2SO_4$$

$$3Fe_2(SO_4)_3 + (NH_4)_2SO_4 + 12H_20 = 2NH_4Fe_3(SO_4)_2(0H)_6 + 6H_2SO_4$$

$$H_2SO_4 + CaO + H_2O = CaSO_4.2H_2O$$

$$H_2SO_4 + CaCO_3 + H_2O = CaSO_4.2H_2O + CO_2$$

Most metal sulphides have been reported as amenable to biooxidation (Karavaiko, 1985; Brierley, 1984; Torma, 1977) and include arsenopyrite (FeAsS), bornite (Cu_5FeS_4), chalcocite (Cu_2S), chalcopyrite ($CuFeS_2$), covellite (CuS), enargite (Cu_3AsS_4), galena (PbS), marcasite (FeS_2), millerite (NiS), molybdenite (MoS_2), orpiment (As_2S_3), pentlandite ($(Fe,Ni)_9S_8$), pyrite (FeS_2), sphalerite (ZnS), stibnite (SbS) and tetrahedrite ($(Cu,Fe)_{12}Sb_4S_{13}$).

In general these reactions proceed via direct bacterial attack as:

$$MS + 2O_2 = MSO_4$$

$$2MS + 2H_2SO_4 + O_2 = 2MSO_4 + 2H_2O + 2S^0$$

$$2S^0 + 3O_2 + 2H_2O = 2H_2SO_4$$

or indirectly via ferric attack as:

$$MS + Fe_2(SO_4)_3 = MSO_4 + 2FeSO_4 + S^0$$

Where M represents a bivalent metal ion (Torma, 1977; Lundgren *et al.*, 1986).

Recovery of uranium has been found to be successful via both indirect oxidation by ferric iron and direct bacterial attack of U^{4+} (Karavaiko, 1985; Lundgren *et al.*, 1986).

2.4 Factors Influencing Biooxidation

Operating factors such as temperature, pH, nutrient availability and supply of O_2 and CO_2 influence the growth and activity of the iron and sulphur oxidising microorganisms used in the biooxidation of sulphide minerals. Comprehensive reviews dealing with these factors and their effects on biological oxidation have been published by Karavaiko (1985), Kelly *et al.* (1979), Lundgren and Silver (1980), and Torma (1977).

The microorganisms involved in biooxidation are mesophilic with optimum growth and biooxidation occurring from 25 to 40 ^oC, with deactivation of the culture occurring in the region of 55 ^oC (Torma, 1977; Lundgren and Silver, 1980). The effects of temperature on the activity of *Thiobacillus ferrooxidans* is also dependant on other parameters such as pH, substrate concentration and the concentration of salts in solution (Karavaiko, 1985).

Thiobacillus ferrooxidans has been reported to survive throughout a pH range of 1 to 5 (Torma, 1977). The optimum pH range for oxidation of various sulphides differs, though many reports conclude that the optimum lies between two and three (Karavaiko , 1985; Torma, 1977). An optimum of between 1,0 and 2,5 for the

oxidation of ferrous iron, zinc sulphide, cobalt sulphide, chalcopyrite, chalcocite, covellite, galena and pyrite has been reported, including the fact that *Thiobacillus ferrooxidans* has been adapted to oxidation at lower pH values (Lundgren and Silver, 1980).

The required nutrients for optimum activity of the microorganisms involved in bio-oxidation include nitrogen, potassium, phosphate, magnesium and calcium (Karavaiko, 1985; Lundgren and Silver, 1980; Torma, 1977). A nutrient medium in common use is the 9K medium of Silverman and Lundgren (1959), in which the energy source is ferrous sulphate. Carbon, necessary for the production of cell mass, is obtained from atmospheric carbon dioxide. An increase in the rate of oxidation of various sulphide minerals with an increase in supply of carbon dioxide has been reported (Karavaiko, 1985; Lundgren and Silver, 1980), and is thought to be related to the pulp density and surface area of sulphide available for oxidation. Carbon dioxide supply may be supplemented by carbonates contained in the ore or concentrate, as well as by addition of limestone for pH control purposes.

Supply of oxygen is of major importance, not only owing to the aerobic nature of the microorganisms, but also for the oxidation of sulphides. As shown by the bio-oxidation reaction of pyrite to ferric sulphate, the stochiometric ratio of oxygen to pyrite required for complete sulphide oxidation is 3,75:1, this is a mass ratio of 1:1, hence the importance of efficient dispersion of oxygen in agitated bio-reactors.

Other factors which have a considerable effect on the rates of biooxidation are the characteristics of the sulphide minerals and the specific bacterial cultures used. These include the presence of toxic elements, electrochemical effects leading to enhanced biooxidation or passivation of intergrown mixed sulphides (Mehta and Murr, 1982; Natarajan and Iwasaki, 1985; Karavaiko *et al.,* 1985), the solubility product of the sulphide (Torma and Sakaguchi, 1978) and the type of conductivity and mechanisms of bacterial action (Karavaiko, 1985). While little can be done to modify these factors in industrial applications, an understanding of their influence on the biooxidation rate is important in predicting the kinetics of the biooxidation of different minerals.

It became evident from the literature that rates and extent of biooxidation were very much influenced by available surface area of sulphide mineral, whether increase was due to finer milling or to an increase in pulp density (Pinches, 1972; Torma, 1977; Chang and Myerson, 1982; Myerson and Kline, 1983; Chaudhury, Sukla and Das, 1985; Hansford and Drossou, 1987). As a study of the effect of surface area or

surface area concentration is central to this project the relevant literature is reviewed in detail.

The increase of exposed surface area in a biooxidation system effectively increases the surface area of sulphide mineral available for both bacterial adsorption and indirect chemical oxidation. Consequently, whether total adsorption of the bacteria onto the surface or just close proximity to the surface is required, increase in surface area should facilitate an increase in biooxidation rate. A detailed review of bacterial attachment as well as the effect of surface area concentration was completed by Drossou (1986).

Scanning electron microscope examinations of the surface of pyrite crystals which had been subjected to prolonged biooxidation showed the presence of both adsorbed bacteria as well as corrosion pits (Bennett and Tributsch, 1978). Location of these pits lent evidence to the theory that bacterial attachment was selective and dependant on crystal structure, particularly deviations such as fracture lines and dislocations in the crystal order. Cultivation of *Thiobacillus ferrooxidans* on synthetically produced single pyrite crystals, in order to investigate the interaction between the bacteria and the pyrite surface, has been reported (Rodriguez-Leiva and Tributsch, 1988). The results indicated the production of an organic film between the bacterium and the sulphide surface. Corrosion pits at different stages of development, correlating with bacterial activity, were also formed. The investigators had no doubt that the mechanism of biooxidation by *Thiobacillus ferroxidans* was heterogeneous whereby the cell attached to the sulphide surface and the reaction occurred in a thin film between the sulphide surface and the bacterial outer membrane.

Similar pore formation was observed while investigating the effect of both bacterial oxidation and chemical, ferric sulphate oxidation on pyrite crystals (Keller, 1982). Different etch patterns were produced by the two oxidation processes, ferric oxidation being characterised by etch pits having symmetries related to crystallographic surface orientations, while bacterial oxidation produced a more complex and irregular pattern. This author suggested no link between bacterial adsorption and etch patterns.

During the biooxidation of auriferous sulphide concentrates for the purpose of gold extraction, polished sections of partially oxidised crystals were examined microscopically (Southwood and Southwood, 1985). In all cases the development of pores penetrating pyrite grains were visible. The depth of these pores varied from

barely discernible pits on the particle surface to pores passing completely through the grains. The pores appeared to be cylindrical and indicated a preferred direction of propagation, in some cases developing in three mutually perpendicular directions. Observations were thus in agreement with, and provided support for, previous suggestions of selective bacterial attachment dependant on imperfections in the sulphide lattice .

Scanning electron microscope investigations of gold-bearing pyrite residues subjected to biooxidation for differing periods showed grooves, pits and pores propagating through the particles (Drossou, 1986). These observations lead the investigator to introduce a kinetic model termed the propagating pore model which will be discussed later.

Growth of *Thiobacillus ferrooxidans* on prills of elemental-sulphur as the sole energy source indicated growth of only adsorbed bacteria and release of progeny into solution once saturation of the sulphur surface had occurred. The patterns of colonisation observed on the sulphur prills suggested that adsorption and growth do not occur homogeneously on the surface, but in regions of distortion (Espejo and Romero, 1987).

The non-stochiometric degradation of coal pyrite has been reported (Andrews, 1988). It was suggested that the preferential oxidation of sulphur, which was observed, implied that sulphur atoms could migrate to the pyrite surface by molecular diffusion which occurred at a much greater rate along dislocations or grain boundaries than through pure crystalline solids. Hence the tendency of the bacteria to adhere to dislocation sites.

Further evidence supporting the observation of attached bacteria include actual enumeration of bacterial populations adsorbed to sulphide surfaces. A range of 30% to 90% of bacteria present being associated with the surface of different sulphides has been reported (Atkins *et al.*, 1986; Myerson and Kline, 1983) with the use of nitrogen and protein determinations. Epifluorescent microscopy has also verified the presence of large populations of adsorbed bacteria during biooxidation of pyrite (Yeh *et al.,* 1987).

Earlier work on the effect of surface area on rates of biooxidation has been reviewed by Torma (1977), who indicated that rates increased with decreasing particle size. A more comprehensive survey by Drossou (1986), and Drossou and Hansford (1987) extended this observation to include variation of surface area not

only by finer grinding but also by increase in solids concentration or pulp density. It was then again concluded that volumetric leach rates were indeed dependant on surface area whether adjusted by varying particle size or solids concentration and that in the region of low surface area, data obtained in either manner coincided, with a linear dependency existing. As surface area increased, the dependency of the rates decreased, indicating that above certain surface area concentrations other factors become rate limiting, possibly due to the high solids concentration.

The conclusion was then drawn that within the region of linear dependance of volumetric biooxidation rate on surface area concentration, it was possible to obtain a physical parameter, the surface biooxidation rate ($kgm^{-2}d^{-1}$), characteristic of a mineral, from the slope of the curve. Drossou (1986) went on to make the assumption that the surface oxidation rate was independent of particle size or solid concentration, and hence surface area concentrations, at least in the region of lower surface area concentrations. This was shown to be true for the biooxidation rates of a pure pyrite concentrate using size fractions between 25 and 106 micron and geometric surface areas. Further work from this group by Chapman (1989) supported the findings of surface area dependance of biooxidation

Other work on the effect of surface area on biooxidation rates will be discussed both when presenting the kinetic models found in the literature and in comparison to results obtained during this project.

2.5 Biooxidation of Pyrite and Arsenopyrite for the Recovery of Precious Metals

The term refractory is used to describe gold bearing ores or concentrates from which gold recovery is not possible when treated by conventional gravity and cyanidation procedures. Some major causes of refractoriness include the presence of submicroscopic gold particles which no amount of milling sufficiently exposes, the presence of carbon active in gold adsorption, or the presence of base metals or pyrrhotite which interfere during the cyanidation process (Swash, 1988; Dry and Coetzee, 1986; Hutchins *et al.*, 1987; Lazer *et al.*, 1986).

A number of options for the recovery of gold occluded within sulphide minerals, as is characteristic of the gold bearing pyrite/arsenopyrite concentrate used for this study, exist. These include pressure oxidation, roasting and bacterial oxidation, all three of which include breakdown of the sulphide minerals (Haines, 1986; Dry and Coetzee, 1986).

A mineralogical investigation of refractory gold bearing ores, including that from Fairview, has been completed by Swash (1988) where it was reported that submicroscopic gold forms a significant portion of the refractory gold in arsenical ores. Analysis using an electron microprobe indicated the presence of higher concentrations of gold in arsenic rich regions. These observations indicated that complete breakdown of the sulphide mineral was necessary in order to expose the gold, unless selective breakdown occurred in gold rich regions resulting in preferential release of the gold.

The seemingly selective biooxidation of sulphide in gold rich regions has been shown to occur, with many investigators reporting only partial sulphide breakdown necessary in order to achieve maximum gold dissolution (Marchant, 1985; Lazer *et al.,* 1986; Hansford and Drossou, 1987). The observations of pores penetrating partially bacterially oxidised pyrite crystals along dislocations and microfractures (Southwood and Southwood, 1985), the fact that the large and incompatible atoms cause instability and distortions within the sulphide lattice (Swash, 1988) and the selective attachment of bacteria to dislocations all confirm the finding that selective breakdown of the sulphide occurs in gold rich regions.

A number of papers dealing with the viability of biooxidation treatment, prior to cyanidation, for the recovery of gold from refractory ore have been presented at conferences. The experimental work on which these papers were based had until recently focused on the relationship between gold recovery and sulphide breakdown rather than on the modelling of the kinetics. What these papers reflect is the level of interest in the biooxidation process; they do, however, not report scientific observations useful for chemical engineering reactor design.

A cost analysis of the direct biooxidation of a gold bearing pyrite/arsenopyrite ore and a flotation concentrate produced from this ore indicated the feasibility of the latter process. The flotation-biooxidation process was also found to be more economically viable than the traditional flotation-roasting process usually employed (Livesey-Goldblatt *et al.,* 1983). A subsequent comparison between pressure oxidation, roasting and biooxidation also indicated biooxidation as being more viable (Haines, 1986).

Gold recovery from carbon containing sulphide concentrates poses two difficulties. Breakdown of the sulphide is necessary in order to liberate occluded gold, as is deactivation of the carbon in order to prevent readsorption of the gold during

cyanidation. Biooxidation of carbon containing sulphides has been most successful, with gold recoveries exceeding those obtained by both roasting and pressure oxidation (Fridman and Savari, 1984; Karavaiko *et al.,* 1985). In both cases preferential oxidation of arsenopyrite was reported as well as maximum gold recovery with incomplete removal of the sulphide mineral.

Biooxidation of several gold bearing pyrite/arsenopyrite concentrates by different bacterial cultures have been compared (Hutchins *et al.,* 1987). These included use of a *Thiobacillus ferrooxidans* culture at 30°C, a facultative "thiobacillus-like" thermophile at 50°C and a *Sulfolobus* species at 60°C. Iron oxidation by the thermophile at 60°C was found to be most rapid.

Laboratory scale batch and continuous testwork followed by pilot plant biooxidation of a pyrite/arsenopyrite flotation concentrate have been reported by Marchant (1985). Results indicated preferential oxidation of arsenopyrite and only partial breakdown of sulphide necessary in order to achieve maximum gold recovery. Iron extraction was found to increase with increasing pulp density up to 10% solids, further increase in pulp density causing a rapid drop in rates.

Similar continuous biooxidation for the recovery of gold and silver from a pyrite flotation concentrate from Porgera, New Guinea, was found to be successful (Lawrence and Gunn, 1985).

Information required for an engineering feasibility study was produced by completing a biooxidation pilot plant test program (Bruynesteyn *et al.,* 1986). A pyrite/arsenopyrite concentrate containing 278 g/t gold, of which 98% was recoverable, was used. Maximum biooxidation rates achieved during continuous operation exceeded those attained during batch tests. Preferential removal of arsenopyrite was noted, while the rate of removal of iron was shown to be more rapid than that for arsenic. This suggested that while arsenic may be preferentially oxidised, the rate of arsenopyrite removal may not exceed that of pyrite.

The feasibility study compared the cost of a 100 tpd biooxidation plant to the cost of both roasting and pressure oxidation. The biooxidation plant was found to be more economically viable. Plant scale up for this study was carried out on an empirical basis, with the authors emphasising the need for a reliable model of the biooxidation process. Marchant and Lawrence (1986), indicated that the response of a refractory sulphide to biooxidation scaled up predictably from bench scale to a 2 tpd

pilot plant, but also emphasised the need for many parameters to be optimised on a much larger scale in order to facilitate plant design.

Biooxidation studies of both a pyrite/arsenopyrite and a pure pyrite concentrate investigating factors affecting biooxidation rates, including pulp density and particle size, have been completed. Rates of pyrite removal achieved during biooxidation of narrowly sized fractions of a pyrite/arsenopyrite concentrate indicated a linear relationship with pyrite surface area when varying particle size. A similar relationship between arsenopyrite oxidation rates and surface area concentration was true only for low surface areas, after which it was likely that parameters other than surface area became limiting. Similar results were shown when increasing surface area by increasing pulp density (Pinches, 1972).

A similar investigation using a pure pyrite concentrate, the surface area of which was varied by use of different size fractions, also indicated a direct relationship between oxidation rates and surface area concentrations (Hansford and Drossou, 1987). This observation led the authors to introduce the use of a surface area oxidation rate (kg m^{-2} hr^{-1}) rather than the more commonly used volumetric oxidation rate (kg m^{-3} hr^{-1}).

A recent study of the biooxidation of a gold bearing pyrite/arsenopyrite concentrate in a single stage and a three stage continuous system has been presented (Pinches *et al.,* 1987). In order to interpret the results a model based on the logistic equation was used. Unlike previous reports this concentrate required almost total break down of the sulphide to achieve maximum gold dissolution. Use of the model enabled the prediction of overall rates for a number of reactor systems. The model facilitated the comparison of the performance of different configurations of reactors and was found to be most useful.

2.6 Kinetic Modelling of Biooxidation

Biooxidation is a very complex process. As a hydrometallurgical process it involves the agitation, aeration and flow of large volumes of slurry, while as a process control problem, control of parameters such as pH, temperature, aeration and flow rates are that much more critical owing to the danger of either deactivation or washout of the bacterial culture. On a more fundamental basis, one is faced with a three phase heterogeneous system in which a number a poorly understood chemical and

bacterially catalysed reactions are occurring, the relative rates of which are not known.

The models attempting to describe biooxidation which have appeared in the literature all seem to fall into two broad categories, either predicting bacterial growth in the system, termed growth models, or leach models, which predict the rate of mineral substrate oxidation. Neither of these categories of models contain parameters which are readily applicable to the prediction of the performance of biooxidation reactors.

The exponential growth of a bacterial culture dependant on a single soluble limiting substrate was proposed by Monod (1949). This relationship was of the same form as the Langmuir adsorption isotherm and Michaelis-Menten enzyme kinetics (Bailey and Ollis, 1977, p345).

Batch oxidation of soluble ferrous sulphate to ferric sulphate by *Thiobacillus ferrooxidans* was found to be well described by Monod kinetics (Lacey and Lawson, 1970). No bacterial numbers were reported, though from the rapid drop in ferrous iron reported, it may be assumed that large and active inocula were used, thus eliminating the lag phase, which is not accounted for by Monod kinetics. Modifications of Monod kinetics to include both substrate and product inhibition by ferrous and ferric iron respectively (Jones and Kelly, 1983), and later to include wall growth of bacteria (Mehta and le Roux, 1974) enabled better descriptions of the continuous oxidation of ferrous sulphate. A model based on the oxidation reaction of ferrous to ferric sulphate and the hydrolysis of ferric iron to ferric hydroxide was constructed (Petrova *et al.,* 1979) and gave an indication of the effect of temperature and pH on the above reactions.

Models considering only the solution reactions have very limited application when considering the dissolution of sulphide minerals, though the form of the Monod kinetics has been retained with the substitution of limiting substrate concentration by the total initial surface area concentration of sulphide mineral (Torma and Sakaguchi, 1978). This study was also based on product formation which was equivalent to metal extraction, rather than bacterial numbers, where metal extraction rates were obtained from the linear section of the curve describing the relationship between metal concentration in solution and time. In each case analytically pure nonferrous sulphides NiS, CoS, ZnS, CdS, CuS, and Cu_2S were used at varying solids concentrations (1 - 14%) in order to vary substrate surface area. Experimental results were found to be in agreement with those predicted by

the model and a correlation between the rate of metal dissolution and solubility product of the metal sulphide found. It was thus suggested that the tendency to dissociation of the substrate, rather than bacterial attachment, be considered a prerequisite for biooxidation.

A trend of model development considering the heterogeneous nature of a biooxidation system may be followed where bacterial attachment has been considered a prerequisite for oxidation to occur.

A model describing bacterial growth on a hydrocarbon source dispersed in a continuous liquid phase was developed (Erickson *et al.*, 1970). This model accounted for growth both in the continuous phase as well as at the interface of the two liquids and adsorption and desorption of the bacteria from this interface.

This model was used as a basis to describe the biooxidation of zinc sulphide where bacterial attachment to the solid surface was presumed a prerequisite for metal dissolution and bacterial growth (Gormeley *et al.*, 1975). Further assumptions included a constant and maximum bacterial growth rate with no contribution to biooxidation being made by the desorbed population. A dynamic interaction between adsorbed and desorbed bacteria was assumed while bacterial growth due to ferrous iron oxidation produced by chemical release of zinc by ferric iron oxidation was assumed negligible. The model, which predicted steady state bacterial populations as a function of dilution rate and surface area concentration, was generally not found to be in agreement with experimental data.

The continuous biooxidation of pyrite was described using the model derived by Gormeley *et al.* (1975) adapted to include bacterial growth both in solution and adsorbed to the solid surface (Chang and Myerson, 1982). In order to fully describe flow of a heterogeneous system, two dilution rates, which could be varied independently, were included in the model, one for the solid phase and the second for the liquid phase. Both experimental results and the model predictions indicated an increase of biooxidation rate with increasing pyrite surface area and decreasing retention time in the reactor. The range of surface areas concentrations studied indicated that high pulp densities must have been used. It is thus strange that levels of ferric iron in solution never exceeded 22 ppm which is exceptionally low. Also strange was the fact that ferrous iron concentrations were always higher than ferric iron if the bacterial culture was active. No indication of the degree of pyrite removal achieved was given.

A model estimating the growth rate of *Thiobacillus ferrooxidans* on a solid substrate was presented and validity of the parameters tested using experimental measurements made during the biooxidation of a zinc sulphide concentrate (Sanmugasunderam *et al.,* 1985). This model, based on that developed by Gormeley *et al.* (1975), was used for the continuous biooxidation of the zinc sulphide using two reactors in series with and without recycle of solids and was found to fit the experimental data well. The values obtained for these parameters (in particular, the surface area occupied by a bacterium) were not in agreement with those of other workers (Chang and Myerson, 1982; Myerson and Kline, 1984) leading the authors to suggest the dependance of parameters on the nature of the mineral and experimental conditions. Surface area measurement either by an air permeability method (Sanmugasunderum *et al.,* 1985) or BET (Chang and Myerson, 1982; Myerson and Kline, 1984) may have contributed to differences.

Removal of pyrite from coal using biooxidation has been modelled in a similar way to the biooxidation of other sulphide minerals. The bacterial mass balance model used by Chang and Myerson (1982) to describe the continuous biooxidation of pyrite was used by Myerson and Kline (1984), with slight adaptations, in their study of the continuous bacterial desulphurization of coal. Myerson and Kline (1983) had previously demonstrated the irreversible adsorption of *Thiobacillus ferrooxidans* to coal particles and hence used an irreversible second order kinetic equation to relate the concentration of adsorbed bacteria to that in solution instead of the Langmuir type adsorption desorption isotherm used previously (Chang and Myerson, 1982). Results indicated increase in bacterial growth rates and hence biooxidation rates with increase in coal surface area and with decrease in required retention time at a fixed surface area concentration. These trends were in agreement with those reported for biooxidation of sulphide minerals. A similar study on the modelling of microbial removal of pyritic sulphur from coal also indicated increasing rates with increasing pulp density, levelling off at high pulp densities. Rates of sulphide oxidation based on particle surface area were also introduced (Kargi and Weissman, 1984).

Various models describing the biological extraction of copper and zinc from ores and concentrates have been proposed. The batch biooxidation of different size fractions of a sphalerite concentrate indicated increased rates with decrease in particle size (Chaudhury, Sukla and Das, 1985). Rate equations describing bio-oxidation kinetics for both diffusion and chemical rate control were applied to the data and it was found that both zinc and copper dissolution from the concentrate

obeyed a shrinking core, chemical controlled reaction, which was first order with respect to the substrate concentrations.

Further biooxidation studies carried out using a zinc, copper and lead containing ore indicated that both copper and zinc oxidation obeyed the model of shrinking core, product layer diffusion control (Chaudhury and Das, 1987).

The sphalerite concentrate studied by (Chaudhury *et al.,* 1985) contained 7 - 8% iron and biooxidation was carried out at a 2% pulp density. The ore used in the second study (Chaudhury and Das, 1987) contained 8,9% iron. Tests were carried out at a 10% pulp density. The higher iron concentrations possibly lead to an increase in jarosite precipitation causing the mechanism to move from chemical reaction control to product layer diffusion control.

Application of a shrinking particle model to the biooxidation of both a chalcopyrite and a zinc sulphide concentrate indicated that zinc extraction was well described while insufficient copper extraction had occurred in order to adequately test the model (Blancarte-Zurita *et al.,* 1985).

A shrinking particle model was derived and used to describe the batch biooxidation of narrowly sized fractions of a pyrite concentrate (Drossou, 1986), but was found to disagree with experimental data. Subsequent to the observation of pore formation in partially oxidised pyrite crystals, similar to those observed by Southwood and Southwood (1985), a propagating pore model was derived (Drossou, 1986; Hansford and Drossou, 1987). This model described three phases, a linear phase where biooxidation rates were constant and all pores active, a phase of decelerating rate, equivalent to pore deactivation, and a stationary phase as bio-oxidation activities ceased. This model also introduced the use of a surface area oxidation rate rather than the more commonly used volumetric oxidation rate. This model was found to describe the experimental data well.

Several other approaches to the modelling of biooxidation systems have also been suggested.

An electrochemical model was successfully used to describe both bacterially aided and sterile oxidation of synthetic nickel sulphide, indicating that the major function of the bacteria was in ferrous iron oxidation (Verbaan and Huberts, 1988).

The accurate analysis of growth of microorganisms in continuous culture is facilitated by the use of an equation which fully describes the entire batch growth curve of that organism. The logistic equation, which describes the lag phase, exponential growth as well as declining growth and the stationary phase is suggested as being suitable (la Motta, 1976).

The logistic equation has been widely used to model human growth (El Lozy, 1978), the growth kinetics of *mycobacterium* sp (Lambrecht *et al.,* 1988), to describe the batch growth of pullulan fermentation (Boa and LeDuy, 1987), to model the production of xanthate gum by batch fermentation (Pinches and Pallent, 1986). It has also been used to describe growth of subterranean clover communities and snails (Fukai and Silsbury, 1976; Plorin and Gilbertson, 1984).

During biooxidation of a mineral substrate the trend of metal extraction follows that of bacterial growth. An adapted version of the logistic equation, whereby bacterial concentrations were replaced by metal extraction during biooxidation, described batch data for the removal of pyrite extremely well (Pinches *et al.,* 1987). Maximum rates of pyrite removal predicted by the model were of the same order as those found experimentally.

A mass balance for a continuous biooxidation reactor including the logistic equation as the rate expression was also found to describe accurately the continuous removal of pyrite. The form of the model presented was shown to be suitable for the characterisation of biooxidation systems and as such will be used in the present study.

CHAPTER 3

THE LOGISTIC MODEL

3.1 Use of the Logistic Equation to Descibe Batch Biooxidation

An unstructured bacterial growth model used to describe batch growth is given by Bailey and Ollis (1977, p359) as

$$\frac{dN}{dt} = kN(1-N/N_m) \qquad 3.1$$

where

- k constant
- N cell number
- N_m maximum population size, usually the saturation population before substrate depletion

This model assumes growth proportional to cell number and inhibition proportional to the square of the population. Integrating Equation 3.1 gives the logistic curve as follows

$$N = \frac{N_0 e^{kt}}{1 - N_0/N_m(1 - e^{kt})} \qquad 3.2$$

where

- N_0 cell number at t = 0
- t time

Equation 3.2 describes a sigmoidal curve where as time, t, tends to infinity, the cell number, N, tends to the stationary population size, N_m. This curve is shown in Figure 3.1 (a), and, as can be seen, is symmetrical about the point of inflection.

A sigmoidal curve is typical of a batch growth curve if the phase of decline is not applicable (Bailey and Ollis, 1977). It is also observed when plotting fractional removal of pyritic sulphur during biooxidation, X, versus time (Pinches *et al.*, 1987) where X is defined as follows

$$X_i = \frac{C_0 - C_i}{C_0}$$

C_0 original amount of pyritic sulphur present, (kg/m^3 slurry)
C_i pyritic sulphur present at time t = *i*, (kg/m^3 slurry)

Two approaches are possible when modelling the removal of pyritic sulphur during biooxidation with logistic kinetics.

(i) Using an equation of the form of Equation 3.1, substituting fraction of pyritic sulphur removed, X_i, for bacterial numbers, N.

$$\frac{dX_i}{dt} = kX_i(1 - X_i/X_m) \qquad 3.3$$

X_m maximum fraction of pyritic sulphur that can be removed. The applicable value of X_m is characteristic of the mineral being oxidised. If all the sulphide can be removed a value of $X_m = 1$ is used.

The justification for this is that the relation between biooxidation of sulphide and time results in a sigmoidal curve which is fitted by an equation of the form of Equation 3.1 or 3.3.

(ii) Equating X, the fraction of pyritic sulphur removed, to N, the cell number. This can be done by using a yield of cells based on pyritic sulphur oxidation as follows.

$$N - N_0 = Y(C_0 - C) \qquad 3.4$$

Assuming that N_0 is very nearly zero and writing Equation 3.4 in terms of the fraction of pyritic sulphur removed, X, gives

$$N = YC_0X \qquad 3.5$$

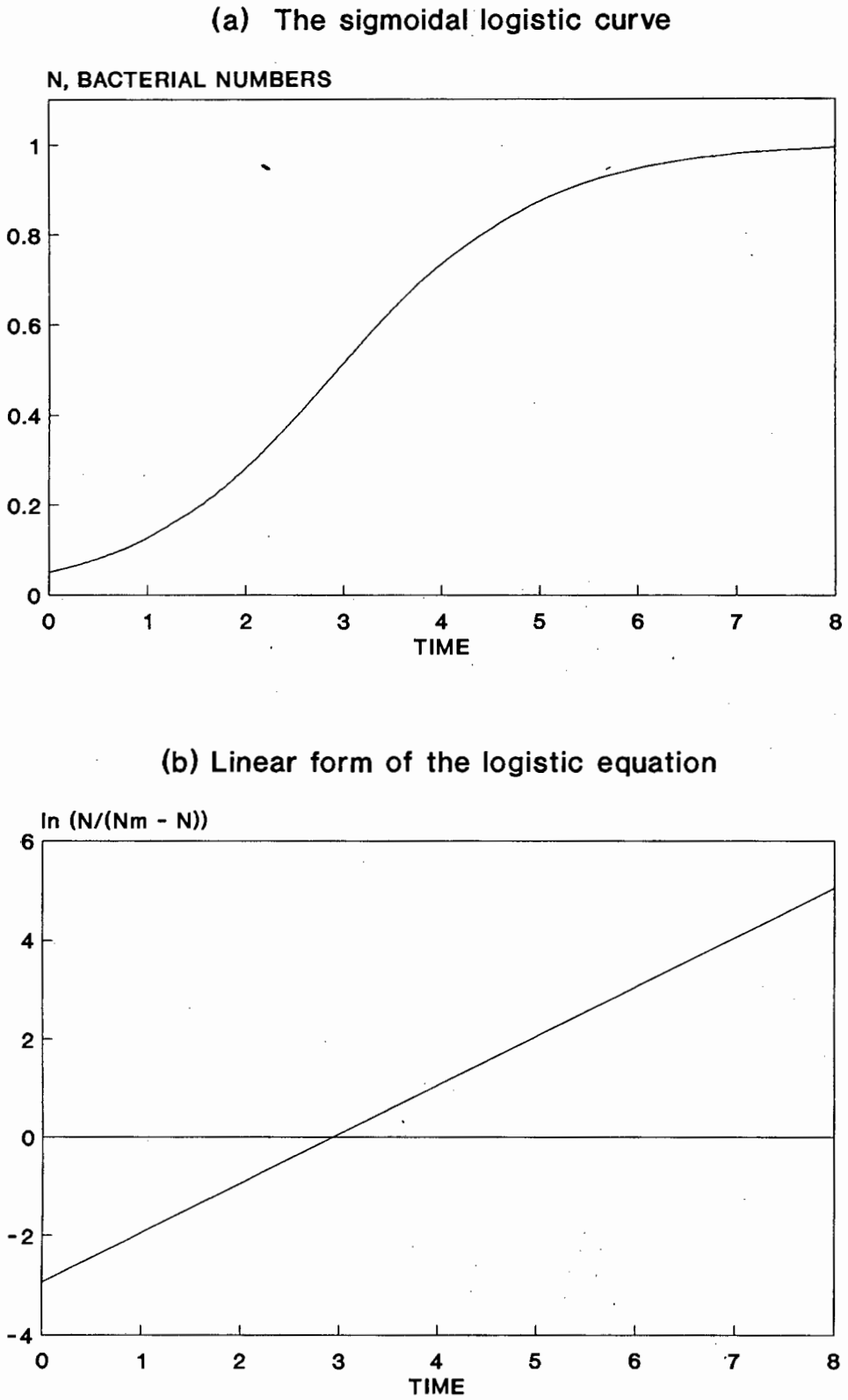

Figure 3.1 The sigmoidal and linear forms of the logistic model.

A different form of Equation 3.2 is given as

$$ln\ \frac{N}{N_m-N} = kt + ln\ \frac{N_0}{N_m-N_0} \qquad 3.6$$

Using Equation 3.5 it follows that

$$\frac{N}{N_m-N_0} = \frac{YC_0X}{YC_0X - YC_0X_m} = \frac{X}{X-X_m}$$

Equation 3.6 then becomes

$$ln\ \frac{X}{X_m-X} = kt + ln\ \frac{X_0}{X_m-X_0} \qquad 3.7$$

Differentiating Eqn. 3.7 results in Eqn. 3.3

Equation 3.6 is that of a straight line. It is this integrated form of the logistic equation which is most useful for determining the constants k, X_0 and X_m for batch data. A typical plot of this form of the equation is shown in Figure 3.1 (b) where $ln(N_0/(N_m-N_0))$ is the intercept and k is the slope.

When applying the logistic model to bacterial growth, the term N_0 in Equation 3.6 is the initial bacterial population. This term is never zero, as an initial inoculum, however small, must always be supplied. When fitting the logistic model in the form of Equation 3.7 to the fraction of pyritic sulphur removed, the term X_0 is included. Under normal conditions the term X_0, the fractional removal of pyritic sulphur, equals zero at the start of a batch test if the sulphide mineral is initially unoxidised, the model thus breaks down at zero time. Another drawback of the logistic model is the prediction of a sigmoidal curve which is symmetrical about the point of inflection. A large inoculum resulting in a negligible lag period could produce results which could be more accurately described by a model of a sigmoidal curve not necessarily symmetrical about the point of inflection. Furthermore, if a mixed sulphide mineral such as a pyrite/arsenopyrite concentrate is being oxidised, initial removal of either iron or sulphur is due to both pyrite and arsenopyrite removal, while during the latter stages of batch biooxidation only pyrite removal

occurs. Extraction curves for both iron and sulphur may thus tend to be assymetrical.

A useful characteristic of the logistic equation is the ease of determination of the maximum rate (la Motta, 1976). This is obtained by setting the second derivative of Equation 3.2 to zero, which gives

$$N = N_m/2 \quad \text{or} \quad X = X_m/2 \qquad 3.8$$

Substituting Equation 3.8 into Equation 3.3 gives the maximum rate of removal as

$$\frac{dX_i}{dt}\Big|_{max} = C_0 k X_m/4 \qquad 3.9$$

Use of Equation 3.9 enables calculation of the maximum rates of removal once values of k and X_m, the logistic parameters, have been obtained. Predicted and experimentally obtained rates may thus be compared.

3.2 Presentation of the Logistic Equation for the Modelling of Continuous Biooxidation.

The logistic growth curve has been used to describe the rate of growth of batch cultures, and can be used directly in the analysis of continuous flow culture in a single reactor (la Motta, 1976). In order to describe the continuous biooxidation of a sulphide mineral in a cascade of reactors, the logistic equation may be applied in a similar manner using fractional removal of a mineral component rather than bacterial numbers (Pinches *et al.*, 1987). The derivation of the mass balance equations are shown below.

Considering a series of continuous stirred tank reactors (CSTR's), the mass balance over the first tank is found to be

$$r_1 = (C_0 - C_1)/T_1 \qquad 3.10$$

where

r_1 rate of removal of pyritic sulphur (kg/m^3 slurry/day)
T_1 retention time in tank 1 (days) [$T_1 = V_1/Q$]

V_1 volume of tank 1 (m^3)
Q the volumetric flowrate of slurry (m^3d^{-1})
C_o Concentration of pyritic sulphur fed to tank 1 (kg/m^3 slurry)
C_1 Concentration of pyritic sulphur in and leaving tank 1 (kg/m^3 slurry)

Equation 3.10 can be written in terms of the fraction of pyritic sulphur removed, X, as follows

$$r_1 = C_0X_1/T \qquad 3.11$$

By definition

$$r_1 = -\frac{dC_1}{dt}$$

$$= C_o\frac{dX_1}{dt}$$

Equation 3.10 then becomes

$$\frac{dX_1}{dt} = \frac{X_1}{T} \qquad 3.12$$

Combining the logistic model, Equation 3.3.

$$\frac{dX_1}{dt} = kX_1(1 - X_1/X_m)$$

with Equation 3.12 results in the following

$$X_1 = X_m(1 - 1/(k_1T_1)) \qquad 3.13$$

This is the mass balance based on logistic kinetics for one Continuous Stirred Tank Reactor or for the first in a series of CSTR's.

The mass balance for the i^{th} tank in a cascade, in terms of X_i which is defined as

$$X_i = (C_0 - C_i)/C_0 \qquad 3.14$$

is given as

$$\frac{dX_i}{dt} = (X_i - X_{i-1})/T_i$$

Combining the above with the logistic equation, Equation 3.3, the following can be derived

$$X_i^2 + X_i X_m \left(\frac{1}{k_i T_i} - 1 \right) - \frac{X_m X_{i-1}}{k_i T_i} = 0$$

Solving the quadratic for X_i results in a more convenient form of the mass balance.

$$X_i = \pm \left| \left(\frac{X_m}{2k_i T_i} - \frac{X_m}{2} \right)^2 + \frac{X_m X_{i-1}}{k_i T_i} \right|^{1/2} - \frac{X_m}{2} \left(\frac{1}{k_i T_i} - 1 \right) \qquad 3.15$$

When $X_{i-1} = 0$, i.e., for the first tank, the negative root applies and Equation 3.14 reduces to Equation 3.13. If the positive root is used when $X_{i-1} = 0$, Equation 3.14 reduces to $X_i = 0$, which is not applicable. For the rest of the cascade the positive root is applied in order to prevent X_i from being negative.

The volumetric rate of sulphide biooxidation in Reactor *i* at steady state, (Pinches *et al.*, 1987) can be given as

$$r_i = \frac{dX_i}{dt} = C_0 (X_i - X_{i-1})/T_i \qquad 3.16$$

This may be compared to the maximum rate as predicted by the logistic kinetics as shown by Equation 3.9, where C_0 is replaced by C_{i-1}

CHAPTER 4

MATERIALS AND METHODS

4.1 Introduction

In this Chapter preparation of the concentrate is discussed as well as the experimental and analytical procedures employed. Analytical procedures will be referenced, if standard, or described in full, as shown in Appendix 1, where necessary.

4.2 Fairview Concentrate

The concentrate used in this study was a pyrite/arsenopyrite concentrate from GENMIN's Fairview Mine near Barberton, Transvaal, South Africa. Material from this origin is currently being processed in a "nominal" 10 ton per day (tpd), biooxidation plant at the mine and continues to be used at GENMIN Process Research[1] for biooxidation pilot plant testwork.

This material is a refractory gold bearing concentrate which, prior to the installation of the biooxidation plant, was treated by roasting so as to break down the sulphide minerals to render the gold accessible to subsequent cyanidation.

The flotation concentrate was received as undried filter cake which was repulped at a slurry specific gravity of 1,5 and fed at 1 *l*/min into a ball mill in order to increase the proportion of material passing 75 micron. This additional milling was carried out in order to follow the procedure employed when running the pilot plant at GENMIN Process Research.

After milling, the material was fed onto an 18" Sweco screen model 1013 in order to separate the bulk concentrate into the following size fractions: +75 micron, -75 +53, -53 +38, -38 +25 and -25 micron

The concentrate was passed through two screens at a time, but in order to achieve efficient separation, each size fraction was rescreened a number of times. Each

1 Private Bag X3, WESTRAND, 1746.

fraction was then filtered, dried and lumps removed to allow all material to pass through an 850 micron screen before sampling material for use.

Chemical analysis and size distribution of the bulk concentrate are given in Tables 4.1 and 4.2.

TABLE 4.1 Chemical composition of the bulk concentrate used for batch testing.

Chemical	Mass %
Iron	24,6
Total Sulphur	22,8
Sulphide Sulphur	22,6
Arsenic	6,0
Silica (SiO_2)	24,9
Gold (g/t)	109,0

The average specific gravity of Fairview concentrate was 3,57 g cm^{-3}.

4.3 Batch Biooxidation

Each batch biooxidation test of 250 *l* was carried out in a 300 *l* agitated reactor. Agitation of the slurry was by overhead mixing at 300 rpm, air was sparged in via a circular sparge ring situated at the bottom of the reactor. The temperature was maintained at 40^{o}C with use of an immersed titanium heating element controlled by an on/off controller.

The culture used was a GENMIN Process Research mixed culture which is a mixed *Thiobacillus* culture that has become very well adapted to the Fairview concentrate.

TABLE 4.2 Microtrac size distribution of the bulk concentrate used for batch testing.

Size (micron)			Mass Retained (%)
	+	212	0,00
-212	+	150	0,54
-150	+	106	3,75
-106	+	75	7,67
-75	+	53	10,13
-53	+	38	13,82
-38	+	28	7,57
-28	+	20	6,14
-20	+	13	6,55
-13	+	9,4	7,32
-9,4	+	6,6	10,55
-6,6	+	4,7	10,98
-4,7			14,98

Each batch biooxidation test was run as follows:

31,25 kg solids, 250 *l* solution containing 184 g ammonium sulphate, 258 g potassium hydroxide and a 10% by volume inoculum. The ammonium sulphate and potassium hydroxide were the only nutrient salts added, following the procedure used on the pilot plant. The resulting slurry had a solids content of 120,8 g/*l* or a liquid to solids ratio of 8:1.

The material was slurried up and brought to a pH of 1,6 with sulphuric acid. A period of pH stabilisation was allowed (usually overnight) before the inoculum was added and a zero time sample removed.

Daily monitoring was as follows:

(i) The reactor was topped up to make up for evaporation losses.
(ii) Samples were removed for soluble iron titrations.
(iii) pH and redox measurements made.

(iv) If sufficient biooxidation had occurred during the previous 24 hours as shown by increase in soluble iron or redox potential, or drop in pH, a 4 *l* sample was withdrawn from the reactor, one of 2 *l* by scooping from the surface, the second by pumping rapidly from the bottom. This was done in order to ensure more reliable sampling.

If the pH dropped below 1,6 it was readjusted using slaked lime (composition given in Appendix 2).

Once removed, the samples were filtered, dried and weighed. Solution samples were further analysed for sulphur and arsenic as described later in this Chapter. A sample of biooxidation product was also retained in case the need for repeat analysis arose, the remaining oxidised product being used for hydrochloric acid washing.

4.4 Hydrochloric Acid Washing of Biooxidation Product

In order to remove the jarosite and ferric iron precipitates as well as any unreacted lime, all which confound calculation of the removal of iron, arsenic and total-sulphur during biooxidation, hydrochloric acid washing of the oxidised product was carried out. Each sample was slurried in a 2,5N solution of hydrochloric acid and bottle rolled for fifteen minutes at room temperature. Residues were then filtered, washed, dried and prepared to 100% passing 850 micron before being split for analysis and further cyanidation.

4.5 Cyanidation

Cyanide leaches were carried out in order to assess gold dissolutions. This was done in agitated beakers using the following procedure.

(i) A 200 g sample was slurried in 400 m*l* tap water (L/S ratio 2:1).
(ii) The pH was raised to above 12 by bulk addition of lime.
(iii) A pH stabilisation period with aeration for 1 hour was allowed prior to the addition of a maximum of 20 kg/t sodium cyanide.
(iv) Cyanide leaching was carried out for 24 hours during which additional lime was added, if necessary, to prevent the pH from dropping below 11.

(v) Cyanidation residues were filtered, washed and dried before being analysed for gold by the fire assay method.

4.6 Analytical Methods

Size analyses of the bulk concentrate and each size fraction produced by screening were done using a Leeds & Northrup microtrac, model 7991-01, particle size analyser. This procedure includes projection of a laser beam through a transparent cell containing a continuous stream of moving particles suspended in water. The amount of material in each size fraction is determined by the amount and direction of the scattering of this beam.

All solid samples, including the feed concentrate and the biooxidation product samples removed at set time intervals, were analysed for gold, iron, total-sulphur, sulphide-sulphur, arsenic and silica. The biooxidation liquors were analysed for total-iron, total-sulphur and arsenic. All analytical procedures are shown in Appendix 1.

CHAPTER 5

RESULTS AND DISCUSSION OF BATCH TESTS

5.1 Introduction

A series of batch biooxidation tests were run on the bulk concentrate and sized fractions of that concentrate in order to establish the dependance of kinetic parameters on particle surface area. Because the composition of these narrow size fractions were not identical, it was also possible to draw conclusions of the dependance of kinetic parameters on chemical composition.

Compositions as well as size distributions and surface areas of each fraction are reported and discussed. The experimentally determined maximum rates of removal of iron, arsenic and sulphide-sulphur, as well as of pyrite and arsenopyrite are examined. The logistic rate constants are then determined and discussed in terms of surface area concentration and element weighted surface area concentration. The effect of sulphide mineral removal on gold dissolution is also investigated.

5.2 Size Separation

Six samples of different sizes, viz. the bulk concentrate and the +75, -75 +53, -53 +38, -38 +25 and -25 micron fractions were produced by wet screening. The size distributions, as determined by microtrac analysis, are shown in Table 5.1. Bar charts of the size distributions are shown in Figure 5.1.

Separation of the bulk concentrate into the narrow size fractions was achieved as indicated by the charts in Figure 5.1. Particles smaller than 28 micron in diameter constituted more than 50% of the bulk concentrate, and were evenly distributed between the intervals from 20 to 4,7 micron, though slightly more reported to the finest interval. This is shown more clearly in Figure 5.1 (f), the chart for the -25 micron fraction. Owing to the degree of fineness, screening of a large amount of bulk concentrate was necessary in order to produce sufficient material for the size fractions of particle diameter greater than 25 micron.

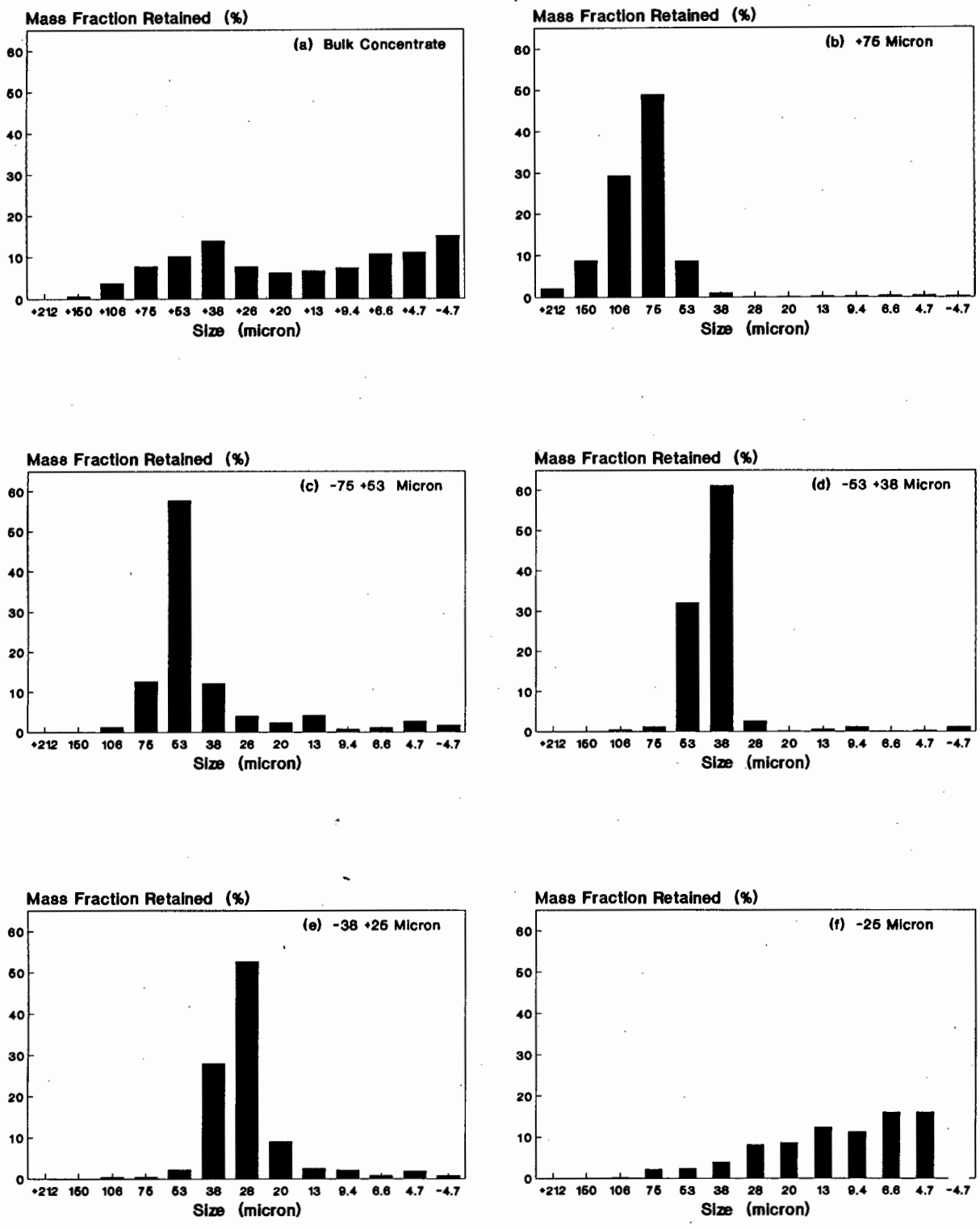

FIGURE 5.1 Microtrac size distributions for the bulk concentrate and narrow size fractions.

TABLE 5.1 Microtrac size distributions of the bulk concentrate and sized fractions.

SIZE		SIZE FRACTIONS					
Micron		Bulk	+75	-75 +53	-53 +38	-38 +25	-25
+212		0,00	2,11	0,00	0,00	0,00	0,00
-212	+150	0,54	8,77	0,00	0,00	0,00	0,00
-150	+106	3,75	29,22	1,21	0,37	0,27	0,04
-106	+75	7,67	48,96	12,63	1,16	0,35	2,14
-75	+53	10,13	8,55	57,65	32,01	2,08	2,28
-53	+38	13,82	0,90	12,10	61,06	27,92	3,84
-38	+28	7,57	0,09	3,91	2,48	52,65	8,04
-28	+20	6,14	0,03	2,29	0,05	8,96	8,66
-20	+13	6,55	0,24	4,13	0,44	2,50	12,35
-13	+9,4	7,32	0,24	0,73	1,11	2,08	11,28
-9,4	+6,6	10,55	0,32	1,09	0,00	0,69	16,05
-6,6	+4,7	10,98	0,32	2,67	0,22	1,81	16,05
-4,7		14,98	0,24	1,58	1,11	0,69	19,26

Table 5.2 shows that the different size fractions had slightly different chemical compositions. The coarsest (+75 micron) and finest (-25 micron) fractions both contained greater proportions of gangue mineral, quoted as SiO_2, and lower proportions of iron, sulphur and arsenic, (sulphide minerals). It also appeared that as the sulphide minerals reported more to the intermediate three fractions, (-75 +53, -53 +35 and -38 +25 micron), the gold content of these fractions also increased, specifically following the trend in arsenic increase. This association of the gold with sulphide minerals and particularly the arsenic is typical of such refractory ores, and hence concentrates. These observations are consistent with those of Swash (1988).

Selective reporting of the sulphide minerals to any specific size fraction was not found by Drossou (1986) when splitting a pure pyrite concentrate into narrow size fractions, though gold content of the finest fraction was lower. Size separation by decantation of a pyrite/arsenopyrite concentrate consisting of only -53 micron material, by Pinches (1972), did result in a similar occurrence with an increase in

sulphide minerals reporting to the coarser fractions. No results of gold deportment were reported.

TABLE 5.2 Chemical composition of size fractions.

SIZE FRACTIONS	ANALYSIS OF SIZE FRACTIONS					
micron	Iron %	Total Sulphur %	Sulphide Sulphur %	Arsenic %	Silica %	Gold g/t
Bulk	24,6	22,8	22,6	6,00	24,9	109,0
+75	23,8	25,6	25,6	3,38	30,0	92,0
-75 +53	30,4	29,9	29,4	6,60	18,8	135,0
-53 +38	32,3	31,4	31,4	7,83	16,3	163,0
-38 +25	30,4	30,4	29,0	10,80	14,4	187,0
-25	21,0	17,3	16,7	5,65	28,8	103,0

Because it was intended to investigate the possible dependance of biooxidation rate on surface area, the manner in which area was calculated is shown below.

Both surface area concentrations and diameters characteristic of each sample were based on size distributions prior to biooxidation. The diameter characteristic of a certain sample, d_c, was calculated using the product of the mass fraction in each size interval and the average diameter and then summing these for each interval, for example:

$$d_c = f_1 d_1 + f_2 d_2 + ... + f_j d_j$$

where

f mass fraction in a specific size interval

d average diameter in a specific size interval

j the number of size intervals as measured by the microtrac

The diameter calculated in this manner will be referred to as the characteristic diameter.

Calculation of surface area concentrations was based on the assumption that all particles were spherical, and as for the characteristic diameters, the average diameter for each size interval and the mass fraction in that interval were used. The initial solids concentration in the suspension was also considered in order to express the surface area in m^2m^{-3} slurry. This is shown in Equation 5.1.

$$\text{Surface area concentration in each size interval} = \frac{\text{volume of solids in that interval} * \text{surface area of an average particle}}{\text{volume of an average particle}}$$

$$= \frac{6 f_j M}{d_s d_j} \qquad 5.1$$

where

M concentration of solids in the slurry (pulp density) [120,8 kgm^{-3}]

d_s sg of solids [3,57 x 10^3 kgm^{-3}]

These results are shown in Table 5.3

TABLE 5.3 Average diameter and surface area concentration for each size fraction.

SIZE FRACTIONS	AVERAGE DIAMETER	SURFACE AREA CONCENTRATION		
	Micron	Total m^2m^{-3} Slurry	Pyrite m^2m^{-3} Slurry	Arsenopyrite m^2m^{-3} Slurry
Bulk	33,17	23 873	8948	3113
+75	108,07	2 482	1122	182
-75 +53	58,26	6 352	3158	911
-53 +38	50,86	5 216	2737	888
-38 +25	35,04	7 429	3389	1744
-25	15,86	31 591	8442	3879

The surface area concentration showed a general increase with decrease in particle size, with exception of the -75 +53 micron fraction. This is however consistent with the presence of more fine material, as shown in Table 5.1. It is evident from these results that fines were not removed to the same extent by each set of screens.

The surface area concentrations of both the bulk and the -25 micron sample were high owing to the presence of large amounts of fines at 56,5% and 83,7% respectively smaller than 28 micron, This can be seen in Table 5.1. These surface area concentrations of 23873 m^2m^{-3} and 31591 m^2m^{-3} were an order of magnitude higher than those obtained for the intermediate fractions.

Two important factors to consider were thus

(i) Distortion of surface area concentration with high proportions of fines.
(ii) Different chemical compositions with size.

Both of these could confound the relationship between biooxidation rate and surface area concentrations. The use of a surface area concentration weighted by the concentration of sulphide mineral present was thus also considered and the suface area concentrations weighted by the pyrite and arsenopyrite content are also shown in Table 5.3. The pyrite and arsenopyrite content of each size fraction are shown in Table 5.16; Calculation of these is described in Section 5.3.3.

5.3 Batch Results

Batch biooxidation tests were run using the bulk concentrate and the sized fractions under conditions described fully in Chapter 4. Total-iron, total-sulphur and arsenic analyses were carried out on the biooxidation and hydrochloric acid wash liquors, while iron, arsenic, total-sulphur, sulphide-sulphur, silica and gold were analysed for in the head and oxidised material. The mass and volume of each sample was recorded, as well as the mass of solids per unit volume of suspension. This was done by filtering and weighing of the dried solids. The analyses of the solid product after both biooxidation and HCl-acid washing are shown in Tables 5.4 to 5.9. Bio-oxidation liquor analyses, as well as those of the acid wash liquors, which were used for mass balance calculations are shown in Appendix 3.

TABLE 5.4 Chemical analysis of the bulk sample after biooxidation and acid washing

TIME	ANALYSIS OF SOLID PRODUCT BULK SAMPLE					
Days	Iron %	Total Sulphur %	Sulphide Sulphur %	Arsenic %	Silica %	Gold g/t
feed	24,6	22,8	22,6	6,0	24,9	109,0
0,0	24,2	24,6	24,6	5,9	26,8	114,0
1,0	23,8	24,1	24,1	6,0	26,9	115,0
3,0	24,1	24,9	24,9	5,1	25,2	116,0
4,0	23,5	23,8	23,8	4,2	26,6	119,0
5,0	22,3	23,5	23,5	3,0	29,7	124,0
6,0	20,8	22,3	22,3	2,4	28,2	128,0
7,0	18,4	20,9	20,1	2,0	32,9	131,0
8,0	14,7	19,4	15,9	1,4	30,8	126,0
11,0	5,4	12,6	6,0	0,3	33,3	125,0
12,0	4,0	11,2	3,5	0,2	33,2	123,0
13,0	2,8	10,5	1,5	0,1	32,2	115,0
14,0	2,3	10,1	0,9	0,1	33,9	118,0

TABLE 5.5 Chemical analysis of the +75 micron sample after biooxidation and acid washing

TIME	ANALYSIS OF SOLID PRODUCT +75 MICRON SAMPLE					
Days	Iron %	Total Sulphur %	Sulphide Sulphur %	Arsenic %	Silica %	Gold g/t
feed	23,8	25,6	25,6	3,4	30,0	92,0
0,0	23,8	24,5	24,0	3,0	32,1	89,3
1,0	23,7	24,4	23,3	2,8	33,7	87,4
4,0	22,8	23,2	21,5	2,2	34,4	88,5
6,0	22,6	25,2	22,5	1,6	32,7	99,0
7,0	21,4	23,3	19,7	1,5	35,4	105,0
8,0	18,7	20,8	17,2	1,3	36,8	109,0
10,0	15,9	17,6	13,9	0,8	40,1	121,0
11,0	13,7	14,9	11,2	0,7	43,4	115,0
12,0	11,5	13,3	8,3	0,6	40,9	95,9
13,0	9,8	12,0	6,3	0,6	41,0	105,0
15,0	6,7	9,1	3,4	0,4	43,4	72,7
18,0	6,3	9,7	1,0	0,4	37,6	84,9
22,0	5,2	9,6	0,2	0,3	35,0	66,4

TABLE 5.6 Chemical analysis of the -75 +53 micron sample after biooxidation and acid washing.

TIME	ANALYSIS OF SOLID PRODUCT -75 +53 MICRON SAMPLE					
Days	Iron %	Total Sulphur %	Sulphide Sulphur %	Arsenic %	Silica %	Gold g/t
feed	30,4	29,9	29,4	6,6	18,8	135,0
0,0	29,3	30,2	30,0	7,5	19,5	139,0
3,0	29,3	30,4	30,2	7,0	19,9	138,0
6,0	30,1	31,0	30,9	7,0	19,1	142,0
10,0	29,9	31,1	31,1	6,6	19,8	143,0
13,0	31,8	32,5	32,4	6,5	18,5	149,0
17,0	30,2	32,5	32,6	5,4	19,7	139,0
21,0	30,8	32,4	32,5	5,1	19,6	142,0
26,0	29,9	33,0	32,7	3,5	20,5	135,0
33,0	30,2	31,5	31,5	1,9	22,4	136,0
34,0	28,7	31,4	31,5	1,7	23,9	142,0
38,0	19,7	25,6	22,0	0,8	24,8	119,0
39,0	10,8	20,3	11,5	0,3	22,1	79,7
40,0	9,0	18,2	8,3	0,1	21,4	82,2
43,0	5,9	15,3	4,9	0,1	24,2	83,3
46,0	5,3	14,1	3,3	0,1	24,5	85,0
51,0	4,9	12,5	1,6	0,1	25,7	77,0

TABLE 5.7 Chemical analysis of the -53 +38 micron sample after biooxidation and acid washing.

TIME	ANALYSIS OF SOLID PRODUCT -53 +38 MICRON SAMPLE					
Days	Iron %	Total Sulphur %	Sulphide Sulphur %	Arsenic %	Silica %	Gold g/t
feed	32,3	31,4	31,4	7,8	16,3	163,0
0,0	33,7	34,2	35,0	11,0	15,9	179,0
1,0	35,4	33,4	33,4	10,2	16,9	182,0
4,0	34,1	34,1	33,8	9,3	17,3	186,0
5,0	32,3	33,1	34,7	7,3	16,8	192,0
6,0	33,3	33,4	34,6	6,2	17,5	195,0
7,0	33,8	33,9	34,0	5,8	18,6	203,0
8,0	29,0	34,0	35,3	5,2	18,7	210,0
11,0	26,4	30,5	24,0	3,4	21,1	218,0
12,0	25,8	30,1	22,0	2,2	22,1	221,0
13,0	18,7	24,9	17,9	1,0	21,3	211,0
14,0	11,7	21,3	12,9	0,7	19,3	170,0
15,0	11,8	21,7	10,0	0,5	21,0	166,0
18,0	4,7	15,9	3,9	0,3	19,6	143,0
20,0	3,2	15,3	2,8	0,3	17,1	112,0
22,0	2,9	14,6	0,6	0,2	18,1	106,0

TABLE 5.8 Chemical analysis of the -38 +25 micron sample after biooxidation and acid washing.

TIME	ANALYSIS OF SOLID PRODUCT -38 +25 MICRON SAMPLE					
Days	Iron %	Total Sulphur %	Sulphide Sulphur %	Arsenic %	Silica %	Gold g/t
feed	30,4	30,4	29,0	10,8	14,4	187,0
0,0	28,7	28,4	28,0	11,3	18,3	197,0
1,0	29,6	30,0	29,0	11,3	15,9	195,0
2,0	31,2	30,6	29,0	11,6	15,5	197,0
4,0	29,5	30,9	30,0	10,6	16,6	204,0
6,0	31,2	30,5	30,5	14,2	16,0	230,0
7,0	30,6	30,7	30,7	13,7	15,0	239,0
10,0	33,5	35,5	34,3	8,2	13,7	222,0
11,0	31,6	34,7	33,4	7,4	15,8	229,0
12,0	31,4	35,2	34,8	6,6	16,8	236,0
13,0	25,6	32,0	30,0	5,6	17,2	231,0
14,0	25,9	31,7	29,7	4,5	19,4	240,0
17,0	16,0	27,0	28,8	1,4	22,2	212,0
18,0	11,5	21,8	13,1	0,9	20,0	220,0
19,0	7,8	18,6	8,4	0,5	27,0	239,0
20,0	3,9	15,3	3,5	0,2	19,7	197,0
21,0	2,5	13,2	1,8	0,2	22,8	187,0
24,0	3,4	13,0	0,8	0,3	15,6	135,0
27,0	5,0	14,2	0,3	0,4	18,7	140,0

TABLE 5.9 Chemical analysis of the -25 micron sample after biooxidation and acid washing.

TIME	ANALYSIS OF SOLID PRODUCT -25 MICRON SAMPLE					
Days	Iron %	Total Sulphur %	Sulphide Sulphur %	Arsenic %	Silica %	Gold g/t
feed	21,0	17,3	16,7	5,7	28,8	103,0
0,0	22,7	19,7	19,2	5,3	31,1	113,0
1,0	21,7	21,5	21,0	5,0	31,9	114,0
4,0	22,0	18,8	18,2	2,1	35,9	128,0
5,0	20,2	18,6	18,1	1,3	37,3	141,0
6,0	16,3	16,8	17,3	0,9	39,8	146,0
7,0	13,5	13,8	13,2	0,6	42,8	155,0
8,0	8,3	8,6	5,0	0,2	40,5	136,0
9,0	5,2	8,7	3,6	0,1	40,2	134,0
10,0	2,7	7,5	1,6	0,1	38,7	121,0
11,0	2,0	6,4	0,4	0,0	40,4	124,0
12,0	2,2	7,7	0,5	0,1	37,5	110,0

5.3.1 Selection of Data Points

Owing to errors in sampling and analysis of the oxidised material, not every data point was found to be valid. A criterion was thus used to exclude invalid points prior to parameter estimation. This was done on the basis of mass balances on iron, sulphur and arsenic.

Knowledge of the mass of solids present in each sample was a prerequisite to calculating mass balances. Mass changes during biooxidation occur owing to the dissolution of sulphide minerals and any carbonate materials present, as well as the precipitation of ferric and arsenic salts, jarosite and calcium sulphate from the addition of lime. The mass per unit volume of slurry is thus not consistent. While every effort was made to ensure accurate sampling, it was decided to employ three methods of mass estimation. These included weighing the mass of solids in a known volume of sample as well as the use of either gold or silica as inert tie substances. Masses were calculated with the use of changes in tie substance content of the oxidised product as follows:

$$M_i = M_0 Z_0 / Z_i$$

where

M_0, M_i concentration of solid in the slurry at times t = 0 and *i*

Z_0, Z_i fraction of the tie substance analysed for at these times.

The availability of accurate zero time mass measurements and chemical analyses, as well as the fact that subsequent gold and silica analyses were likely to be more accurate than the true mass determinations, were motivation for the calculation of mass changes in this manner.

The weighed, gold and silica based solid masses were each used as the basis for the determination of mass balance ratios of the elements arsenic, iron and total-sulphur for each sample.

A mass balance ratio using iron, for example, was defined as follows:

$$\text{Mass Balance Ratio} = \frac{\text{Fe in BIOX Liquor} + \text{Fe in HCl Wash Liqour} + \text{Fe in BIOX Residue}}{\text{Fe in Feed}}$$

This ratio could be calculated using the chemical analyses for iron, arsenic and total-sulphur combined with masses based on weight, silica or gold, thus giving nine mass balance checks for each sample. A ratio of one indicated a perfect mass balance and in general an exclusion criterion of values outside 0,9 and 1,1 was adopted. When more than one mass balance ratio satisfied the criterion the average mass was used for further calculations.

This procedure is best illustrated in Figures 5.2 to 5.7 where the ratios for each element based on measured masses, silica and gold, as well as the chosen points are shown for each batch test.

In general the most reliable mass balance ratios were calculated using the total-sulphur analyses. These were more sensitive to discrepancies in the measured and calculated masses as, especially towards the end of the batch tests, more sulphur than iron or arsenic remained in the residue, generally as sulphate precipitates which had not been completely removed through acid washing. All batches followed this trend with the exception of the smallest size fraction for which both the iron and arsenic ratios were more reliable. Where each mass was excluded by the mass balance criterion, no result for extent of removal was calculated.

The difficulty encountered in obtaining accurate measurements of the degree of biooxidation is typically a problem associated with the oxidation of an arsenopyrite/pyrite concentrate where iron, arsenic and sulphate all precipitate. When studying the biooxidation of, for example, copper or zinc sulphide, the copper and zinc appearing in solution is an accurate measure of the degree of oxidation.

In the latter stages of each batch, more so with those running for a longer period of time, the samples gave low values for gold when analysed by the fire assay method. This is shown in Tables 5.4 to 5.9. It was not possible to determine the cause of this, however it may have been owing to accumulation of fine liberated particles of gold at the bottom of the reactor or the production of some material which interfered with the fire assay. No similar phenomenon was mentioned in the literature.

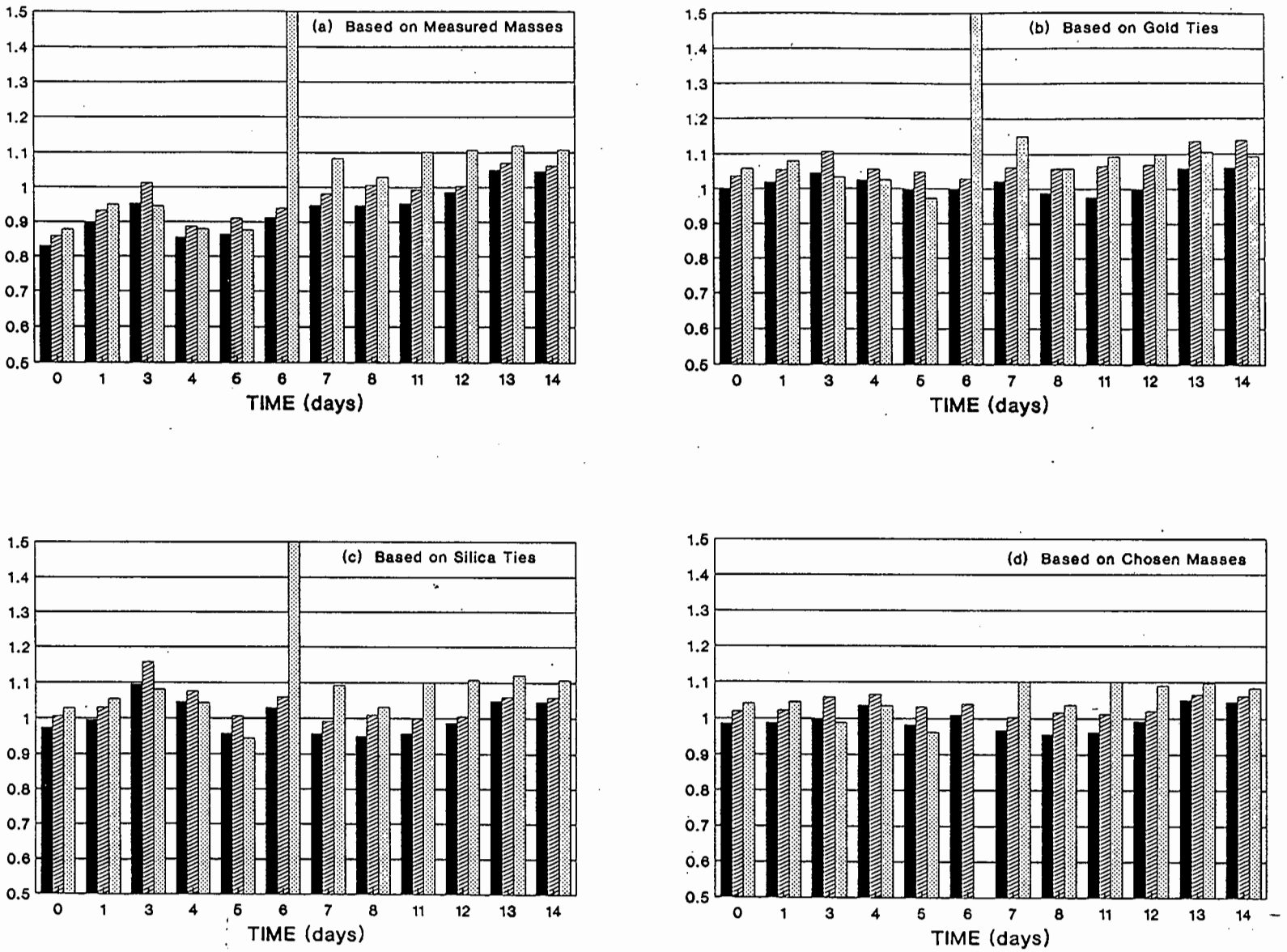

FIGURE 5.2 Mass balance ratios for iron (▬), sulphur (▨) and arsenic (▭) for the bulk concentrate.

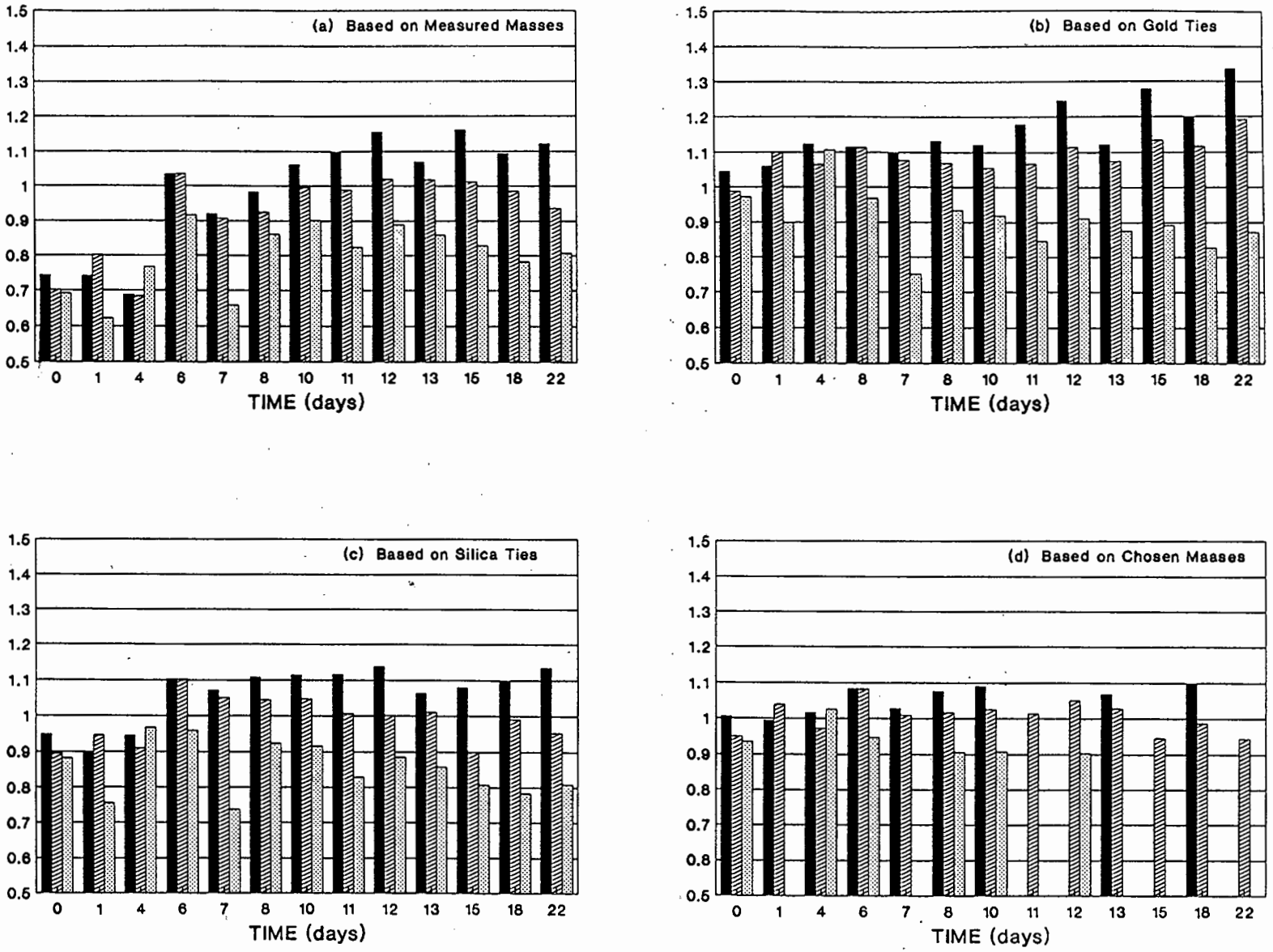

FIGURE 5.3 Mass balance ratios for iron (■), sulphur (▨) and arsenic (▩) for the +75 fraction.

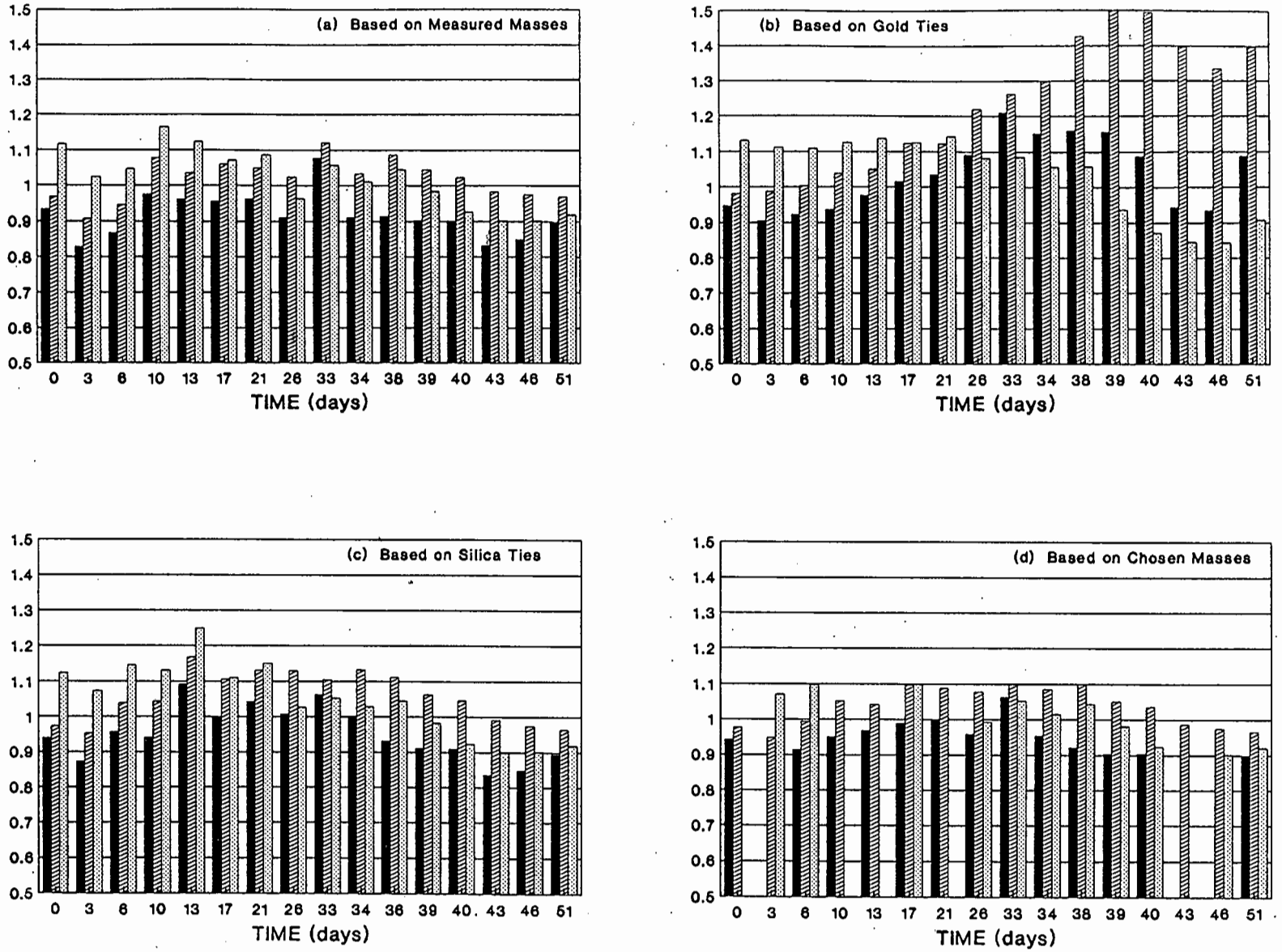

FIGURE 5.4 Mass balance ratios for iron (▬), sulphur (▨) and arsenic (▩) for the -75 +53 fraction.

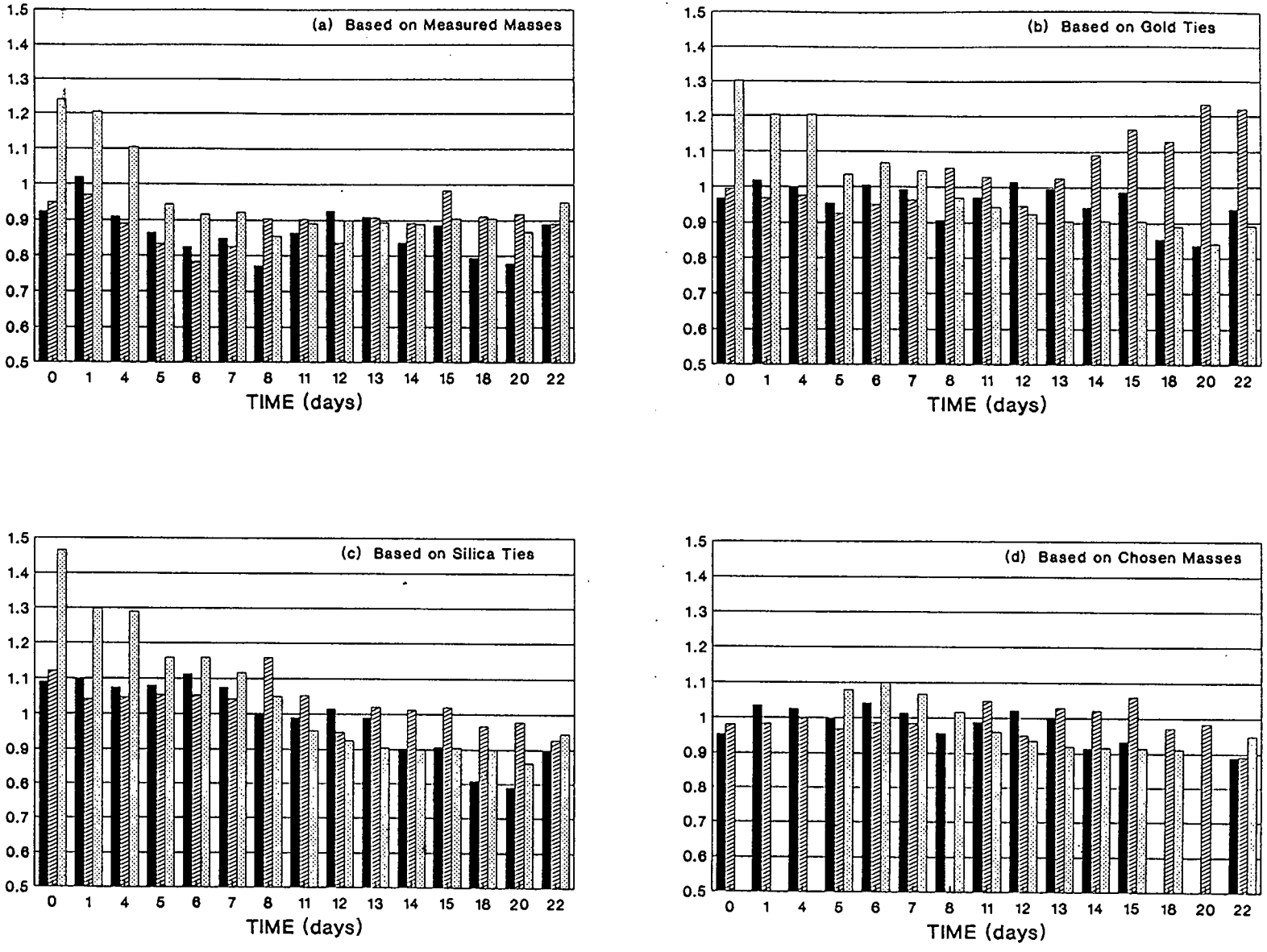

FIGURE 5.5 Mass balance ratios for iron ( ), sulphur (▨) and arsenic (▩) for the -53 +38 fraction.

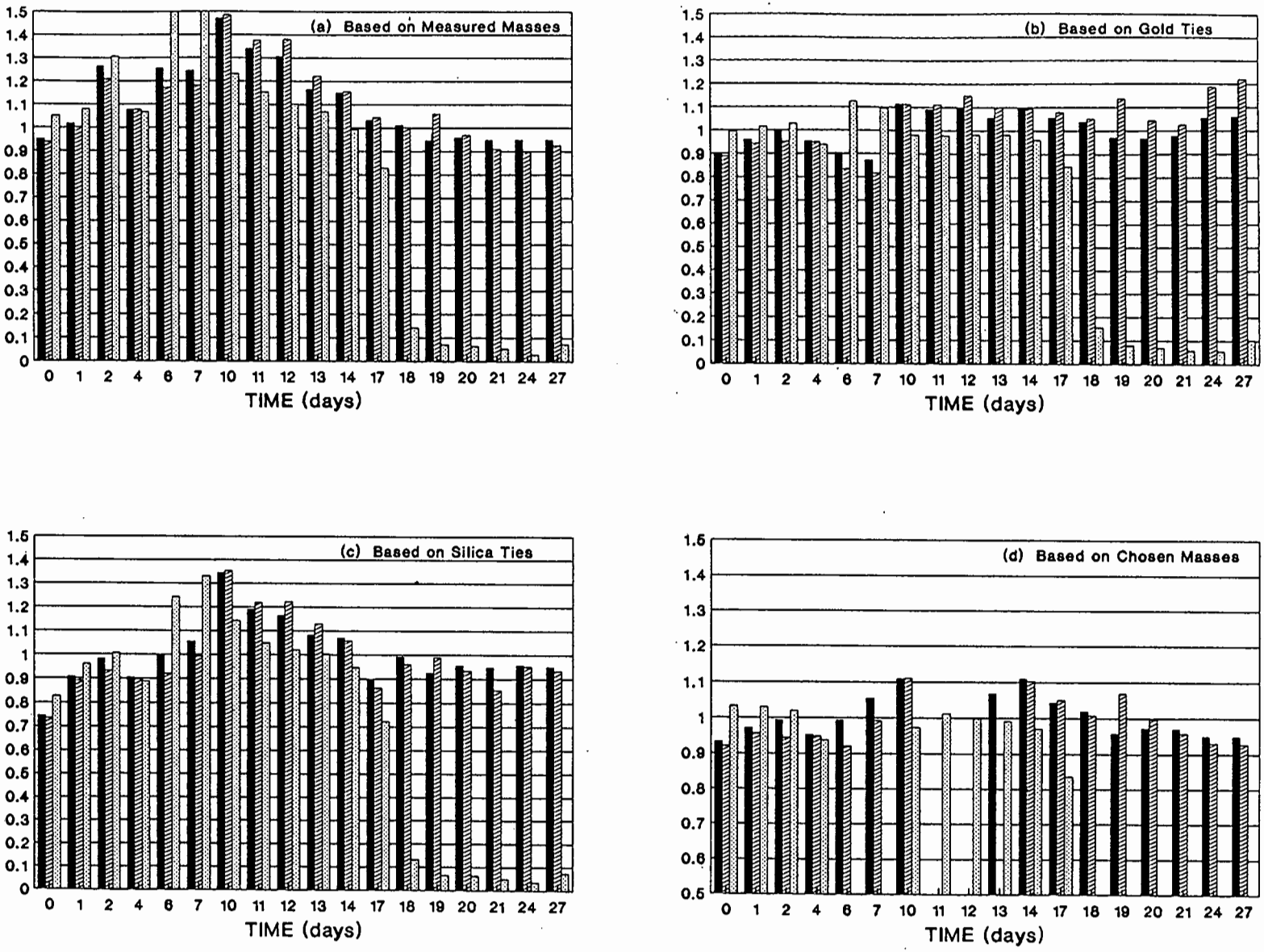

FIGURE 5.6 Mass balance ratios for iron ( ), sulphur (▨) and arsenic (▩) for the -38 +25 fraction.

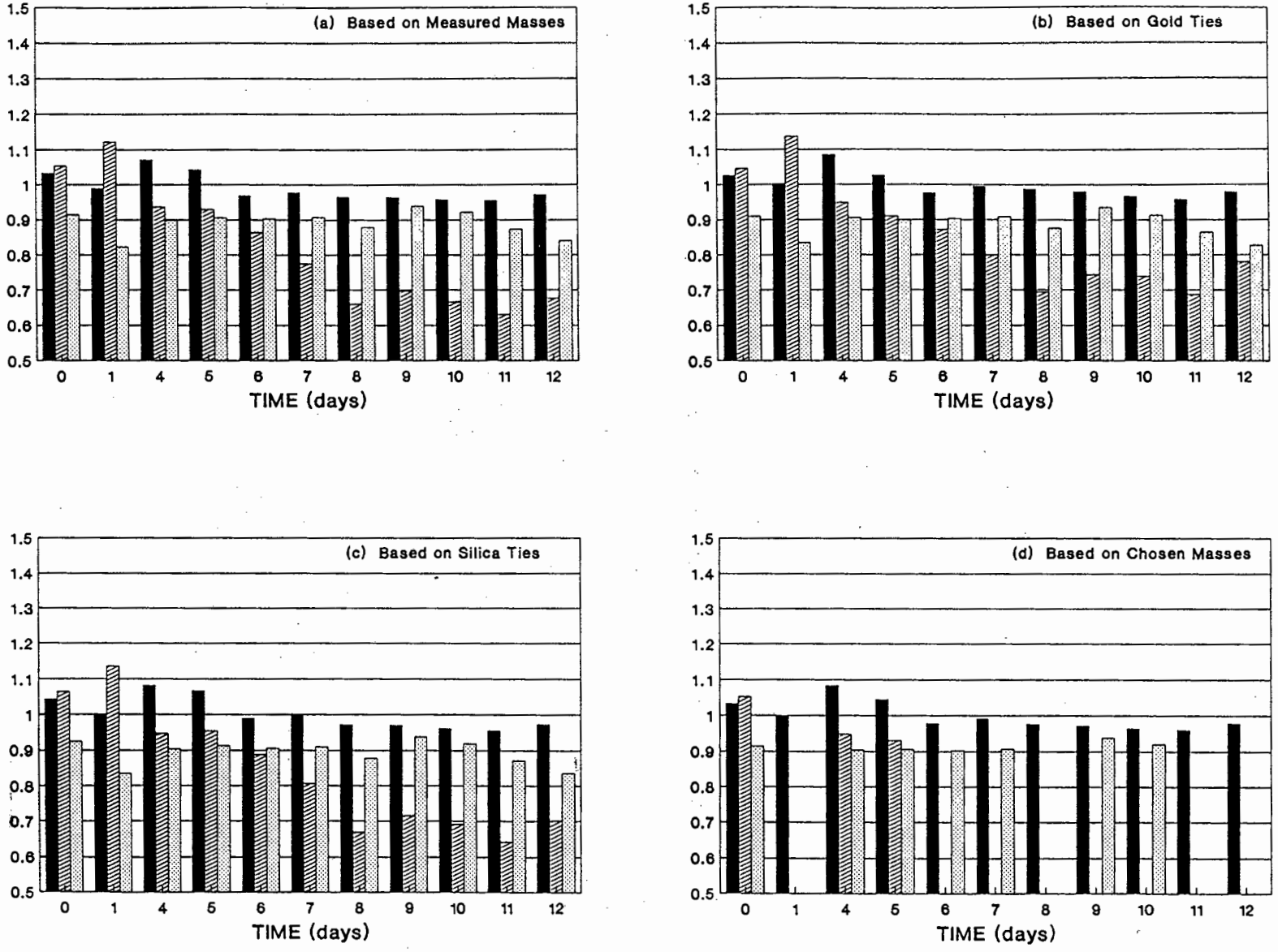

FIGURE 5.7 Mass balance ratios for iron ( ), sulphur (▨) and arsenic (▩) for the -25 fraction.

5.3.2 Time Course Biooxidation Results

The time course removal of sulphide-sulphur, iron and arsenic during each batch biooxidation run are plotted in Figures 5.8 and 5.9, where the solid curves represent the best fit of the logistic equation to the selected data points and the straight line segments represent the best straight line fit to the linear portion of the curve. The data sets are shown in Tables 5.10 to 5.15. Fitting of the logistic equation is discussed in Section 5.3.5.

Fractional removal of any component was calculated as follows:

$$X_i = \frac{C_0 - C_i}{C_0} \qquad 5.2$$

where

X_i	fractional removal of component at time *i*
C_0, C_i	concentrations of component in the slurry at time t = 0 and *i*, and C = MZ (kgm^{-3})
M	concentration of solids in the slurry (kgm^{-3})
Z	fraction of component present in solid

In all cases the results followed the shape of a sigmoidal curve. This corresponded to a pattern of an initial lag phase, a period of maximum growth which was linear, prior to a stationary phase.

All batches displayed lag periods ranging from 4 to 6 days, with the exception of the -75 +53 micron batch. The extended lag occurring was attributed to a delay between running of the +75 and the -75 +53 batch during which the culture may have become less active before being used to inoculate the -75 +53 micron batch. With the exception of this discrepancy no regular pattern seemed to govern the length of the lag phase.

After the lag each batch underwent a period of linear growth as shown by the removal of sulphide-sulphur, iron and arsenic (Figures 5.8 and 5.9). As will be discussed later, this slope was used as a measure of maximum oxidation rate, and in units of d^{-1}, was termed the specific rate of removal. In all cases the rate of oxidation decreased after the linear phase and finally ceased. This appeared to be owing to exhaustion of the sulphide minerals being oxidised.

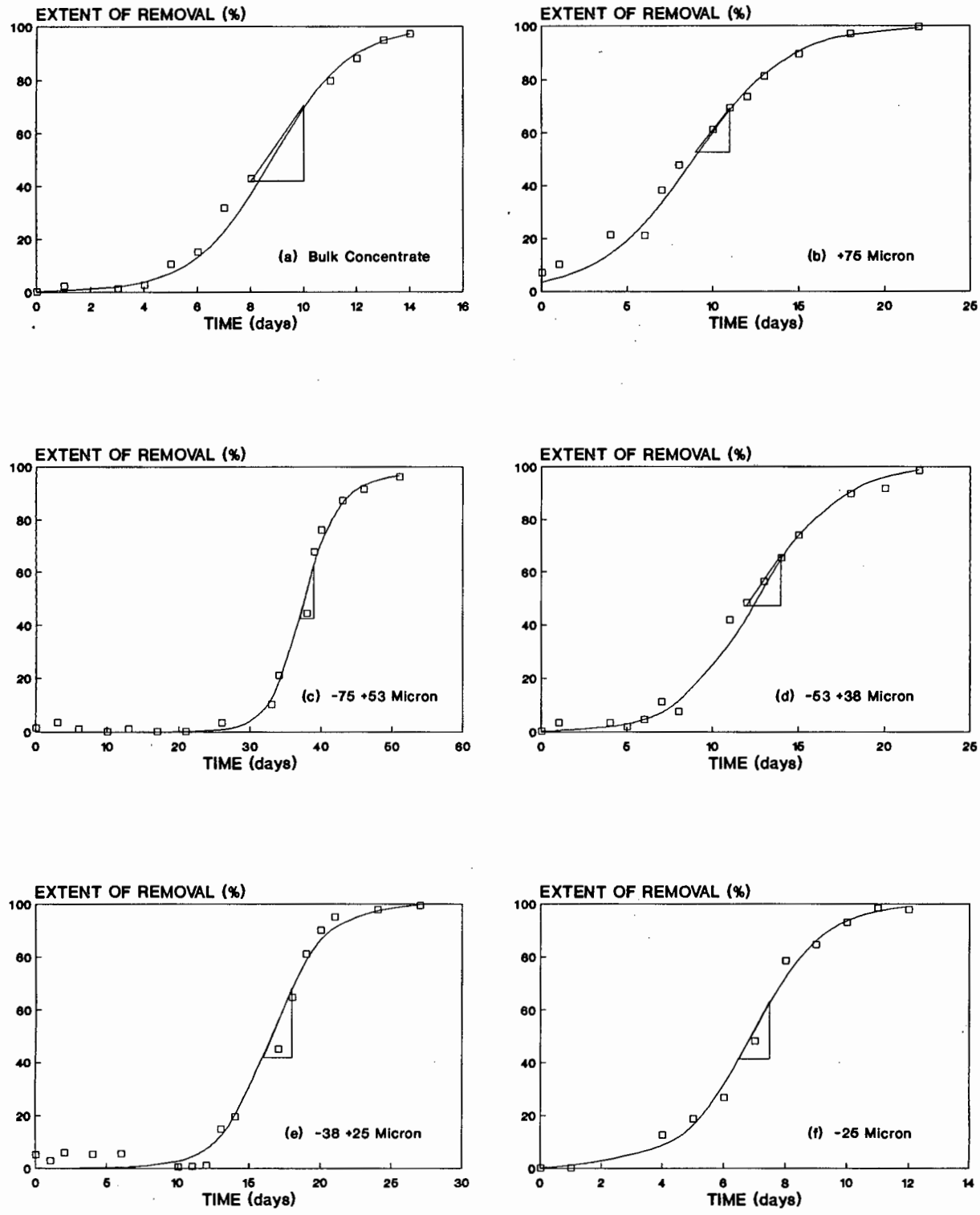

FIGURE 5.8 Time course removal of sulphide-sulphur for each size fraction showing the slope of the linear portion of the experimentally determined curve. Chosen points (□), fit of the logistic equation (——).

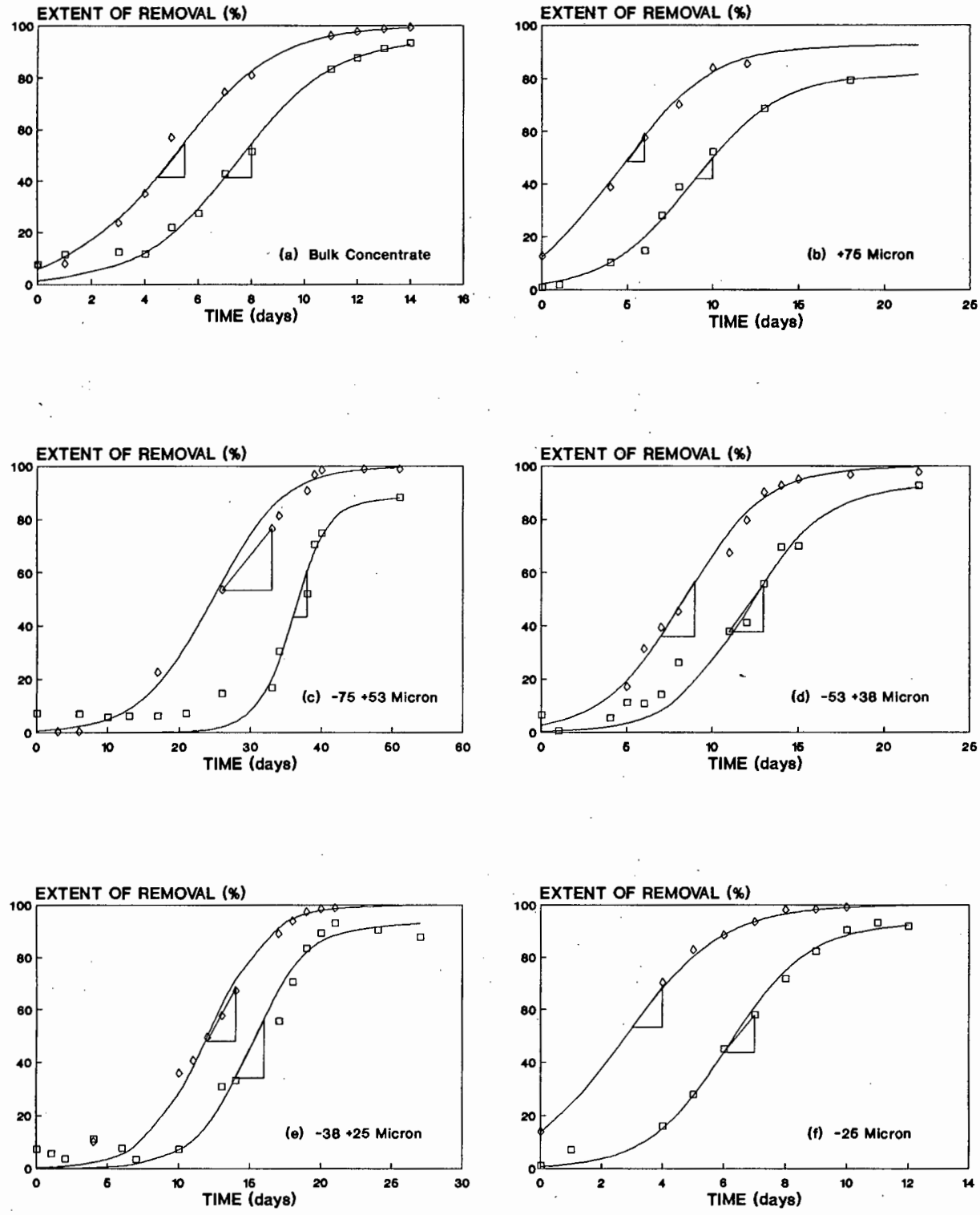

FIGURE 5.9 Time course removal of iron and arsenic for each size fraction showing the slopes of the linear portions of the experimentally determined curves. Chosen points: iron (□), arsenic (◇), fit of the logistic equation (——).

TABLE 5.10 Final masses, extents of removal of iron, arsenic and sulphide-sulphur, and gold dissolutions for the bulk sample after bio-oxidation and acid washing.

TIME	FINAL MASSES, EXTENTS OF REMOVAL AND GOLD DISSOLUTIONS BULK SAMPLE				
	Final Mass	Extents of Removal			Gold Dissolution
		Iron	Sulphide Sulphur	Arsenic	
Days	g	%	%	%	%
feed	120,7	8,8	-2,0	-5,7	34,8
0,0	113,4	7,5	-2,3	7,3	41,5
1,0	110,7	11,2	2,2	7,9	39,9
3,0	108,2	12,2	1,2	23,5	46,9
4,0	111,8	11,5	2,5	35,0	54,8
5,0	104,1	21,8	10,3	56,7	66,3
6,0	104,0	27,1	14,9	65,4	74,1
7,0	92,6	42,6	31,7	74,3	82,2
8,0	98,4	51,3	42,7	80,9	87,1
11,0	92,7	83,1	79,6	96,0	94,8
12,0	93,6	87,4	88,0	97,7	96,7
13,0	94,7	91,1	94,7	98,6	96,9
14,0	89,1	93,1	97,0	99,3	97,6

TABLE 5.11 Final masses, extents of removal of iron, arsenic and sulphide-sulphur, and gold dissolutions for the +75 micron sample after biooxidation and acid washing.

TIME	FINAL MASSES, EXTENTS OF REMOVAL AND GOLD DISSOLUTIONS +75 MICRON SAMPLE				
	Final Mass	Extents of Removal			Gold Dissolution
		Iron	Sulphide Sulphur	Arsenic	
Days	g	%	%	%	%
feed	120,7	-0,8	2,5	1,8	35,7
0,0	119,7	0,8	7,0	12,5	39,3
1,0	119,2	1,6	10,1	19,4	36,9
4,0	113,3	10,0	21,1	38,6	57,2
6,0	108,5	14,6	21,0	57,5	74,1
7,0	97,0	27,7	38,1	65,3	80,3
8,0	94,2	38,7	47,6	70,0	82,8
10,0	86,6	52,0	61,0	83,9	88,9
11,0	84,8	59,6	69,3	86,3	86,0
12,0	99,0	60,4	73,4	85,4	91,4
13,0	92,6	68,4	81,8	86,4	96,6
15,0	97,0	77,4	89,3	90,0	96,6
18,0	95,1	79,2	96,9	90,2	97,6
22,0	100,8	81,8	99,3	92,6	96,5

TABLE 5.12 Final masses, extents of removal of iron, arsenic and sulphide-sulphur, and gold dissolutions for the -75 +53 micron sample after biooxidation and acid washing.

TIME	FINAL MASSES, EXTENTS OF REMOVAL AND GOLD DISSOLUTIONS -75 +53 MICRON SAMPLE				
	Final Mass	Extents of Removal			Gold Dissolution
		Iron	Sulphide Sulphur	Arsenic	
Days	g	%	%	%	%
feed	120,7	2,3	-3,1	-9,5	30,8
0,0	116,6	6,9	1,4	-10,2	32,1
3,0	113,6	9,3	3,3	0,2	37,8
6,0	113,7	6,7	1,0	0,1	34,4
10,0	115,7	5,7	-1,4	4,0	38,8
13,0	108,6	5,9	0,9	10,9	41,7
17,0	114,2	6,0	-4,9	22,6	48,2
21,0	110,9	6,9	-1,6	29,0	53,8
26,0	104,9	14,5	3,3	53,4	60,3
33,0	101,3	16,6	10,1	76,3	76,7
34,0	89,1	30,3	20,9	81,3	81,9
38,0	89,7	51,8	44,4	90,7	91,0
39,0	100,4	70,5	67,5	96,9	95,8
40,0	103,6	74,6	75,8	98,3	95,4
43,0	92,7	85,1	87,2	98,8	97,7
46,0	92,5	86,6	91,4	98,7	98,1
51,0	89,0	88,1	96,0	98,8	98,1

TABLE 5.13 Final masses, extents of removal of iron, arsenic and sulphide-sulphur, and gold dissolutions for the -53 +38 micron sample after biooxidation and acid washing.

TIME	FINAL MASSES, EXTENTS OF REMOVAL AND GOLD DISSOLUTIONS -53 +38 MICRON SAMPLE				
	Final Mass	Extents of Removal			Gold Dissolution
		Iron	Sulphide Sulphur	Arsenic	
Days	g	%	%	%	%
feed	120,7	18,4	8,4	1,7	-
0,0	108,2	6,5	0,1	-25,9	29,1
1,0	109,8	0,3	3,2	-18,5	31,0
4,0	108,4	5,2	3,3	-6,8	38,6
5,0	107,3	11,1	1,7	17,1	53,7
6,0	104,7	10,6	4,4	31,3	63,9
7,0	99,1	14,1	11,1	39,2	67,8
8,0	99,4	26,0	7,4	45,3	73,7
11,0	92,0	37,7	41,7	67,3	89,2
12,0	89,1	41,0	48,3	79,4	92,8
13,0	92,7	55,5	56,2	90,0	94,7
14,0	102,2	69,3	65,2	92,7	96,6
15,0	100,0	69,7	73,6	94,8	97,4
18,0	100,3	87,9	89,6	96,6	98,4
20,0	114,8	90,6	91,6	96,7	97,5
22,0	99,1	92,6	98,5	97,6	98,5

TABLE 5.14 Final masses, extents of removal of iron, arsenic and sulphide-sulphur, and gold dissolutions for the -38 +25 micron sample after biooxidation and acid washing.

TIME	FINAL MASSES, EXTENTS OF REMOVAL AND GOLD DISSOLUTIONS -38 +25 MICRON SAMPLE				
	Final Mass	Extents of Removal			Gold Dissolution
	Mass	Iron	Sulphide Sulphur	Arsenic	
Days	g	%	%	%	%
feed	120,7	2,7	-0,4	-11,4	29,6
0,0	118,8	7,1	5,0	-3,0	35,0
1,0	117,4	5,3	2,8	-1,7	32,6
2,0	113,6	3,4	5,9	-1,1	28,9
4,0	110,6	11,0	5,2	10,0	38,3
6,0	108,6	7,6	5,3	-18,3	35,4
7,0	115,9	3,4	-1,6	-21,8	36,3
10,0	101,7	7,2	0,4	35,8	60,7
11,0	104,3	10,2	0,5	40,6	65,1
12,0	99,5	14,8	1,0	49,4	74,8
13,0	99,4	30,7	14,8	57,6	80,9
14,0	94,9	33,0	19,5	67,1	85,5
17,0	102,3	55,4	45,1	88,9	93,7
18,0	94,6	70,4	64,6	93,8	94,6
19,0	79,2	83,2	81,0	97,1	95,7
20,0	102,3	89,1	89,8	98,4	98,3
21,0	102,5	93,0	94,9	98,8	97,8
24,0	106,4	90,1	97,6	98,0	99,0
27,0	91,8	87,5	99,3	96,9	98,9

TABLE 5.15 Final masses, extents of removal of iron, arsenic and sulphide-sulphur, and gold dissolutions for the -25 micron sample after biooxidation and acid washing.

TIME	FINAL MASSES, EXTENTS OF REMOVAL AND GOLD DISSOLUTIONS -25 MICRON SAMPLE				
	Final Mass	Extents of Removal			Gold Dissolution
		Iron	Sulphide Sulphur	Arsenic	
Days	g	%	%	%	%
feed	120,7	9,3	0,3	20,2	33,6
0,0	110,6	0,9	-5,4	14,0	46,6
1,0	108,6	7,1	-13,1	20,4	48,4
4,0	97,0	15,8	12,4	70,1	77,7
5,0	90,6	27,8	18,7	82,7	88,5
6,0	85,6	45,0	26,6	88,2	90,5
7,0	79,3	57,8	48,1	93,3	95,0
8,0	87,0	71,5	78,4	98,0	96,7
9,0	87,2	82,1	84,4	98,2	97,4
10,0	91,9	90,2	92,7	98,9	97,9
11,0	89,6	92,9	98,3	99,5	98,1
12,0	97,2	91,6	97,6	99,3	98,0

The time course oxidation of arsenic revealed that in each case arsenic dissolution preceded both iron and sulphide dissolution and reached completion typically two to three days prior to complete oxidation of the iron and sulphide. These results are consistent with those of Pinches (1972), Bruynesteyn *et al.* (1986), Karavaiko *et al.* (1985) and Marchant (1985) who also found that arsenic oxidation preceded iron oxidation. Several of these investigators have interpreted these results as indicating a faster rate of arsenopyrite removal. However, as this study will show, the rates were not faster, and on examination of the literature it is possible that preferential removal of arsenic was mistakenly interpreted as faster removal. An exception has been reported by Pinches (1972) when studying the biooxidation of the narrowly sized fractions of a pyrite/arsenopyrite concentrate all passing 53 micron. Tests were conducted at a very low pulp density, viz 1,5% and results for the removal of iron appeared to exhibit two rates. The initial rate was shown to correspond to arsenopyrite and pyrite removal, while the second rate only to pyrite removal. Results shown for the 26,3 to 36,9 micron fraction and the 3,3 to 7,4 micron fraction showed higher volumetric rates of oxidation for arsenic than for iron. This was only shown to occur during biooxidation at the very low pulp densities. Results reported for tests carried out at higher pulp densities did not display this double rate. It is thus possible that this differentiation is discernible only at very low pulp densities.

5.3.3 Linear Biooxidation Rates

The specific rates of removal of iron, arsenic and sulphide-sulphur were obtained from the slopes of the linear regions of the curves of fractional removal of these elements. In order to determine the rates of pyrite and arsenopyrite oxidation for comparative purposes it was necessary to make the following assumptions.

(i) All arsenic was present as arsenopyrite; the rates of arsenic and arsenopyrite oxidation on a molar basis were thus equal.

(ii) The remaining sulphur was present as pyrite, the molar rate of pyrite removal was thus equal to:
(Rate of sulphide-sulphur removal - rate of arsenic removal)/2.

The amount of iron not accounted for could be calculated, and was slightly in excess in each case. This may have been owing to association of some arsenic with the pyrite (Swash, 1988), indicating that these assumptions were not entirely correct.

Alternatively, oxidation of the sulphide minerals may have begun, in which case a proportion of the iron may have been associated with iron oxides and not sulphides.

The measured specific rates of removal of iron, arsenic and sulphide-sulphur as well as the calculated rates for arsenopyrite and pyrite removal are shown along with the feed concentrations of pyrite and arsenopyrite in Table 5.16.

Calculation of absolute rates of iron, arsenic, sulphide-sulphur and pyrite removal (mol m^{-3} d^{-1}) were possible from the specific rates as follows.

Absolute rate = Specific rate * molar concentration in feed

TABLE 5.16 Feed concentrations of arsenopyrite and pyrite, and their specific rates of removal.

SAMPLE	FEED CONTENT		SPECIFIC RATES OF REMOVAL			
	Arseno-pyrite %	Pyrite %	Arseno-pyrite d^{-1}	Pyrite d^{-1}	Iron d^{-1}	Sulphide Sulphur d^{-1}
Bulk	13,04	37,48	0,1312	0,1442	0,1339	0,1428
+75	7,35	45,19	0,0942	0,0817	0,0813	0,0825
−75 +53	14,34	49,72	0,0336	0,1087	0,0876	0,1015
−53 +38	17,02	52,48	0,1034	0,0948	0,0893	0,0957
−38 +25	23,47	45,61	0,1000	0,1362	0,1092	0,1305
−25	12,28	26,72	0,1538	0,2268	0,1411	0,2163

The molar concentrations of arsenopyrite and pyrite were calculated using the same assumptions as (i) and (ii) mentioned previously, thus allowing calculation of the absolute rates. The absolute rates of removal are shown in Table 5.17

The specific rates of removal as shown in Table 5.16, while indicating that in general the removal of arsenopyrite and pyrite were similar, also showed a trend towards an increase in rate with increase in surface area. This was the case for both the

removal of pyrite and arsenopyrite though the relationship between the specific rate of arsenopyrite removal and surface area seemed more linear than for pyrite removal.

As shown in Table 5.17, the absolute rates of removal of arsenopyrite were lower than those for pyrite for each batch. The rates for the +75 and -75 +53 fraction were both low, increasing to 12,7 - 17,4 mol m^{-3} d^{-1} for the other 4 batches. The low rate obtained for the -75 +53 batch was possibly owing to the long lag phase exhibited by this batch as mentioned in the previous section. These rates, excluding that for the -75 micron batch did not seem to show any trend with surface area concentration except for a general increase and then levelling off or even dropping.

TABLE 5.17 Absolute rates of removal of iron, arsenic, sulphide-sulphur and pyrite and asenopyrite.

SAMPLE	ABSOLUTE RATE OF REMOVAL (mol m^{-3} d^{-1})				
	Iron	Arsenic	Sulphide Sulphur	Pyrite	Arsenopyrite
Bulk	71,2	12,7	121,5	54,4	12,7
+75	41,2	5,1	79,5	37,2	5,1
-75 +53	57,6	3,6	112,3	54,4	3,6
-53 +38	62,3	13,1	113,2	50,1	13,1
-38 +25	71,8	17,4	142,5	62,5	17,4
-25	64,0	14,0	136,0	61,0	14,0

The relationship between the specific and absolute rates and the total surface area concentration are shown in Figure 5.10. A possible explanation for this increase and then levelling off of the absolute removal rates may be that at low surface areas the removal is very dependant on the surface area available. As it increases other factors become limiting. The trend for specific rates with surface area do seem to be linear. The implication of this is the existence of constant fractional removal rate per available surface area, rather than one expressed as kg $m^{-2}d^{-1}$

The differences of mineral composition of each size fraction was brought to attention earlier in the Chapter. So as to ascertain the effect of the varying grade of sulphide on the rates of mineral removal, the relationship between the rates of removal of and surface areas of either pyrite or arsenopyrite were also considered. These are shown in Figures 5.11 and 5.12 and it is quite evident that the relationship between the specific rates of removal of arsenopyrite and the arsenopyrite surface area is linear. The relationship between the specific rates of pyrite removal and pyrite surface area is also possibly linear, but would need to be confirmed. The relationship between the specific rate of iron removal and pyrite surface area also seems linear.

For low surface area concentrations of both pyrite and arsenopyrite there was a strong dependence of the absolute rate constants for arsenic, iron, sulphide-sulphur and pyrite on surface area; however at increased surface areas the dependence was not as strong. This can be seen from Figures 5.11 and 5.12. A possible explanation may be owing to an observation made by Swash (1988) that the sulphide minerals break down more readily than the gangue minerals during milling. Further milling did thus not produce a larger surface area of sulphides but further increased the surface area of the gangue minerals.

Approximate surface area oxidation rates for the linear portions of these curves were 1,81 g m^{-2} d^{-1} for arsenopyrite removal with respect to arsenopyrite surface area and 2,23 g m^{-2} d^{-1} for pyrite, 1,31 g m^{-2} d^{-1} for sulphide-sulphur and 1,18 g m^{-2} d^{-1} for iron removal with respect to pyrite surface area. These results are comparable to the value of 1,52 g m^{-2} d^{-1} for the removal of pyrite (Chapman, 1989).

The dependence of the absolute rates of arsenic removal on arsenopyrite surface area concentrations are in agreement with the findings of Pinches (1972). However, this is not true for oxidation of the iron component of the pyrite which was found by Pinches (1972) to have a linear dependence on pyrite surface area. A comparison of results obtained in this study and those obtained by Pinches (1972) are shown in Figure 5.13. As mentioned, the trend for arsenic removal is similar, while results for iron removal from pyrite differ by a factor of ten. This discrepancy could not be explained.

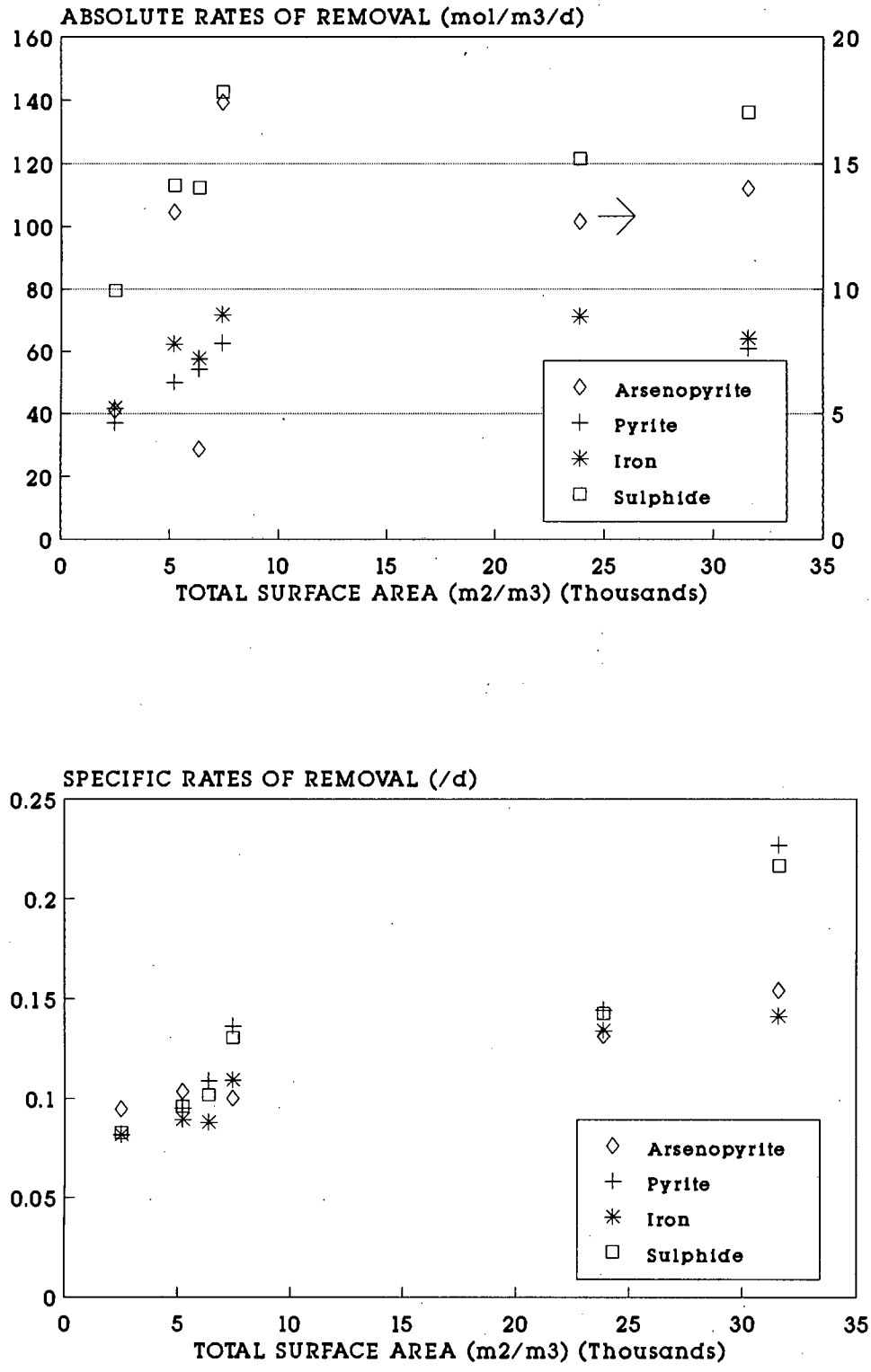

FIGURE 5.10 Relationship between specific and absolute rates of removal and total surface area.

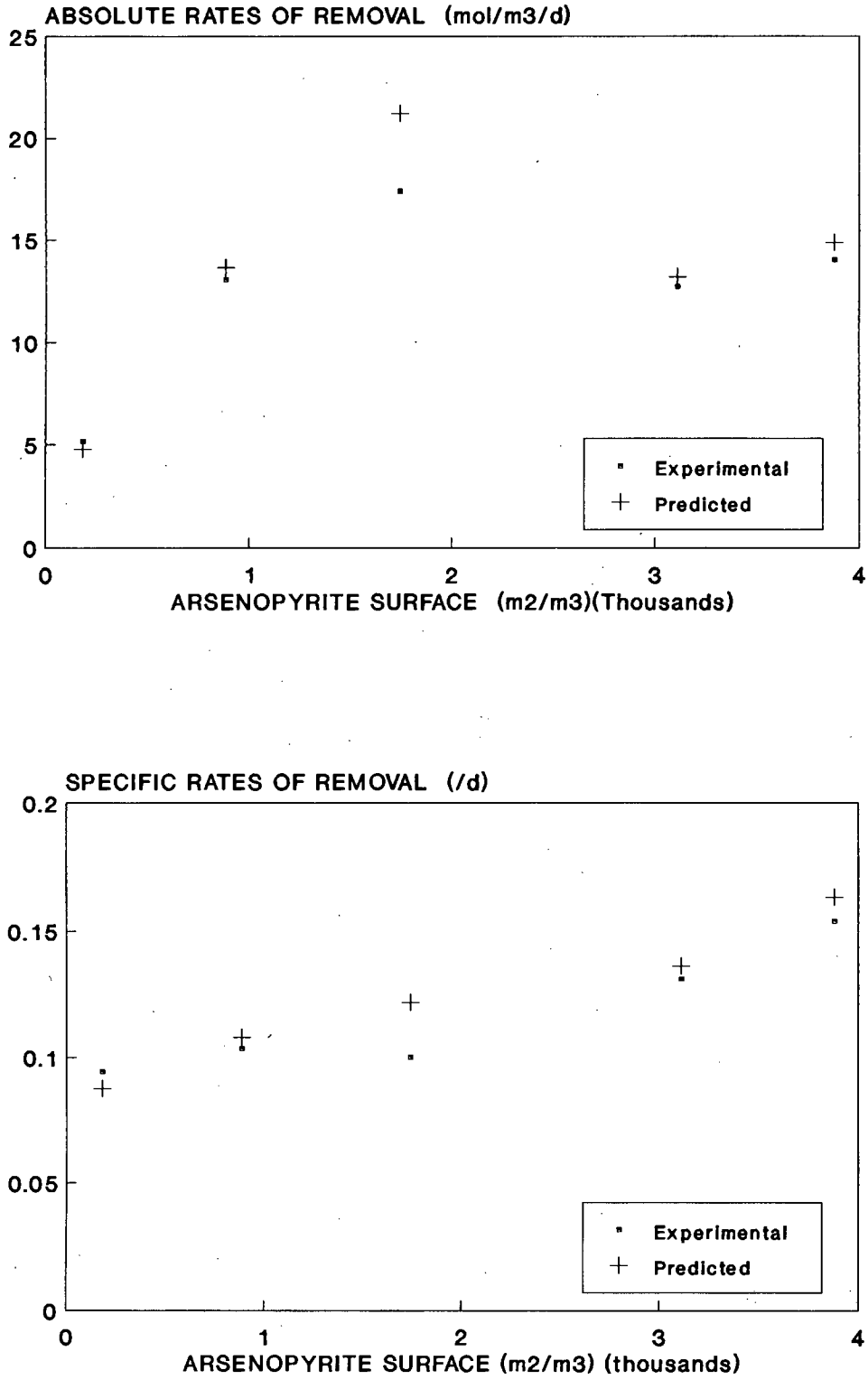

FIGURE 5.11 Relationship between the specific and absolute rates of removal of arsenopyrite and arsenopyrite surface area.

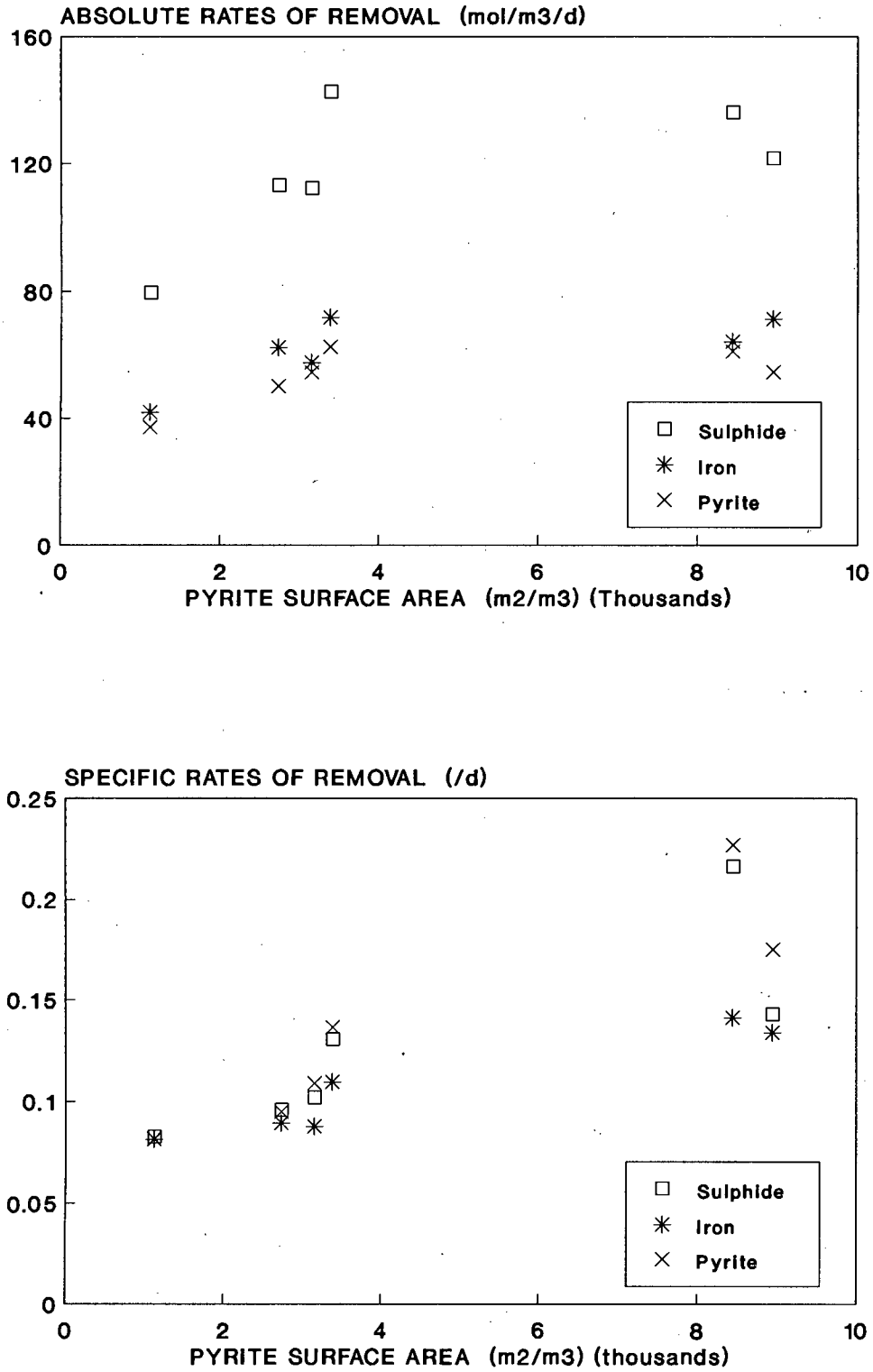

FIGURE 5.12 Relationship between the specific and absolute rates of removal of iron, sulphide-sulphur and pyrite and pyrite surface area.

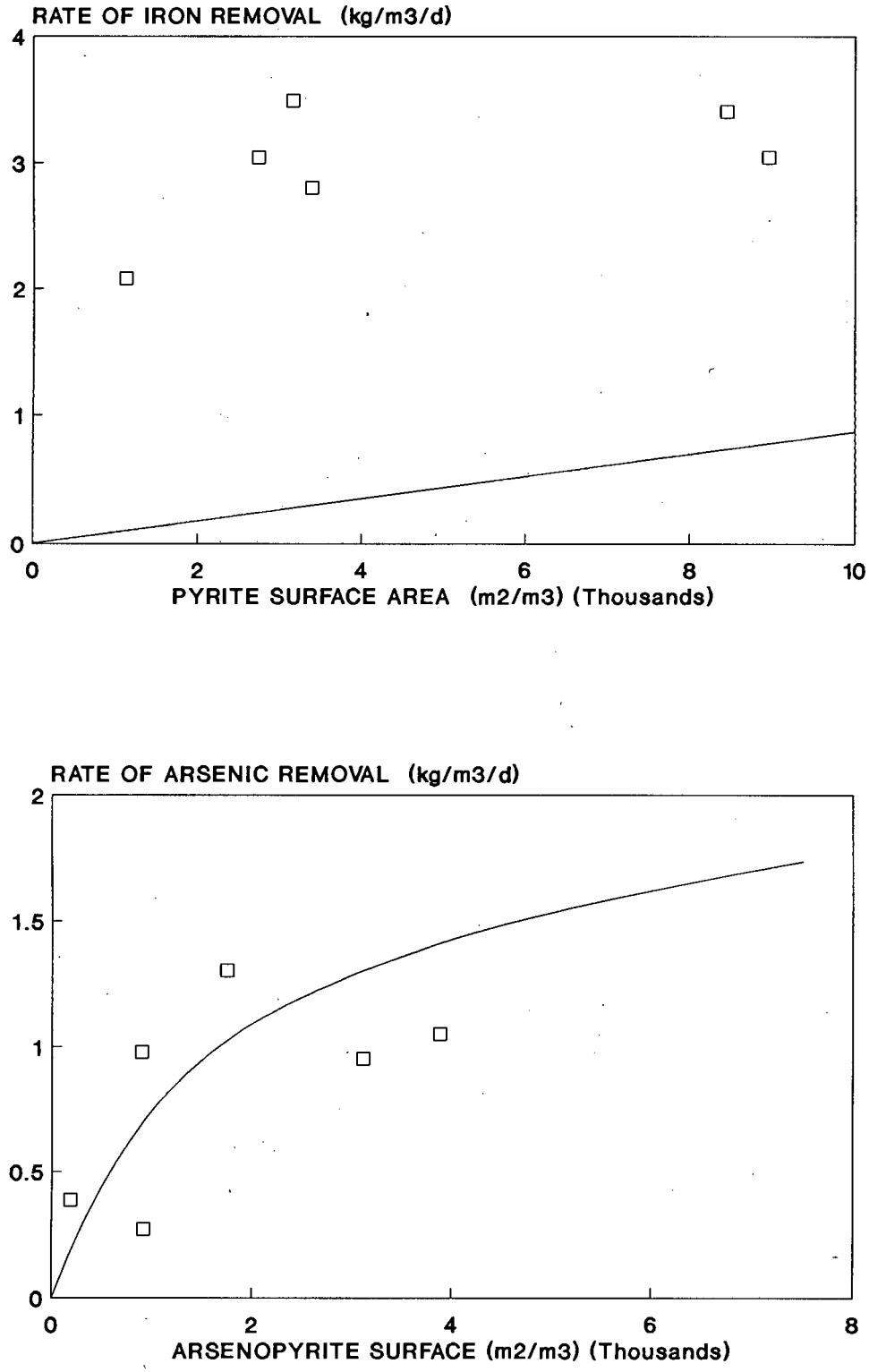

FIGURE 5.13 Relationship between the removal rate of iron from pyrite and pyrite surface area and arsenic removal and arsenopyrite surface area, compared to literature values (——) (Pinches, 1972).

5.3.4 Gold Liberation

As biooxidation has been considered as an alternative method of gold liberation from sulphide minerals, this study was initiated in order to determine the relationship between the extent of pyrite and arsenopyrite removal and the extent of gold liberation. Gold dissolutions were determined by cyanidation and subsequent fire assay of the tails. Time course gold dissolution results for each batch are shown in Tables 5.10 - 5.15 and Figure 5.14. The relationships between gold dissolution and both arsenic and sulphide removal are shown in Figure 5.15.

The time course data indicated that gold and arsenic removal preceded that of iron and sulphide-sulphur. Representing this slightly differently, (Figure 5.15) a direct relationship between gold dissolution and arsenic removal was evident, whereas the curve of gold dissolution versus sulphide breakdown indicated that there was selective biooxidation of those regions of the sulphide lattice rich in gold.

The relationship between gold liberation and sulphide removal, as shown in Figure 5.15, indicated a rapid increase in gold dissolution with minimal sulphide breakdown. Subsequent to this any further improvement required a far greater removal of the sulphide.

This was true for all batches with the exception of the +75 micron batch where, owing to the coarseness of the particles, removal of a greater amount of sulphide material was required in order to liberate the gold. In spite of this, up to 97% gold dissolution was achieved by the end of the run indicating the ability of bacterial action to liberate the gold particles given sufficient time.

The linear dependence of gold liberation on arsenic removal is consistent with the observations of Swash (1988). Furthermore the liberation of gold from the pyrite may be explained by the disruption of the pyrite crystal lattice owing to the inclusion of the larger gold atoms and hence selective oxidation in these areas.

This direct association between gold recovery and arsenic removal provides a valuable plant process control parameter for assessing biooxidation efficiency of this concentrate. The degree of arsenic removal can be used to predict the extent of gold liberation. When determining extent of arsenic removal it is necessary to determine total arsenic removed from the original crystal lattice, that is, all arsenic not remaining as arsenoprite. This includes arsenic in solution as well as any having reprecipitated as ferric arsenate.

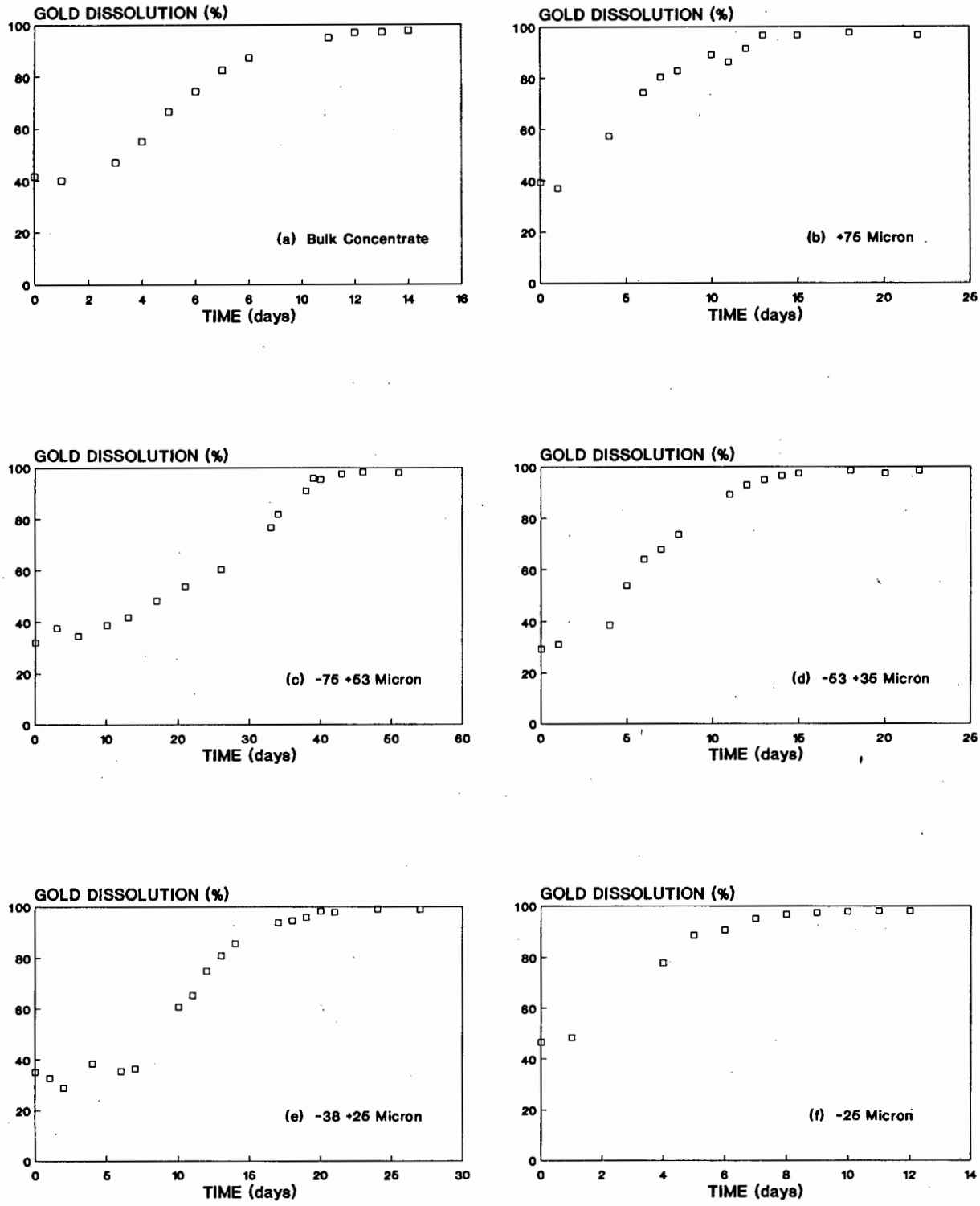

FIGURE 5.14 Time course gold dissolution for the batch biooxidation of each size fraction.

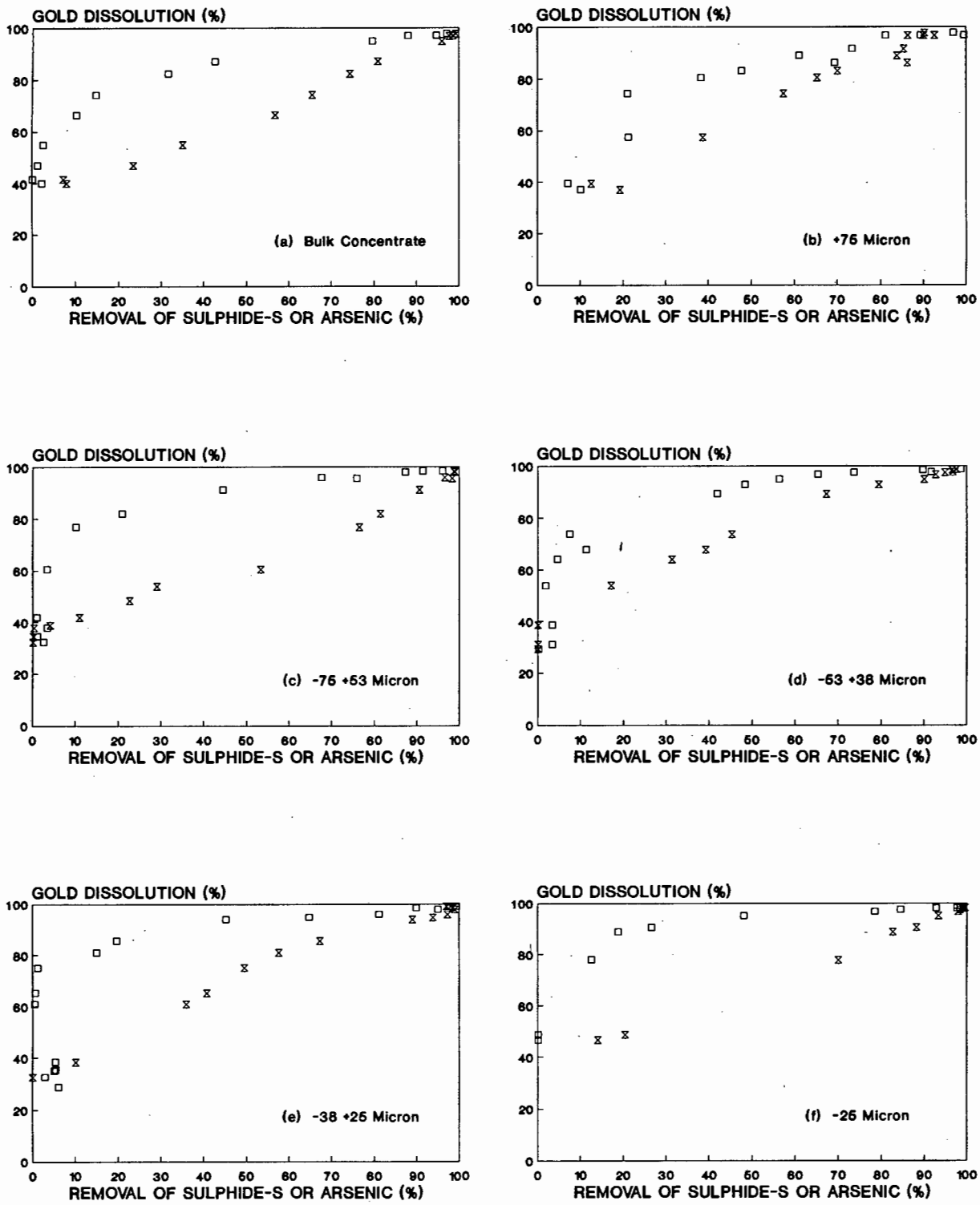

FIGURE 5.15 The relationship between gold dissolution and sulphide-sulphur or arsenic removal; sulphide-sulphur (□), arsenic (⧖).

5.3.5 Use of the Logistic Equation to Describe Batch Biooxidation Data

The logistic equation, which has traditionally been used to describe bacterial growth, has been shown to readily describe the biooxidation process and to include a rate parameter useful in predicting biooxidation reactor performance (Pinches *et al.*, 1987). Analysis of the effect of particle surface area on the rate of biooxidation was an important aspect of this project and was facilitated by the use of a model which included parameters specifically of use for design and scale-up purposes which indicated any effects owing to the variation of surface area.

The logistic equation was fitted to points selected from the complete data set, where selection was based on the consistency of mass balances. In addition, several points during the lag and latter stages of the batches were eliminated. The rationale behind this was firstly, not to be limited by the inherent symmetry of the logistic model and secondly, as the primary objective was to characterise the concentrate for continuous treatment, the linear portion of the curve, the period of maximum rate of biooxidation, was most important. Therefore, as the lag and stationary phase are not critical during continuous operation the logistic equation was used to describe the linear portion of the biooxidation curve accurately and not forced to fit the lag and latter stages.

The solids curves on Figures 5.8 (sulphide) and 5.9 (iron and arsenic) show the progress of removal of sulphide-sulphur, arsenic and iron as described by logistic kinetics.

As shown in the Figures, the curves predicted using this model described the experimental data accurately, with the exception of results which did not follow a symmetrical curve as with the iron removal in the -75 +53 micron sample or the arsenic in the -25 micron sample. It is also evident that in some cases the predicted curve did not follow the experimental points at the beginning of the biooxidation period.

The logistic model parameters X_0 and k, obtained from the best linear least squares fit of each set of experimental data, are shown in Table 5.18, along with the values of r^2, which with a few exceptions, were all above 98, indicating an acceptible fit of the logistic equation to the data. In general for sulphide-sulphur and arsenic removal, the value of X_m, the maximum possible removal was taken as 100%. As can be seen from Figures 5.8 and 5.9 this was generally a valid assumption. Where necessary slightly lower values were used, as was the case with iron removal, where

partial removal was more likely owing to incomplete removal of iron during acid washing than during biooxidation. Alternatively a curve fitting routine could have been used to solve for all three unknown parameters.

The maximum rate of removal could be calculated from the logistic rate constant k as shown by Equation 3.9. Table 5.19 shows the rates predicted by the logistic equation and those determined experimentally. The experimental rates were obtained from the linear portion of the time course curves as described previously. Correlation between the experimental and predicted rates demonstrate the usefulness of the logistic model.

Biooxidation rates for the bulk concentrate at 11,1% pulp density (w/v) the size of which was 64% passing 53 micron were:

Iron	3,98	kg m^{-3} d^{-1}
Arsenic	0,95	kg m^{-3} d^{-1}
Sulphide S	3,89	kg m^{-3} d^{-1}
Pyrite	6,53	kg m^{-3} d^{-1}

Pinches (1972) obtained rates of 4,39 kg $m^{-3}d^{-1}$ and 1,65 kg $m^{-3}d^{-1}$ for iron and arsenic respectively at a similar pulp density and material 100% passing 53 micron. The higher surface area concentration available may account for the higher rates. For a low arsenic containing pyrite concentrate Pinches *et al.* (1987) obtained a pyrite removal rate of 7,60 kg $m^{-3}d^{-1}$. This material, containing 54,5% pyrite and trace amounts of arsenopyrite, was very fine at 80% passing 38 micron. A pulp density of approximately 15% must have been used. This pyrite removal rate implied an iron removal rate of 3,54 kg $m^{-3}d^{-1}$ which is comparable to the 3,98 kg $m^{-3}d^{-1}$ obtained in this study.

Rates of 1,39; 1,42 and 1,70 kg $m^{-3}d^{-1}$ for the removal of iron from a pure pyrite concentrate were obtained for the following three size fractions; -38 micron, -53 +38 micron and -75 +53 micron. The geometric surface area concentration in each case was 2681 m^2m^{-3} (Chapman, 1989). As can be seen from Table 5.19 these rates were lower than those obtained for similar size fractions during this study. These results indicated faster rates of biooxidation in the presence of arsenopyrite.

With the use of a mixed culture, Helle and Onken (1988) demonstrated a maximum rate of 6,90 kg m^{-3} d^{-1} for the batch removal of pure pyrite. The material used

was 90% passing 60 micron, consisted of 83% pyrite and a 10% pulp density was used. The corresponding rate of iron removal was 3,22 kg m^{-3} d^{-1} which is slightly lower than the iron removal rate obtained in this study and those obtained by Pinches *et al.* (1987).

TABLE 5.18 Model parameters for the fit of the logistic equation to the extent of removal of sulphide-sulphur, iron and arsenic.

SAMPLE	LOGISTIC MODEL PARAMETERS											
	SULPHIDE-SULPHUR				IRON				ARSENIC			
	k d^{-1}	X_0 %	Xm %	r^2	k d^{-1}	X_0 %	Xm %	r^2	k d^{-1}	X_0 %	Xm %	r^2
Bulk	0,683	0,3	100	0,99	0,568	1,4	95	1,00	0,546	5,8	100	1,00
+75	0,373	3,5	100	0,99	0,403	2,2	82	0,98	0,379	12,4	93	1,00
-75 +53	0,428	0,0	97	0,98	0,502	0,0	88	0,99	0,207	0,6	100	0,96
-53 +38	0,462	0,3	100	0,97	0,464	0,4	93	0,99	0,432	2,7	100	0,98
-38 +25	0,556	0,0	100	0,96	0,514	0,0	93	0,97	0,488	0,3	100	0,98
-25	0,907	0,2	100	0,98	0,792	0,7	93	0,98	0,653	13,8	100	0,99

TABLE 5.19 Predicted and experimentally determined maximum rates of removal of sulphide-sulphur, iron, arsenic, pyrite and arsenopyrite.

SAMPLE	MAXIMUM RATES OF REMOVAL ($kg\ m^{-3}\ d^{-1}$)									
	Sulphide -Sulphur		Iron		Arsenic		Pyrite		Arseno-pyrite	
	Pred	Exp	Pred	Exp	Pred	Exp	Pred	Exp	Pred	Exp
Bulk	4,66	3,89	4,00	3,98	0,99	0,95	7,92	6,53	2,15	2,07
+75	2,88	2,55	2,37	2,34	0,39	0,39	5,10	4,46	0,78	0,84
-75 +53	3,69	3,60	4,07	3,21	0,41	0,27	6,57	6,52	0,90	0,58
-53 +38	4,38	3,63	4,21	3,48	1,02	0,98	7,37	6,01	2,22	2,12
-38 +25	4,87	4,57	4,39	4,01	1,59	1,30	7,83	7,50	3,46	2,83
-25	4,57	4,36	4,67	3,58	1,11	1,05	7,66	7,32	2,41	2,28

CHAPTER 6

PRESENTATION AND DISCUSSION OF PILOT PLANT DATA

6.1 Background to Pilot Plant Operation

Continuous pilot plant biooxidation was begun by GENMIN Process Research a number of years ago to gain insight into, and experience of running a plant of this nature, as little information on continuous biooxidation was available.

Laboratory scale batch and continuous biooxidation gave the foundation upon which the pilot plant operation was based. Optimisation of many parameters including operating temperature, pH, pulp density, bacterial inocula, nutrient flowrate and composition and recycles had to be attempted.

The first six months of pilot plant operation included variation and optimisation of the above mentioned parameters. Once the plant was running suitably and had reached stable operation, the flowrate of slurry was increased periodically to ascertain the optimum retention time. The average composition and size analysis of the Fairview concentrate fed to the pilot plant is shown below in Table 6.1.

Table 6.1 Analysis of Fairview concentrate used for pilot plant testing

CHEMICAL ANALYSIS		SIZE ANALYSIS	
Component	Analysis %	Size micron	Mass Retained %
Total-Sulphur	23,2	+71	4-6
Sulphide-Sulphur	22,9	+56	8-11
Iron	24,7	+48	4-5
Arsenic	5,5	+36	5-6
		+28	10-11
Gold (g/t)	143,6	+20	7-8
		-20	50-60

All pilot plant operating information and data was obtained from the GENMIN report (Ming and Olën, 1986).

The biooxidation pilot plant consisted of five 5 m^3 rubber lined tanks. The tanks were baffled and agitation was by means of overhead stirrers, the shafts and impellers also being rubber lined. Compressed air was introduced into each tank via a stainless steel sparge ring situated below the impeller.

The first two tanks were used in parallel and constituted a primary stage. The combined flow from these tanks then cascaded into a series of three tanks. The use of the first two tanks in parallel played an important role in bacterial population increase and stability. The fact that the retention time in the first stage was effectively doubled was responsible for this. The plant configuration was thus maintained as such, as preferable to using all five tanks in series. A schematic diagram of the plant is shown in Figure 6.1.

Flotation concentrate received from the mine was slurried and screened. All material passing 100 micron screen was utilised directly. The oversized material was remilled and rescreened prior to use. The plant feed was maintained at a pulp density of 120 kg m^{-3}, equivalent to 11% solids (w/v) as often termed in the literature, (liquid to solid ratio of 8:1). This is a lower pulp density than that used by Bruynesteyn *et al.* (1986), of 200 kg m^{-3}. This low pulp density was originally chosen to prevent the build up of arsenic, ferric or other possible toxic products of the biooxidation process to levels exceeding the tolerance of the culture. After adaptation of the culture it was possible to increase the pulp density of the slurry. This in turn, increased the output of the plant.

Temperature in the plant was maintained at 40 ^{o}C. Daily monitoring of the pH was carried out and adjustment made to 1,6 using approximately 250 to 300 *l* of plant lime daily (analysis shown in Appendix 2). No breakdown of lime addition to individual tanks was recorded. Necessary nutrients were fed continuously to the two primary tanks as well as to Tank 2. Initially the nutrients contained a slightly modified version of the 9K nutrient medium of Silverman and Lundgren (1959). During the course of the pilot plant operation changes were made to the nutrient medium, and it was soon found that most of the required trace elements were supplied by the concentrate and the lime. However, during the period of stable operation from which the steady state data was obtained, the nutrient medium contained only sources of nitrogen, potassium and phosphate.

Initially the biooxidation plant was run at a retention time of twelve days. Owing to the low flowrate the primary tanks were fed hourly with pre-weighed packages of concentrate while water was added continuously. Once stable operation at a specific retention had been demonstrated, the feed rate was increased.

Each tank was sampled on a weekly basis. Both solid and solution samples were analysed in the same manner as described in Chapter 4 for samples taken during batch testing. Analyses included total-iron, total-sulphur, sulphide-sulphur and arsenic analyses of the solids and iron, sulphate-sulphur and arsenic analyses of the solution. No hydrochloric acid washing of the biooxidation product produced during continuous operation was carried out. Results of the iron, arsenic and total-sulphur analyses of the biooxidation product thus included both the residual material which had not been oxidised as well as any iron, arsenic or jarosite salts which may have precipitated. The removal of these elements from the solids could thus not be accurately calculated. Gold liberation was ascertained by subsequent cyanidation of the oxidised product.

6.2 Pilot Plant Data

The following sets of data were collected during operation of the pilot plant

(i) Liquid and solid flowrates into and out of the plant.
(ii) Chemical analysis of the solids.
(iii) Solution analyses.
(iv) Pulp density of the slurry.

The degree of biooxidation was determined using the extent of sulphide-sulphur breakdown. Sulphide-sulphur oxidation was used as the basis for this investigation owing to its fundamental importance in the process. As well as being the most reliable measurement of the degree of biooxidation, it is the break down of the sulphide minerals which lead to gold liberation. Owing to precipitation of iron, arsenic and sulphur as jarosite, ferric arsenate and other salts, total-iron, total-sulphur and arsenic could not be regarded as reliable measurements of the removal of the sulphide minerals. For the same reason iron and sulphur concentrations in the solution could not be regarded as valid measurements of the process.

In order to determine sulphide-sulphur breakdown rates it was necessary to have accurate estimates of the mass flowrate of solids between tanks. This flowrate did

not remain constant through the cascade but was affected by decrease in mass owing to biooxidation and increases in mass owing to jarosite precipitation and lime addition. Furthermore, solids concentration changed owing to constant evaporation of water caused by agitation and aeration at 40 ^{o}C.

With regard to evaporation, it was found that up to 1,3% of the liquid volume of a tank could be lost per day. This constituted approximately 5% of the total flowrate through the plant if it was running at a four day retention time. Lime addition accounted for between a 200 to 300 *l* increase in volume, representing between 85 and 115 kg of calcium sulphate precipitating over the entire cascade.

During the operation of the pilot plant no accurate measurements of volumetric flowrates and lime addition were made for each individual tank. It was thus not possible to determine the mass flowrates between tanks accurately; therefore, as a close approximation, it was assumed that there were equal volumetric flowrates of slurry between each tank.

With this assumption of constant volumetric flowrate, Q, and the knowledge of the concentration of solids in the slurry, M, and the sulphide-sulphur analysis, Z, the fractional removal of sulphide sulphur, X, could be calculated as follows.

$$X = 1-(ZM)_i/(ZM)_0$$

where

X	fractional removal of sulphide sulphur
Z	sulphide sulphur analysis (fraction)
M	solid content of slurry (kg solid m^{-3} slurry)

subscripts

0,i	referring to the feed stream and i^{th} reactor in the cascade

The periods of operation from which the steady state data were obtained included operation at 12, 10, 8, 6 and 4 days retention time respectively. The set of results collected for each tank for the duration of the run at a specific retention time was averaged before calculation of rates and fitting the logistic model. Results obtained for each of the primary tanks were also averaged as these were expected to be duplicates. The condensed set of data to which the logistic model was fitted is shown in Table 6.2.

The rate of removal of sulphide sulphur was calculated using Equation 3.16 and an average value for the sulphide content of the feed of C_0 = 27,66 kg m^{-3}. These rates are also shown on Table 6.2. A maximum rate of sulphide-sulphur removal of about 8,85 kg m^{-3} d^{-1} was achieved in the first stage.

This seems lower than the 16,4 kg $m^{-3}d^{-1}$ for the removal of the sulphide-sulphur constituent of a relatively pure pyrite concentrate as reported by Pinches *et al.* (1987). These tests were run at a 15% pulp density with material sized at 80% passing 38 micron. In order to make these results more comparable the rates may be quoted in units of grams of sulphide-sulphur removed per kilogram of concentrate fed per day, as follows, 109,3 g (kg feed)$^{-1}$ d^{-1} (Pinches *et al.*, 1987) and for this study 73,3 g (kg feed)$^{-1}$ d^{-1} which, while lower, is more comparable. These rates of removal may also be quoted with respect to the sulphide content of the feed material, they then become 375 g (kg sulphide)$^{-1}$ d^{-1} (Pinches *et al.*, 1987), and 320 g (kg sulphide)$^{-1}$ d^{-1} for this study. The fineness of sample used by Pinches *et al.* (1987) could explain the slightly higher rate reported. A value of 48,7 g (kg feed)$^{-1}$ d^{-1} (111 g (kg sulphide)$^{-1}$ d^{-1}), for sulphide-sulphur removal from a pure pyrite was quoted by Helle and Onken (1988) which is much lower than that determined in this study. Most commonly results are reported in the literature in units of kg m^{-3} d^{-1} which complicates the comparison of rates of oxidation, as differences in solid content of the slurries and sulphide content of the concentrates, is not taken into consideration. However, if rates are reported as g (kg sulphide)$^{-1}$ d^{-1}, comparisons are much more valid.

It must be noted that this pilot plant was operated in order to ascertain whether it was possible to operate a biooxidation cascade of this size. Parameters such as nutrient addition and the effect of recycles and changes in flowrates were assessed, as well as the degree of sulphide removal possible. The pilot plant was neither operated, nor samples suitably treated to provide data strictly appropriate for modelling purposes and therefore kinetic parameters determined are not expected to be all that accurate and strictly comparable to those of Pinches *et al.* (1987) who ran tests specifically in order to determine kinetic parameters.

The rate of sulphide-sulphur oxidation obtained for the batch biooxidation of the bulk concentrate was 3,89 kg m^{-3} d^{-1} which is less than half the rate of oxidation of the 8,85 kg m^{-3} d^{-1} calculated for the continuous operation. A similar increase in rates from batch to continuous was shown by Pinches *et al.* (1987).

Table 6.2 Steady State Pilot Plant Data: Retention times through the cascade, sulphide-sulphur removal and experimentally determined rates of sulphide-sulphur removal.

STAGE	RETENTION* days	SULPHIDE-SULPHUR REMOVED %	REMOVAL RATE $kgm^{-3}d^{-1}$
	Total plant retention of four days		
Primary	1,61	51,5	8,85
Stage 2	2,42	64,9	4,60
Stage 3	3,22	84,4	6,70
Stage 4	4,03	81,5	
	Total plant retention of six days		
Primary	2,42	59,9	6,86
Stage 2	3,62	86,0	5,98
Stage 3	4,83	89,6	0,82
Stage 4	6,04	92,7	0,71
	Total plant retention of eight days		
Primary	3,22	66,1	5,68
Stage 2	4,83	85,8	3,38
Stage 3	6,44	95,0	1,58
Stage 4	8,05	96,7	0,29
	Total plant retention of ten days		
Primary	4,03	71,9	4,94
Stage 2	6,04	88,4	2,27
Stage 3	8,05	96,3	1,09
Stage 4	10,06	97,4	0,15
	Total plant retention of twelve days		
Primary	4,83	76,6	4,39
Stage 2	7,25	90,5	1,59
Stage 3	9,66	97,3	0,78
Stage 4	12,08	97,7	0,05

* Total retention time at that point of the cascade.

6.3 Fitting the Logistic Model to Continuous Data

When fitting the logistic model to the continuous data the unknown parameters k and X_m were solved for by considering the data for each tank separately. Equation 3.13 was fitted to the data for the primary tanks using a linear least squares routine. This gave the values of k_1 and X_{m1} which were then used to predict theoretical values of X_1. Equation 3.15 was fitted to the data from the second tank using the predicted values of X_1. A Nelder-Mead non-linear optimisation routine shown in Appendix 4 was developed and used to solve for k_2 and X_m. This was done similarly for tanks 3 and 4. Figure 6.1 shows a schematic diagram of the continuous plant for which these parameters were found.

It must be noted that the residence time, T_i, is the residence time in tank *i* and not the overall residence time, t_i, of the material in the cascade, i.e.,

$$T_2 = V_2/Q$$
$$t_2 = (V_1 + V_2)/Q$$

Table 6.3 shows the modelling parameters through the cascade as predicted by logistic kinetics.

Table 6.3 Logistic model parameters.

Stage	Maximum Removal, X_m	Rate constant, k d^{-1}	(Sum of errors)^2
Primary Stages	0,880	1,3500	$8,0 \times 10^{-3}$
Stage 2	0,979	0,9703	$1,4 \times 10^{-3}$
Stage 3	0,993	1,3000	$2,5 \times 10^{-4}$
Stage 4	0,999	0,3129	$8,0 \times 10^{-4}$

Calculation of the logistic rate constants, k, for the biooxidation of a predominantly pyrite concentrate in two different single stage continuous reactors gave values of 1,32 d^{-1} and 0,767 d^{-1} (Pinches *et al.*, 1987). These results indicate enhanced oxidation in the former reactor, which the author associated with lower pH. These rates were also higher than the value of 0,683 d^{-1} obtained during batch

biooxidation. The values obtained in this study are comparable to those obtained by Pinches *et al.* (1987).

Values of k obtained for the single stage continuous operation of different size fractions of a pure pyrite concentrate, while maintaining a similar surface area, were in the region of 0,28 d^{-1} to 0,35 d^{-1}, again indicating the slower rate of oxidation of a pure pyrite (Chapman, 1989). This study, however, also indicated similar values of k for both batch and continuous oxidation.

Figure 6.2 shows the experimental data as well as the curves predicted by the logistic parameters for each stage of the pilot plant cascade. The data for stage 1 appears linear, additional data points at lower retention times are thus required to confirm the shape of this curve, and to give greater credibility to the values of the rate parameters for each stage.

6.4 Prediction of Cascade Performance Using the Logistic Model

Using the values of the modelling parameters obtained it was possible to investigate the performance of a number of cascades in which the tanks were differently configured, and also to assess how sensitive the prediction of the experimental data was to the value of k_i, the logistic rate constant in reactor *i*.

Figure 6.3 shows the experimental results, as well as the predicted curve generated using different values of the rate constant k_i. Curves generated using the correct values described the data well, slightly higher or lower values of k did not predict the experimental data as accurately for the primary stage or tank 2. Progressing through the cascade it was evident that the model became increasingly less sensitive to variations in the value of the rate constant k. Regarding the fourth tank, even large variations in the value of k caused negligible shift of the curve. Evaluation of the $(\text{sum of errors})^2$ for the fit of the logistic equation to data from stages two, three and four, and forcing the value of k, the rate parameter, to k = 1,35 gave values of $1{,}3 \times 10^{-2}$; $3{,}1 \times 10^{-4}$ and $9{,}3 \times 10^{-3}$ respectively, indicating that a value of k = 1,35 could be applicable throughout the cascade.

A degree of insensitivity is thus apparent when fitting the logistic equation to data and could be a short coming of either the logistic equation or the Nelder-Mead non-linear optimisation routine. Continuous cascade biooxidation results reported by Bruynesteyn *et al.* (1986) and Pinches *et al.* (1987) did either not include a

breakdown of data for each stage or at sufficient retentions to enable verification of this insensitivity on other results.

The performance of five cascades of different tank configuration was compared. Each consisted of five equal volume tanks. The configurations considered were:

(i) 5 tanks in series
(ii) A primary stage of 2 tanks in parallel, followed by 3 tanks series
(iii) A primary stage of 3 tanks in parallel, followed by 2 tanks series
(iv) A primary stage of 4 tanks in parallel, followed by a fifth tank
(v) A primary stage of 5 tanks in parallel

Tank volume, and hence, cascade volume was kept constant. Total flowrate, Q, into the cascade was also kept constant in order to keep overall retention time consistent. Using the logistic model and the values of k obtained for each tank, curves were generated of final sulphide-sulphur removal versus overall retention time, t, in the cascade. These are shown for each of the five cascades in Figure 6.4.

The performance curves clearly show that the cascade consisting of five tanks in parallel is least effective, unless very low sulphide removal is required. Options (ii) and (iii) finally give similar results, with cascade (iii) performing far better initially than even cascade (i). At higher conversions, above 80% removal of sulphide-sulphur, cascade (i) out performs the other three, but this only occurs at retention in the cascade of greater than seven days.

Ultimately biooxidation is being carried out to achieve maximum gold liberation. If gold recovery is adequate with minimal removal of sulphide a cascade such as options (iv) and (v) with large initial stages would be adequate. If a high fractional removal of sulphide is required, use of a cascade with a slightly larger primary stage followed by a number of tanks in series is recommended. The benefit of the slightly larger primary stage, as in option (ii), is the reduction of the risk of wash-out of the bacterial culture.

Having examined these different configurations it appears that a multiple first stage does give optimum performance. It is reassuring that this theoretical approach confirms the almost intuitive basis upon which the multiple first stage configuration was initially decided on for pilot and demonstration plant purposes (van Aswegan *et al.*, 1988).

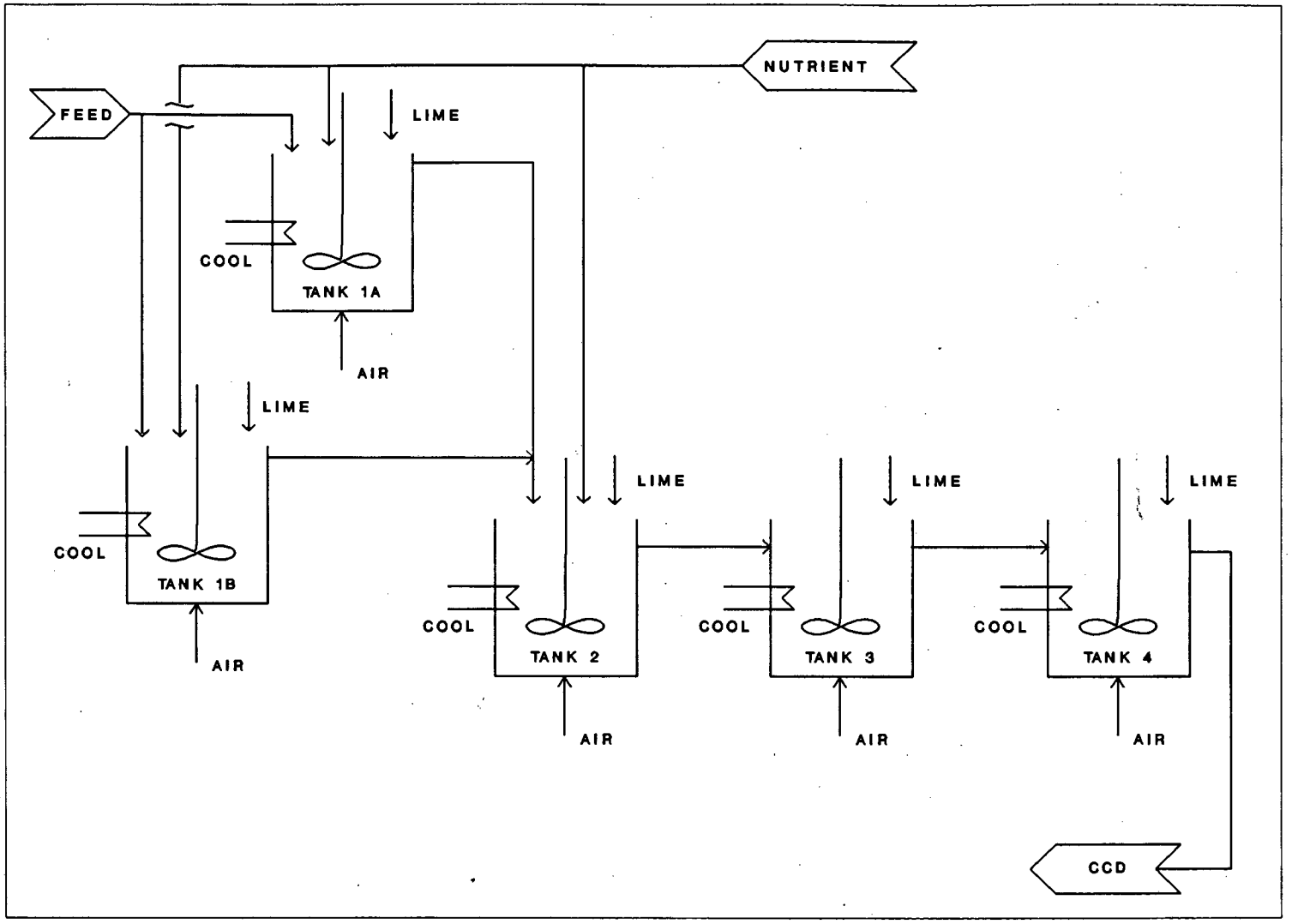

Figure 6.1 Diagram of the continuous pilot plant cascade.

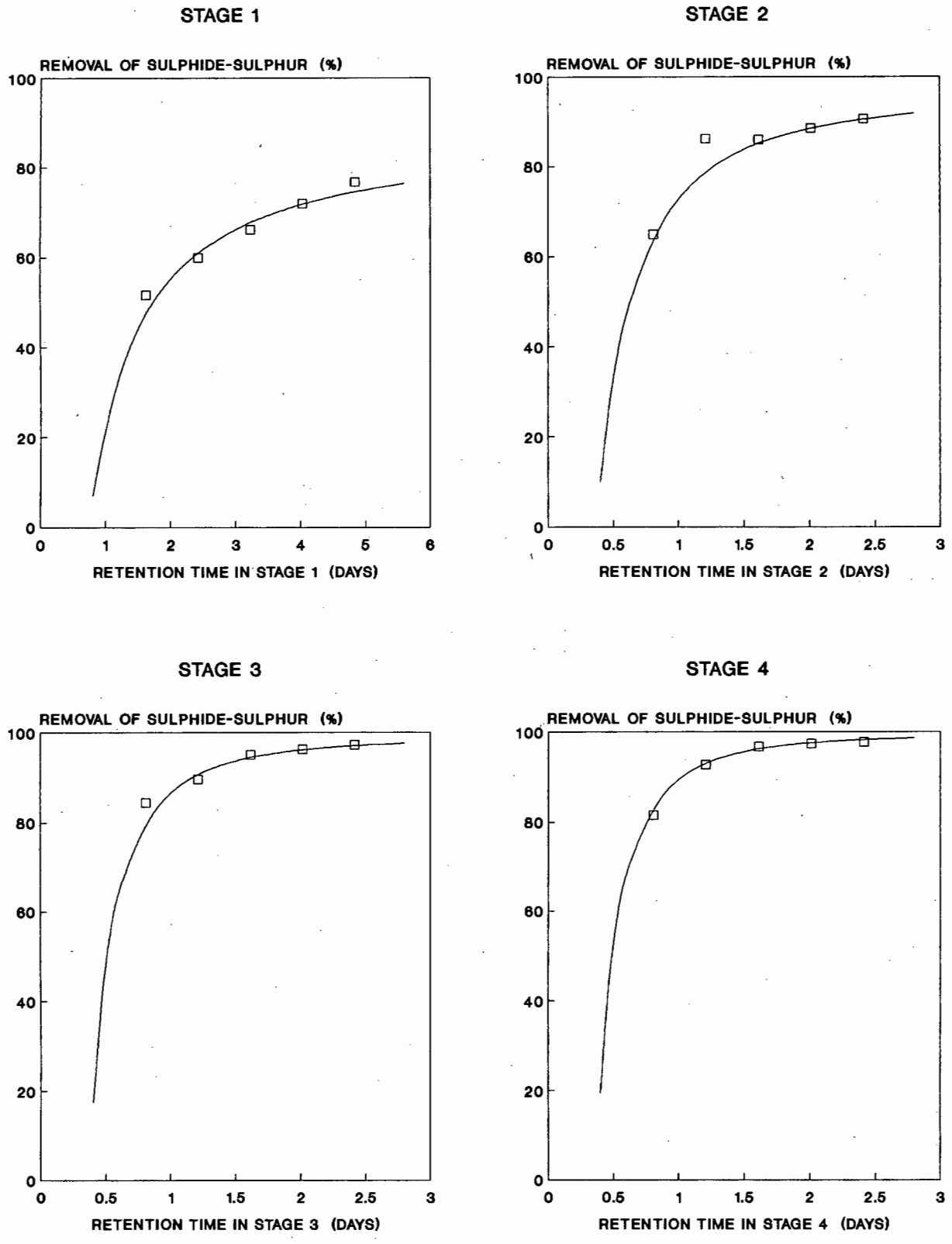

Figure 6.2 Fit of pilot plant data for each stage using the logistic equation.

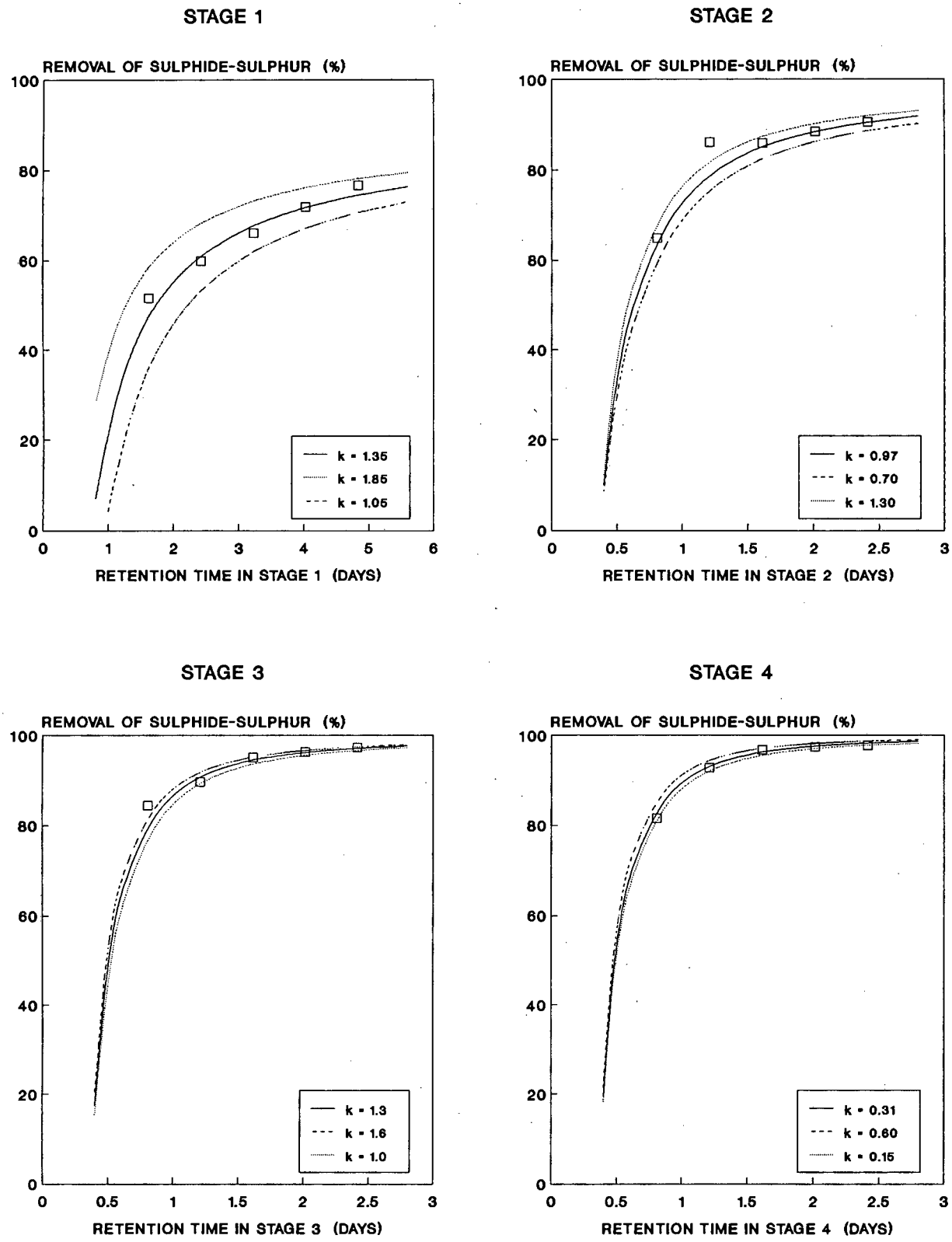

Figure 6.3 Fit of pilot plant data for each stage using the logistic equation and varying values of the parameter k.

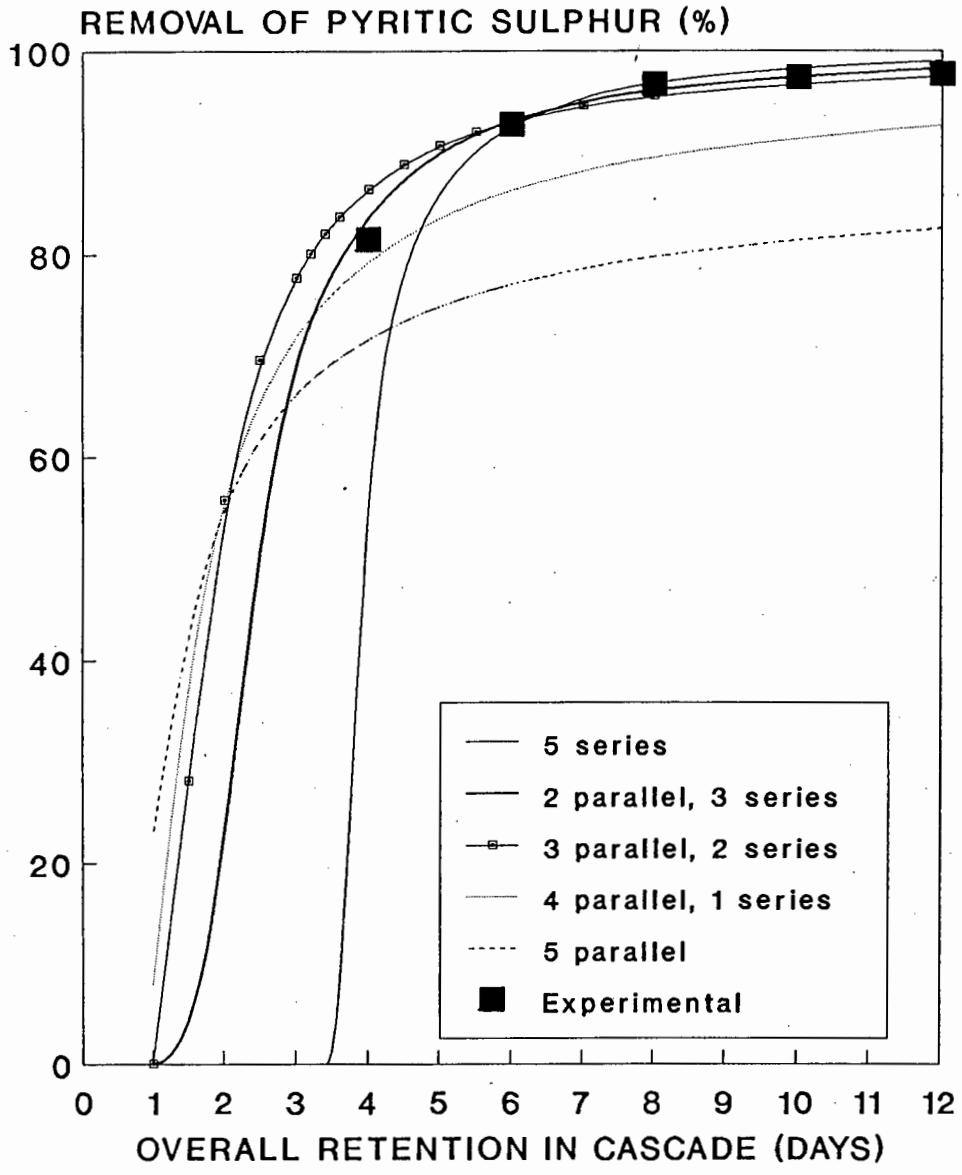

Figure 6.4 Theoretical performance curves for five configurations of a five tank continuous cascade compared to the experimental results obtained for the pilot plant run.

CHAPTER 7

CONCLUSIONS AND RECOMMENDATIONS

7.1 Conclusions

The objectives of this project were:

(i) to investigate the dependence of the batch biooxidation rate on particle surface area to enable recommendation of milling requirements for optimisation of the biooxidation process.

(ii) to establish a procedure for the determination of kinetic parameters on which to base the design of biooxidation reactors.

(iii) to analyse existing continuous pilot plant data, specifically for testing the validity of kinetic parameters determined by analysis of the batch data.

The conclusions may be summarised as follows:

(i) Splitting of the bulk concentrate into narrow size fraction resulted in selective reporting of the sulphide minerals to certain size fractions. Consequently, the dependence of the rates of removal on specific mineral surface areas as well as on the total surface was investigated.

(ii) Assessment of iron and arsenic removal during biooxidation required the removal of precipitates from the biooxidation product by HCl-acid washing.

(iii) Sulphide-sulphur, iron and arsenic removal results were found to be more consistent when a selection criterion for data points was introduced. Calculation of the removal of the aforementioned components required quantification of the mass changes during biooxidation. While the mass of solids per unit volume of slurry was measured during sampling, the analysis of inert substances, such as gold and silica, gave a reliable mass tie. Mass balance ratios were therefore calculated using the measured masses and those calculated from the gold and silica ties. Values not satisfying a

selection criterion were discarded. If more than one value was accepted, these were averaged.

(iv) The trends for the batch removal of sulphide-sulphur, iron and arsenic followed the form of a sigmoidal curve, viz. a lag phase, followed by a period of maximum oxidation which was linear, and then a stationary phase as substrate became depleted.

(v) Arsenic removal from the bulk concentrate preceded that of iron and sulphide-sulphur. Specific removal rates (d^{-1}) of these components were similar (As - 0,13; Fe - 0,13; S^{2-} - 0,14), while on a molar basis sulphide-sulphur and iron removal rates were higher (As - 13 mol m^{-3} d^{-1}; Fe - 71 mol m^{-3} d^{-1}; S^{2-} - 122 mol m^{-3} d^{-1}).

(vi) The maximum rate of removal of each component could be obtained from the linear portion of the fractional removal versus time curves. This rate, termed the specific removal rate (d^{-1}), was more useful for comparative purposes than the absolute rate (mol m^{-3} d^{-1}), as differences in sulphide grades were taken into consideration.

(vii) Dependence of the specific rate of arsenic removal on arsenopyrite surface was linear, while absolute rates increased to a certain extent, and then no further. The difference in trends may be explained by the selective reporting of the arsenopyrite to the lower surface area fractions; hence, on a molar basis, the rate of removal remained static. This was due to a lower arsenopyrite content rather than to no further increase in rates with increase in surface area.

(viii) Dependence of the rates of iron and sulphide-sulphur on pyrite surface area followed similar trends to those of arsenopyrite, but need confirmation. The dependence of the absolute rates on pyrite surface area was not found to be linear. This is contrary to literature studies, but may also be due to variation in sulphur grade of each fraction.

(ix) Gold dissolution was found to be linearly dependent on arsenic removal and to increase rapidly with initial sulphide-sulphur removal, before levelling off. Complete sulphide oxidation was not necessary to ensure the maximum gold dissolution, implying preferential bacterial attack in gold rich regions of the

crystal lattice. The results also indicate association of the gold with the arsenopyrite.

(x) The logistic model described the batch data well, with good correlation between predicted and experimental rates of removal, except where the removal-time curves were not symmetrical.

(xi) Sulphide-sulphur oxidation during continuous bioooxidation was also well described by the logistic model; however discrepancies between batch ($k = 0{,}683\ d^{-1}$) and continuous ($k = 1{,}35\ d^{-1}$) parameters could not be reconciled.

(xii) Prediction of cascade performance with the logistic equation is possible, but only on the basis of selection of the optimum reactor configuration to achieve a required sulphide oxidation.

7.2 Recommendations

(i) Surface area concentrations were calculated using the average particle diameter in each size interval. Surface area measurement may however be more accurate.

(ii) To assess the effect of surface area, each sample should be milled separately to a specific degree of fineness to prevent the complication of differing chemical compositions.

(iii) Use of the Gompertz model (Richards, 1959), of which the logistic equation is a special case, should be assessed as data is not required to be symmetrical.

(iv) Sulphide oxidation obtained from continuous pilot testing at four days retention and more was already too high to allow for proper assessment of the logistic equation which becomes insensitive to variations in kinetic parameters at high extents of removal. Generation of sulphide oxidation results at lower retentions is required.

REFERENCES

ANDREWS, G.F. (1988), The selective adsorption of *Thiobacilli* to dislocation sites on pyrite surfaces. *Biotechnol. Bioeng.*, **31**, 378-381.

ATKINS, A.S., POOLEY, F.D. and TOWNSLEY, C.C. (1986), Comparative mineral sulphide leaching in shake flasks, percolation columns and pachuca reactors using *Thiobacillus ferrooxidans. Process Biochem*, **21**(1), 3.

BAILEY, J.E. and OLLIS, D.F. (1977), "Biochemical engineering fundamentals", McGraw Hill, New York

BENNETT, J.C. and TRIBUTSCH, H. (1978), Bacterial leaching patterns on pyrite crystal surfaces. *J. Bacteriol.*, **134**, 310-317.

BLANCATE-ZURITA, M.A., BRANION, R.M.R. and LAWRENCE, R.W. (1985), Application of a shrinking particle model to the kinetics of microbiological leaching, in *Fundamental and Applied Biohydrometallurgy*, Proceedings of the Sixth International Symposium on Biohydrometallurgy, Vancouver, B.C., Canada, August 1985, LAWRENCE, R.W., BRANION, R.M.R and EBNER, H.G., Eds. (Elsevier, Amsterdam, 1986), 243-253.

BOA, J.M. and LEDUY, A. (1987), Pullulan from peat hydroxylate fermentation kinetics. *Biotechnol. Bioeng.*, **30**, 462.

BRIERLEY, C.L. (1984), Microbial mining : Technology, status and commercial opportunities. *World Biotech. Rep.*, **1**, 599, Online Publishers Ltd., Pinner, UK.

BRUYNESTEYN, A., HACKL, R.P. and WRIGHT, F. (1986), The BIOTANKLEACH process, in *Gold 100*, Proceedings of the International Conference on Gold, Vol **2**: *Extractive Metallurgy of Gold.*, Johannesburg, SAIMM (1986), 353-365.

CHANG, Y.C. and MYERSON, A.S. (1982), Growth models of the continuous bacterial leaching of iron pyrite by *Thiobacillus ferrooxidans. Biotechnol. Bioeng.*, **24**, 889.

CHAPMAN, J.T. (1989), The batch and continuous bacterial leaching kinetics of a refractory gold-bearing pyrite concentrate. *MSc(Eng) Thesis*, University of Cape Town.

CHAPMAN, J.T., HANSFORD, G.S. and PINCHES, A. (1989), Batch and continuous bacterial leaching kinetics of a refractory gold-bearing concentrate. Paper presented at Biohydrometallurgy 89, Jackson, Wyoming, , 13-18 Aug 1989.

CHAUDHURY, G.R., SUKLA, L.B. and DAS, R.P. (1985), Kinetics of biochemical leaching of sphalerite concentrate. *Metall Trans B*, Vol **16B**, 667.

CHAUDHURY, G.R. and DAS, R.P. (1987), Bacterial leaching - Complex sulphides of copper, lead and zinc. *Int. J. of Min. Proc.*, **21**, 57.

COLMER, A.R. and HINKLE, M.E. (1947), The role of microorganisms in acid mine drainage: a preliminary report. *Science*, **106**, 253.

DROSSOU, M. (1986), The kinetics of the bioleaching of a refractory gold bearing pyrite concentrate. *MSc(Eng) Thesis*, University of Cape Town.

DRY, M.J. and COETZEE, C.F.B. (1986), Recovery of gold from refractory ores, in *Gold 100*, Proceedings of the International Conference on Gold, Vol **2**: *Extractive Metallurgy of Gold*. Johannesburg, SAIMM (1986), 259-274.

EL LOZY, M. (1978), A critical analysis of double and triple logistic growth curves. *Annals of Human Biology*, **5**, 389-394.

ERICKSON, L.E., FAN, L.T., SHAH, P.S., and CHEN, M.S.K. (1970), Growth models of cultures with two liquid phases: 4. Cell adsorption, drop size distribution and batch growth. *Biotechnol. Bioeng.*, **12**, 713.

ESPEJO, R.T. and ROMERO, P. (1987), Growth of *Thiobacillus ferrooxidans* on elemental sulphur. *Appl. Environ. Microbiol.*, **53(8)**, 1907.

FRIDMAN, I.D. and SAVARI, E.E. (1984), Advantages of bacterial leaching in treating gold - antimony - arsenic concentrates containing carbon. *Non-Ferrous Metals*, **25**, 102.

FUKAI, S. and SILSBURY, J.H. (1976), Responses of subterranean clover communities to temperature: I Dry matter production and plant morphogenesis. *Aust. J. Plant. Physiol.*, **3**, 527.

GORMELEY, L.S., DUNCAN, D.W., BRANION, R.M.R. and PINDER, K.L. (1975), Continuous culture of *Thiobacillus ferrooxidans* on a zinc sulphide concentrate. *Biotechnol. Bioeng.*, **17**, 31-49.

GROUDEVA, V.I., GROUDEV, S.N. and MARKOV, K.I. (1985), A comparison between mesophilic and thermophilic bacteria with respect to their ability to leach sulphide minerals, in *Fundamental and Applied Biohydrometallurgy*, Proceedings of the Sixth International Symposium on Biohydrometallurgy, Vancouver, B.C., Canada, August 1985, LAWRENCE, R.W., BRANION, R.M.R and EBNER, H.G., Eds. (Elsevier, Amsterdam, 1986), 484-485.

HAINES, A.K. (1986), Factors influencing the choice of technology for the recovery of gold from refractory arsenical ores, in *Gold 100*, Proceedings of the International Conference on Gold, Vol **2**: *Extractive Metallurgy of Gold*, Johannesburg, SAIMM (1986), 227-233

HANSFORD, G.S. and DROSSOU, M. (1987), A propagating pore model for batch bioleach kinetics of refractory gold bearing pyrite, in *Biohydrometallurgy*, Proceedings of the International Symposium, Warwick, (1987). NORRIS, P.R. and KELLY, D.P., Eds. (Science and Technology Letters, Surrey, 1988), 345-358.

HARRISON, A.P. (1984), The acidophilic Thiobacilli and other acidophilic bacteria that share their habitat. *Ann. Rev. Microbiol.*, **38**, 265-292.

HELLE, U. and ONKEN, U. (1988), Continuous microbial leaching of a pyrite concentrate by *Leptospirillum* - like bacteria. *Applied Microbial. and Biotechnol.*, **28**, 553-558.

HUTCHINS, S.R., DAVIDSON, M.S, BRIERLEY, J.A. and BRIERLEY, C.L. (1986), Microorganisms in reclamation of metals. *Ann. Rev. Microbiol.*, **40**, 311-336.

HUTCHINS, S.R., BRIERLEY, J.A. and BRIERLEY, C.L. (1987), Microbial pretreatment of refractory sulphide and carbonaceous gold ores, for presentation at the 116th Annual AIME Meeting, Denver, Colorado, February 1987.

JONES, C.A. and KELLY, D.P. (1983), Growth of *Thiobacillus ferrooxidans* on ferrous iron in chemostat culture: Influence of product and substrate inhibition. *J.Chem. Tech. Biotechnol.*, **33**B, 241-261.

KARAVAIKO, G.I. (1985), Microbiological processes for the leaching of metals from ores - State-of-the-art review. TORMA, A.E., Ed. Centre of International Projects, GKNT, Moscow.

KARAVAIKO, G.I., CHUCHALIN, L.K., PIVOVAROVA, T.A., YEMEL'YANOV, B.A. and DOROFEYEV, A.G. (1985), Microbiological leaching of metals from arsenopyrite containing concentrates, in *Fundamental and Applied Biohydrometallurgy*, Proceedings of the Sixth International Symposium on Biohydrometallurgy, Vancouver, B.C., Canada, August 1985, LAWRENCE, R.W., BRANION, R.M.R and EBNER, H.G., Eds. (Elsevier, Amsterdam, 1986), 115-126.

KARGI, F. and WEISSMANN, J.G. (1984), A dymanic mathematical model for microbiological removal of pyritic sulphur from coal. *Biotechnol. Bioeng.*, **26**, 604-612.

KELLER, L. (1982), Acid bacterial and ferric sulphate leaching of pyrite single crystals. *Biotechnol. Bioeng.*, **24**, 83-96.

KELLY, D.P., NORRIS, P.R. and BRIERLEY, C.L. (1979), Microbiological methods for the extraction and recovery of metals, in *Microbial Technology: Current State, Future Prospects*, 29th Symposium of the Soc. of Gen. Microbiology. BULL, A.T., RATLEDGE, C. and ELLWOOD D.C., Eds. 264-308.

LACEY, D.T. and LAWSON, F. (1970), Kinetics of the liquid-phase oxidation of acid ferrous sulphate by the bacterium *Thiobacillus ferrooxidans*. *Biotechnol. Bioeng.*, **12**, 29-50.

LAKSHMANAN, V.I. (1986), Industrial views and applications: Advantages and limitations of biotechnology, in *Biotechnology and Bioengineering Symposium No 16.* (John Wiley & Sons, 1986), 351-361.

LAMBRECHT, R.S., CARRIERE, F.C. and COLLINS, M.T. (1988), A Model for analyzing growth kinetics of a slowly growing *mycobacterium* sp. *Appl. Environ. Microbiol.*, **54(4)**, 910-916.

LA MOTTA, E.J. (1976), Kinetics of continuous growth cultures using the logistic growth curve. *Biotechnol. Bioeng.*, **18**, 1029-1032.

LAWRENCE, R.W. and GUNN, J.D. (1985), Biological pre-oxidation of pyritic gold concentrate, in *Session on Frontier Technology in Mineral Processing*, the 1985 AIME Annual Meeting, New York.

LAZER, M.J., SOUTHWOOD, M.J. and SOUTHWOOD, A.J. (1986), The release of refractory gold from sulphide minerals during bacterial leaching, in *Gold 100*, Proceedings of the International Conference on Gold, Vol **2**: *Extractive Metallurgy of Gold.*, Johannesburg, SAIMM (1986), 287-297.

LIVESEY-GOLDBLATT, E., NORMAN, P. and LIVESEY-GOLDBLATT, D.R. (1983), Gold recovery from arsenopyrite/pyrite ore by bacterial leaching and cyanidation, *Progress in Biohydrometallurgy*, Cagliari, 1983, 627-641.

LUNDGREN, D.G. and SILVER, M. (1980), Ore leaching by bacteria. *Ann. Rev. Microbiol.*, **34**, 263-283.

LUNDGREN, D.G., VALKOVA-VALCHANOVA, M., and REED, R. (1986), Chemical reactions important in bioleaching and bioaccumulation, in *Biotechnology and Bioengineering Symposium No 16.* (John Wiley & Sons, 1986), 7-

MARCHANT, P.B. (1985), Continuous vat biooxidation of a refractory arsenical sulphide concentrate, Presented at the 17th Canadian Mineral Processors Conference, Ottawa, Ontario, January 1985.

MARCHANT, P.B. and LAWRENCE, R.W. (1986) Considerations for the design, optimisation and control of continuous biological tank leaching operations to enhance precious metals extraction, in *Gold 100*, Proceedings of the International Conference on Gold, Vol **2**: *Extractive Metallurgy of Gold.*, Johannesburg, SAIMM (1986), .

MEHTA, A.P. and LE ROUX, N.W. (1974), *Biotechnol. Bioeng.*, **16**, 559.

MEHTA, A.P. and MURR, L.E. (1982), Kinetic study of sulphide leaching by galvanic interaction between chalcopyrite, pyrite and sphalerite in the presence of *Thiobacillus ferrooxidans* (30^{o}C) and a thermophilic microorganism (55^{o}C). *Biotechnol. Bioeng.*, **24**, 919-940.

MING, N. and OLEN, C.M. (1986), GENMIN Process Research Report, Bacterial leaching of sulphide minerals for gold liberation

MONOD, J. (1949), The growth of bacterial cultures. *Ann. Rev. Microbiol.*, **3**, 371-394.

MYERSON, A.S. and KLINE, P.C. (1983), The adsorption of *Thiobacillus ferrooxidans* on solid particles. *Biotechnol. Bioeng.*, **25**, 1669-1676.

MYERSON, A.S. and KLINE, P.C. (1984), Continuous bacterial coal desulphurization employing *Thiobacillus ferrooxidans*. *Biotechnol. Bioeng.*, **26**, 92-99.

NATARAJAN, K.A. and IWASAKI, I. (1985), Mineral-microbe interactions in the leaching of complex sulphides, in *Microbiological Effects on Metallurgical Processes*, AIME annual meeting, New York, February, 1985. CLUM, J.A. and HAAS, L.A., Eds.

NORRIS, P.R. and PARROT, L. (1985), High temperature, mineral concentrate dissolution with *Sulfolobus*, in *Fundamental and Applied Biohydrometallurgy*, Proceedings of the Sixth International Symposium on Biohydrometallurgy, Vancouver, B.C. Canada, August 1985. LAWRENCE, R.W., BRANION, R.M.R and EBNER, H.G., Eds. (Elsevier, Amsterdam, 1986), 355-365

OLSON, G.J. and KELLY, R.M. (1986), Microbiological metal transformations: Biotechnological applications and potential. *Biotechnol. Progress*, **2**(1), 1-15.

PETROVA, T.A., GALAKTIONOVA, N.A., KARAVAIKO, G.I., KRYLOV, Y.M. and MOSHNYAKOVA, S.A. (1979), Mathematical growth model of *Thiobacilus ferroxidans* on ferrous iron medium. *Microbiology*, **48**(2), 185-189

PINCHES, A. (1972), The role of microorganisms for the recovery of metals from mineral materials. *PhD Thesis*, University of Wales, Cardiff.

PINCHES, A. and PALLENT, J. (1986), Rate and yield relationships in the production of xanthan gum by batch fermentations using complex and chemically defined growth media. *Biotechnol. Bioeng,*, **28**, 1484-1496.

PINCHES, A., CHAPMAN, J.T., TE RIELE, W.A.M. and VAN STADEN, M. (1987), The performance of bacterial leach reactors for the preoxidation of refractory gold-bearing sulphide concentrates, in *Biohydrometallurgy*, Proceedings of the International Symposium, Warwick, (1987). NORRIS, P.R. and KELLY, D.P., Eds. (Science and Technology Letters, Surrey, 1988), 329-344.

PLORIN, G.G. and GILBERTSON, D.E. (1984), Equations for describing the growth of the schistosome host snail *Biomphalaria glabrata*. *J. Parasit.*, **70**(1), 43-47.

RICHARDS, F.J. (1959), A flexible growth function for empirical use. *J. of Experimental Botany*, **10**(29), 290-300.

RODRIGUEZ-LEIVA, M. and TRIBUTSCH, H. (1988), Morphology of bacterial leaching patterns of *Thiobacillus ferrooxidans* on synthetic pyrite. *Arch. Microbiol.*, **149**, 401-405.

SANMUGASUNDERAM, V., BRANION, R.M.R. and DUNCAN, D.W. (1985), A growth model for the continuous microbiological leaching of a zinc sulphide concentrate by *Thiobacillus ferrooxidans. Biotechnol. Bioeng.*, **27**, 1173-1184.

SILVERMAN, M.P. and LUNDGREN, D.G. (1959), Studies on the chemo-autotrophic iron bacterium *Ferrobacillus ferrooxidans*, 1. An improved medium and harvesting procedure for securing high cell yields. *J. Bacteriol.*, **77**, 642.

SOUTHWOOD, M.J. and SOUTHWOOD, A.J. (1985), Mineralogical observations on the bacterial leaching of auriferous pyrite: A new mathematical model and implications for the release of gold, in *Fundamental and Applied Biohydrometallurgy*, Proceedings of the Sixth International Symposium on Biohydrometallurgy, Vancouver, B.C., Canada, August 1985, LAWRENCE, R.W., BRANION, R.M.R and EBNER, H.G., Eds. (Elsevier, Amsterdam, 1986).

SWASH, P.M. (1988), A mineralogical investigation of refractory gold ores and their beneficiation, with special reference to arsenical ores. *J. S. Afr. Inst. Min. Metall.*, **88**(5), 173-180.

TORMA, A.E. (1977), The role of *Thiobacillus ferrooxidans* in hydrometallurgical processes, in *Advances in Biochemical Engineering, New Substrates*, GHOSE, F.K., FIETCHTER, A. and BLAKEBROUGH, N. Eds. (Springer-Verlag, New York), **6**, 1-37.

TORMA, A.E. and SAKAGUCHI, H. (1978), Relation between the solubility product and rate of metal sulphide oxidation by *Thiobacillus ferrooxidans. J. Ferment. Technol.*, **56**(3), 173-178.

VAN ASWEGAN, P.C., MARAIS, H.J. and HAINES, Dr A.K. (1988), Design and operation of a commercial bacterial oxidation plant. Paper presented at the Perth International Gold Conference, Perth, Western Australia, 28 Oct - 1 Nov 1988, 144.

VERBAAN, B and HUBERTS, R. (1988), An electrochemical study of the bacterial leaching of synthetic Ni_3S_2. *Int. J. of Min. Proc.*, **24**, 185-202.

YEH, T.Y., GODSHALK, J.R., OLSON, G.J. and KELLY, R.M. (1987), Use of epifluorescence microscopy for characterizing the activity of *Thiobacillus ferrooxidans* on iron pyrite. *Biotechnol. Bioeng.*, **30**, 138-146.

APPENDIX 1

ANALYTICAL PROCEDURES

I Analytical Procedures for Solid Residues

- A Iron
- B Arsenic
- C Total-Sulphur
- D Sulphide-Sulphur
- E Silica
- F Gold

II Analytical Procedures for Liquor Samples

- A Iron
- B Total-Sulphur
- C Arsenic

A. IRON ON RESIDUE

See footnote of Section II A, Iron in solution.

B. ARSENIC ON RESIDUE

1. REAGENTS
   - 1.1 Hydrochloric acid
   - 1.2 Nitric acid
   - 1.3 diArsenic trioxide
   - 1.4 Sodium hydroxide
   - 1.5 Distilled water used throughout
   - 1.6 Aqua Regia - concentrated: 3 Parts HCl to part 1 HNO_3 prepared fresh for each batch of samples. Any excess aqua regia is diluted 1:1 with water to provide item 1.7.
   - 1.7 Aqua Regia 1:1 : See 1.6 above.
   - 1.8 Arsenic Stock Solution - 1000 ppm: Weigh out 1,3203 g of As_2O_3 and dissolve with gentle heating in the minimum of strong NaOH solution. Wash into a 1000 m*l* volumetric flask, add 50 m*l* HNO_3 and dilute to the mark with water.
   - 1.9 Arsenic Working Standards, 20 ppm and 100 ppm: Using burettes and volumetric flasks, dilute appropriate amounts of the 1000 ppm arsenic solution to give 20 and 100 ppm arsenic solutions. Add Aqua Regia to make the solutions 20% in respect to Aqua Regia.

2. DISSOLUTION

   The samples are prepared to pass a 180 micron sieve. Weigh out 1 g of sample into a 100 m*l* beaker. Add 20 m*l* of concentrated Aqua Regia, swirl and cover with a glass cover slip immediately. Include a reagent blank and 1 sample check in every 10 samples. Place the beakers in front of a hotplate set at 95^{o}C in a fume chamber and leave overnight i.e. $\pm$ 16 hours. Place the beakers on the hotplate, raise the temperature and bring to the boil, or alternatively place on a low hotplate (100^{o}C) for $\pm$ 1 hour, raise the temperature and bring to the boil. Remove from the hotplate and cool. Wash into a 100 m*l* volumetric flask and dilute to the mark. Mix well and

allow to settle. Dilution = 1 g/100 m*l*. If an absorbance reading is obtained greater than that of the 100 ppm standard, dilute the sample solution by pipetting 5 m*l* of the solution into a 50 m*l* volumetric flask, add 20 m*l* of 1:1 Aqua Regia and dilute to the mark. Mix well. Dilution = 1 g/1000 m*l*.

3. PROCEDURE

The solutions are "read" on 1275 instrument using the following parameters:

H C lamp - Hilger at 5 mA
Slit - 1,0 nm S.B.P.
Wave length - 193,7 nm
Automatic background correction required.
Fuel acetylene (1,5 cm red feather)
Support nitrous oxide
Burner height setting 10 (+ 7 mm below optical axis)
Mode 3 sec integration.

Calibration

Zero on distilled water.
20 ppm As standard calibrated to read 20,0.
100 ppm As standard "curve corrected" to read 100,0.
The reagent blank (usually zero) is subtracted from all readings.

4. CALCULATION

Net reading x 100/100,0 x dilution = ppm As
ppm/10000 = % As
The minimum value reported is 50 ppm.

Footnote:
Omit dissolution procedure for liquor samples

C. TOTAL SULPHUR

1. INTRODUCTION

This method is also applicable to solid residues of alkaline origin.

2. PRECISION

The lowest reported indication is <0,005% i.e the detection limit is 0,01%.

3. REAGENTS

3.1 10% barium chloride: Weigh 100 g Merck barium chloride (GR) into a 600 cm^3 beaker, dissolve in distilled water and then make to 1*l*.

3.2 HCl: CP grade.

3.3 1:1 ammonium hydroxide - NH_4OH (AR): 500 cm^3 NH_4OH + 500 cm^3 distilled water.

3.4 Bromothymol blue 0.1%: 1 g dissolved in 1 *l* 95% ethanol.

3.5 Nitric/Chlorate Mixture: Dissolve 50 g potassium chlorate in 1000 m*l* concentrated nitric acid. Store in a glass stoppered amber bottle.

3.6 Ascorbic acid.

4. APPARATUS

4.1 400 m*l* beakers.

4.2 Watch glasses.

4.3 Filter funnels for 12,5 cm papers.

4.4 Whatman 542 filter papers (12,5 cm diameter) or equivalent.

4.5 Hotplates.

4.6 Measuring cylinders.

4.7 Filter-funnel stands.

4.8 Porcelain crucibles (30 m*l*s).

4.9 Muffle-furnace.

4.10 Muffle trays (Salamander trays).

4.11 Lifter for muffle trays.

5. PROCEDURE

5.1 Weigh 2,0 g of the well mixed sample into a 250 m*l* beaker.

5.2 Add 100 m*l* hot distilled water, cover and boil for five minutes.

5.3 Filter through a MN, S & S 590 or Whatman 542 paper and wash twice with hot water. Wash the solids in the paper back into the original beaker.

5.4 Add 20 m*l* nitric/chlorate mixture and evaporate to dryness at a low temperature, being particularly careful to prevent loss by spraying. Preferably leave overnight to bake.

5.5 Cool slightly and add 5 m*l* HCl and carefully evaporate to dryness. Add a further 5 m*l* HCl and again take to dryness.

5.6 Bake for one hour at about 120°C to dehydrate the silica. Cool and add 5 m*l* HCl and 25 m*l* hot distilled water. Boil to dissolve all soluble salts.

5.7 Carefully add 10 m*l* 1:1 NH_4OH to the boiling solution and boil for one minute and filter on a 12,5 cm MN, S & S 590 or Whatman 542 filter paper. Wash the beaker, paper and precipitate six times with hot distilled water. Discard the precipitate.

5.8 Add 3 drops of bromothymol blue to the clear filtrate and neutralise with HCl, add 2 m*l* HCl in excess for every 100 m*l* of filtrate.

5.9 Bring solution to the boil, then cool to 80 °C and add ascorbic acid crystals until all iron has been reduced. Add 25 m*l* of barium chloride solution slowly to prevent co-precipitation of metal salts. Allow to stand overnight.

5.10 Filter through a MN, S & S 589/6 or Whatman 542 paper and wipe the inside of the precipitation beaker and stirring rod with a quarter of a filter paper and add this to the main filter paper. Wash the beaker, paper and precipitate six times with hot distilled water.

5.11 Transfer the filter paper to a tared porcelain crucible. Place the crucible into a cold muffle. Bring temperature up to 800°C and maintain for 20 minutes allowing a flow of air through the muffle.

5.12 Remove and cool in a desiccator and weigh.

6. CALCULATION

(Wt of precipitate x 0,1374 x 100)/2 = % Total sulphur (See note)

or (Wt of crucible and contents - Wt of crucible) x 6,87 = % Total sulphur

Note: Similar versions of this method have been widely employed in the S A gold mining industry for many years. Water-soluble sulphur species in residues are usually negligible. If it is suspected that water-soluble sulphur species are present in the residue then the filtrate from 5.3 must be treated as from 5.8 onwards and the mass of barium sulphate recorded. This must be converted to % S (see Calculation 6) and added to the original % S to give a true % TOTAL SULPHUR.

D SULPHIDE-SULPHUR

1. INTRODUCTION

This method is applicable to solid residues.

2. PRECISION

The lowest reported indication is <0,005% i.e. the detection limit is 0,01%.

3. REAGENTS

3.1 10% barium chloride solution.

3.2 Hydrochloric acid (CP).

3.3 Nitric acid/chlorate mixture: dissolve 10 g potassium chlorate in 200 m*l* concentrated nitric acid (CP).

3.4 Magnafloc filter aid.

3.5 Ascorbic acid.

4. APPARATUS

4.1 400 m*l* beakers.

4.2 Watchglass covers.

4.3 Filter funnels for 12,5 cm papers.

4.4 12,5 cm Whatman filter papers No 542 or equivalent (i.e. the finest/slowest filter papers).

4.5 Hotplates and laboratory muffle furnace.

4.6 25 m*l* measuring cylinder.

4.7 Filter funnel stands.

4.8 Porcelain crucibles.

4.9 Muffle trays (Salamander trays).

4.10 Lifter for muffle trays.

5. PROCEDURE

5.1 1 g of sample is boiled in 400 m*l* beaker with 100 m*l* of 10% Na_2CO_3 to remove sulphates soluble in Na_2CO_3 solution.

5.2 Filter through a Whatman 542 or equivalent fine/slow paper and wash five times with hot distilled water allowing the filter to drain completely between washings.

5.3 Transfer residue and filter paper to a 400 m*l* beaker.

5.4 Add 20 m*l* nitric acid/chlorate mixture and heat, taking to dryness.

5.5 Add 10 m*l* concentrated hydrochloric acid (A.R.) and heat to dryness. Do this three times.

5.6 Add 10 m*l* concentrated hydrochloric acid and 100 m*l* distilled water and boil.

5.7 Cool and add 1 - 2 m*l* Magnafloc. Filter and wash five times through a Whatman 542 (or the finest/slowest paper available) allowing the filter to drain completely between washings.

5.8 Add about 0,5 g ascorbic acid to the filtrate (to prevent co-precipitation of iron).

5.9 Bring to the boil and add 20 m*l* 10% barium chloride solution. Allow to return to the boil.

5.10 Cover with watchglass and stand at room temperature, preferably overnight.

5.11 Filter through a Whatman 542 or equivalent slow paper. (See Note at end of method).

5.12 Fold paper and precipitate into a weighed porcelain crucible. Place in muffle and allow temperature to rise to 800^{o}C. Maintain this temperature for 5 minutes. Allow a slight current of air through the muffle during ignition to enable the paper to burn away. Switch off muffle and remove crucibles to cool in a desiccator.

5.13 Re-weigh to get mass of the barium sulphate precipitate.

6. CALCULATION

Mass of $BaSO_4$ x 0,4116 x 100 = % Sulphide-sulphur

Note:

For biooxidation samples it may be necessary to filter through a weighed 0,45 micron millipore membrane filter. In this case the membrane filter is dried in an air oven at 110^{o}C before re-weighing.

E. SILICA

1. INTRODUCTION

This method is best suited to chromites and magnetites.

2. PRECISION

Values less than <0,01% SiO_2 are not reported.

3. REAGENTS

3.1 Hydrochloric acid.

3.2 Sulphuric acid, (1:1 sulphuric acid - 1:1 v/v distilled water to concentrated sulphuric acid).

3.3 Hydrofluoric acid.

3.4 Gelatine solution (1,5% solution).

3.5 Sodium peroxide.

4. APPARATUS

4.1 Platinum crucibles.

4.2 Hotplate and desiccator.

4.3 Whatman 541 filter papers (12,5 cm) or equivalent.

4.4 Filter funnels for 12,5 cm papers.

4.5 Filter stand.

4.6 Zirconium crucibles.

4.7 LP gas burners.

4.8 Appropriate glassware.

5. PROCEDURE

5.1 Weigh 0,3 g and 0,5 g of sample into a zirconium crucible for chromites and magnetites respectively.

5.2 Add 10 times the mass of sodium peroxide to that of sample, mix well.

5.3 Heat the crucible and sample matrix over a low Bunsen flame to char the matrix (this prevents loss of sample by spitting). Gradually increase the temperature till the mass has melted and fuse at a dull red heat for about 2 minutes swirling the mixture to allow complete fusion. Finally increase the temperature to a cherry red colour and swirl for 1 minute (NOTE 1).

5.4 Cool and lixiviate in about 100 m*l* distilled water in a 400 m*l* squat beaker washing all adhering sample from crucible with distilled water.

5.5 Add 50 m*l* concentrated HCl. Rinse and remove crucible.

5.6 Evaporate to deliquescence.

5.7 Cool. Carefully add 50 m*l* concentrated H_2SO_4.

5.8 Heat till SO_3 fumes are evolved, fume strongly for a further 10 min.

5.9 Cool and add (with caution NOTE 2) 100 m*l* distilled water and 15 m*l* concentrated HCl. Bring to the boil (± 2 minutes).

5.10 Cool slightly and whilst still warm add 20 m*l* of 1,5% gelatine solution. Stir well and allow to stand for 15 minutes.

5.11 Filter through Whatman 541 paper and wash twice with hot 10% HCl.

5.12 Wash a further five times with hot water.

5.13 Transfer drained filter paper to a tared platinum crucible. Ignite at $800^{o}C$ for 1 hour. Remove and cool in a desiccator.

5.14 Weigh the platinum crucible and residue.

5.15 Add 1 m*l* distilled water, two drops of 1:1 sulphuric acid and about 5 m*l* hydrofluoric acid and carefully take to dryness on a hot plate. Heat over an open flame to drive off any residual sulphuric acid and to convert any residues to their oxides.

5.16 Cool and weigh. Weight loss (from 5.14) may be expressed as percentage silica (NOTE 3).

6. CALCULATION

(Loss in Mass)/(Sample Mass) x 100 = % Silica

Note 1:

At this stage no solid particles should be visible in melt. If present persist for a longer period.

Note 2:

Add the distilled water by running it slowly down the side of the beaker swirling at all times to prevent the mixture from being concentrated in one area. Once the reaction has ceased (after addition of 20 - 30 m*l* water) the remaining water and acid may be added normally.

Note 3:

If the difference in wt between the tared crucible and that of the final wt after HF treatment is greater than 0,02 g, the analysis should be repeated as the residue will be a mixture of SO_4 oxides giving erroneous results.

F. GOLD: FIRE ASSAY

1. INTRODUCTION

The fire assay involves converting the gangue of the ore by means of a flux and heat to a slag which can be separated from the precious metals. The latter are collected in metallic lead formed during fusion. The reduced lead falls as a lead rain to the bottom of the mass forming a lead button. The resulting lead button in cupelled in an oxidising furnace leaving the precious metals in the cupel. The bead is then parted in nitric acid. The resulting bead is weighed on a micro balance and the value calculated and reported in grams per ton.

2. PRECISION

The assay balance is capable of weighing to 1 microgram plus or minus 1 throughout the range. The balance is calibrated with certified weights. Samples are done in triplicate. A 10% coefficient of variation is allowed at value of 0,5 g/t or less.

3. MATERIALS

3.1 Sodium Carbonate Anhydrous Na2CO3 (Soda): Forms sodium meta-silicate with quartz in the ore

$Na_2CO_3 + SiO_2 = Na_2SiO_3 + CO_2$ (Na_2SiO_3 = Slag)

3.2 Borax (Sodium Tetraborate) $Na_2B_4O_7$: Borates are more fluid than silicates at the same temperature, and are added to thin the slag allowing the lead globules and particles of precious metals to settle, and act as an acid flux dissolving basic metal oxides.

3.3 Litharge PbO: Readily fuses with silicates both basic and double basic. Dissolves most metallic oxides. Provides the lead rain collecting the gold and silver in the sample.

3.4 Carbon (in the form of cake flour): This is added to reduce the litharge to lead. $2\,PbO + C = 2\,Pb$.

3.5 The above reagents are blended in the following proportion forming the residue flux.

Sodium carbonate	43,0 kg
Borax	17,3 kg

Litharge	25,0 kg
Cake flour	2,4 kg
Paraffin	500 m*l* added to reduce dust

This is mixed in a rotating blender for 20 minutes. A blank fusion using 120 g pure silica instead of sample is done as in procedure 6 to check lead button weight, which should be 80 grams, and possible precious metals contamination.

3.6 Silver Nitrate Solution: Dissolve 3,24 g silver in a minimum amount of nitric acid, make up to 1*l*

3.7 Diluted Nitric Acid, SG 1,13

3.8 Concentrated Nitric Acid 55%: Using distilled water dilute the acid to a SG of 1,13 using a hydrometer.

Note: Diluted and concentrated nitric must be tested for chlorides using silver nitrate. Any indication of chlorides (cloudiness) is detrimental to the parting process.

4. EQUIPMENT

No 5 furnace crucibles (economic fireclay) - 860 m*l* total volume.
No 10 cupels (2 Gonard light industries) - 160 g magnesite
20 m*l* porcelain cups (parting cups).
Flux mixing bottles- eg. hospital male urine bottle.
Fusion furnace 50 KPa - 675mm x 1190 mm.
Cupellation furnace 3 KVA - 570 mm x 880 mm.

5. SAMPLE PREPARATION

5.1 The sample is checked and dried if moist.
5.2* Screened through a 160 micron screen.
5.3 Well matted (blended).

* The plus fraction produced by screening is ground in a pestle and mortar to pass through the screen and mixed back into the sample.

6. PROCEDURE

6.1 Fluxing

The sample is spread out on a piece of manilla paper and matted for an additional minute. Using a 250mm stainless steel spatula, small dips are taken over the whole area in order to obtain a representative portion of the sample. 150g of the sample is mixed with 400g residue flux. 3 drops of silver solution are added. This has a dual function, it will act as a collector for the gold and it will aid in removing the silver normally found associated with the gold during the nitric acid parting process.

6.2 Fusion

The sample is fused in a fusion furnace at a temperature of 1150 ^{o}C for 50 minutes. The fusion is complete when tranquil. The fusion is poured into conical cast iron moulds. When cool, the mould is inverted to remove the solidified pour. The slag phase is separated from the lead button which is hammered free of any slag.

6.3 Cupellation

Is the process whereby the lead is removed from the precious metal. The cleaned lead button is placed in a preheated No 10 cupel and loaded into a muffle furnace at 980 ^{o}C. The lead is oxidised into litharge and absorbed by the cupel leaving a gold and silver alloy prill. This process normally takes approximately one hour. NB!! any adhering slag will react with the cupel surface and cause losses of precious metals through absorption.

$$2\,Pb + O_2 = 2\,PbO$$

6.4 Parting

The prill is removed from the cupel and flattened to provide a larger surface area for acid attack to remove cupel dross. The prills are placed in porcelain cups and 10 m*l* preheated nitric acid (SG 1,13) is added. These are then heated on a hot plate and kept at a temperature of 160 ^{o}C for 5 minutes. 0,5 m*l* concentrated nitric acid is then added and left for a further 5 minutes. The resultant gold prill is washed three times with distilled water to remove any traces of silver nitrate, then dried on the hot plate and annealed for three minutes in a temperature controlled annealing muffle at 900 ^{o}C.

6.5 Weighing

The gold prills are weighed on a micro balance and the gold content of the sample calculated in g/t

6.6 Reporting

Values are reported to three significant figures in g/t.

SECTION II. ANALYTICAL PROCEDURES FOR LIQUOR SAMPLES.

A. TOTAL IRON IN SOLUTION

1. INTRODUCTION

The amount of iron in solution can be judged by the intensity of the yellow-amber colour of the solution. If the intensity of the colour is high a low aliquot is taken for titration eg 20 m*l*. Otherwise use 50 or 100 m*l*.

2. PRECISION:

1 m*l* of standard dichromate is equivalent to 0,005585 g Fe. The endpoint is a very sharp transition from green to purple. In the hands of an experienced analyst great precision is possible, and duplicates differing by no more than 0,05 g/*l* can easily be achieved. Arsenic interferes, as do coloured impurities on suspensions which mask the colour - transition at the endpoint.

3. REAGENTS

3.1 0,1 N Potassium Dichromate: Dissolve 4,9032 g potassium dichromate in distilled water and make up to one litre. The dichromate should be oven-dried i.e. 2 hours at $110^{o}C$.

3.2 Acid Mixture: Add 320 m*l* 1:1 sulphuric acid to 600 m*l* distilled water and then add 80 m*l* phosphoric acid, (1:1 sulphuric acid - 1:1 v/v distilled water to concentrated sulphuric acid).

3.3 Concentrated hydrochloric acid.

3.4 Stannous Chloride: Dissolve 100 g stannous chloride (H_2O) in 100 m*l* concentrated HCl by warming on a hotplate. Cool and make up to 1 litre with distilled water.

3.5 Mercuric Chloride (Saturated): Boil 120 g mercuric chloride in 1 litre of distilled water. Cool and make up to 2 litres with distilled water.

3.6 Indicator Solution: Dissolve 1 g Barium diphenylamine sulphonate in 100 m*l* concentrated sulphuric acid. Sodium diphenylamine sulphonate may also be used.

3.7 24 - 28% NU_4OH.

3.8 NH_4Cl.

4. APPARATUS

4.1 Aspirator for stock $K_2Cr_2O_7$ solution connected to an A-grade self-filling 50 m*l* burette.

4.2 Assorted pipettes and a glass stirring rod.

4.3 Hotplate.

5. PROCEDURE

5.1 Pipette 20 or 50 m*l* aliquot of solution into a 250 m*l* beaker. Add about 10 m*l* concentrated HCl (NOTE 1).

5.2 Boil for 5 minutes and add stannous chloride solution dropwise until the iron colour is completely discharged. Add one extra drop.

5.3 Cool solution to room temperature and add about 10 m*l* mercuric chloride solution and about 10 m*l* acid mixture (3.2).

5.4 Add 3 - 4 drops of indicator solution (3.6) and titrate with standard potassium dichromate. Add the dichromate dropwise towards the endpoint with stirring rod until one drop produces an intense purple-violet coloration which is permanent.

6. CALCULATION

Titre x 0,005585 x 1000/(m*l*s aliquot) = g/*l* Fe(T)

Footnote: For total iron on a solid: Fuse 0,3 g solid with 6 g sodium peroxide in a zirconium crucible. Leach with about 100 m*l* 15% HCl. Boil. Then proceed as from 5.2.

Note 1: If arsenic, and/or interfering impurities are present, these may be removed by bringing the aliquot to the boil, adding ± 2 g ammonium chloride and precipitating the group 3 ion out with ammonium hydroxide. Separate by filtration through a Whatman 540 paper, washing with hot distilled water. Wash the precipitate into the original beaker, reassemble the paper and dissolve traces of Group 3 from the paper with 50 m*l* of 20% hot HCl solution giving the paper two final washes with hot distilled water. If a high concentration of interferants are present it would be advisable to continue finally as from 5.2.

B. TOTAL SULPHUR IN SOLUTION.

1. INTRODUCTION

This method is suitable for both conventional and biooxidation solutions.

2. PRECISION

The lowest reported indication is < 0,005% i.e. the detection limit is 0,01%.

3. REAGENTS

3.1 Barium chloride (10% solution).
3.2 Hydrochloric acid C.P.
3.3 Ascorbic acid.
3.4 Bromine.

4. APPARATUS

4.1 400 m*l* beakers with watch glasses to match.
4.2 Filter funnels for 12,5 cm papers.
4.3 650 ml Phillips beakers.
4.4 Whatman 542 or MN, S & S 589/5 filter papers (12,5 cm diameter).
4.5 Hotplate/s.
4.6 Measuring cylinder (25 m*l*).
4.7 Porcelain crucibles (30 m*l* capacity).
4.8 Muffle furnace.
4.9 Muffle trays (Salamander trays).
4.10 Fork to lift muffle trays.
4.11 Filter funnel stand.
4.12 5 m*l* pipette.

5. PROCEDURE

5.1 Pipette 5 m*l* sample into a 400 m*l* beaker.
5.2 Add 3 drops of liquid bromine and stand for 15 minutes at room temperature.
5.3 Add 100 m*l* distilled water, 15 m*l* of HCl and boil.
5.4 Cool to approximately 80^{o}C and add a spatula-tip (about 0,25 g) ascorbic acid if the resulting solution shows iron colour.
5.5 Bring to the boil again and add about 25 m*l* $BaCl_2$ solution slowly to prevent co-precipitation of other metals and boil for 1 minute.

5.6 Remove from hotplate and allow to stand at least four hours - preferably overnight.

5.7 Filter through an MN, S & S 589/6 or a Whatman 542 paper collecting filtrated in a 650 m*l* Phillips beaker. Remove adhering $BaSO_4$ by wiping the beaker with 2 x a quarter circle of filter paper (moistened with distilled water). Wash precipitate well with 6 to 8 washes of hot distilled water, discarding the filtrate.

5.8 Transfer residue and filter paper to a dry clean tared 30 m*l* porcelain crucible and place in a cold muffle (use salamander tray for convenience).

5.9 Dry contents in the muffle at $100^{o}C$, ignite for 20 minutes at $800^{o}C$.

5.10 Cool the porcelain crucible and contents in a desiccator and weigh.

5.11 Evaluate sulphur by weighing.

S(T) g/*l* = (A - B) x 0,13735 x 1000/5 = (A-B) x 27,47

A = Difference in mass between crucible plus sample and the tared dry crucible.

B = Difference in mass between crucible plus reagent blank and the tared dry crucible.

C. ARSENIC IN SOLUTION.

See footnote of Section I B, Arsenic on solid residue.

APPENDIX 2

ANALYSIS OF PLANT LIME

COMPONENT	MASS %
Al	0,12
As_2O_3	0,01
Ca	50,74
Co	0,002
Cr	0,0005
Cu	0,002
Fe	0,12
K	0,013
Mg	0,65
Mn	0,52
Na	0,004
Ni	0,0006
PO_4^{2-}	0,0
Total-Sulphur	0,0
SiO_2	1,35
Ti	0,004

APPENDIX 3

ANALYSES OF BIOOXIDATION AND HCL-WASH LIQUORS

TABLE A3.1 Chemical analysis of biooxidation and acid-wash liquors for the bulk sample

TIME	ANALYSIS OF LIQUORS BULK SAMPLE							
	BIOOXIDATION LIQUORS				HCL-WASH LIQUORS			
Days	Volume ml^{-1}	Iron g/l	Total Sulphur g/l	Arsenic g/l	Volume ml^{-1}	Iron g/l	Total Sulphur g/l	Arsenic g/l
feed					208	10,2	0,8	1,9
0,0	968	2,2	4,0	0,4	213	5,9	0,4	3,2
1,0	973	2,9	5,3	0,5	210	9,4	0,5	3,2
3,0	965	3,6	5,9	0,9	203	9,5	1,3	4,7
4,0	975	4,0	6,6	1,7	220	10,9	0,8	5,8
5,0	978	5,6	7,9	2,8	198	11,5	0,8	6,6
6,0	965	6,8	8,4	3,0	215	15,4	4,0	30,0
7,0	988	10,3	11,1	3,7	193	15,9	4,3	12,3
8,0	971	13,6	11,9	4,9	179	12,6	4,1	7,5
11,0	984	25,4	19,3	8,1	177	3,4	3,1	0,4
12,0	977	27,6	20,9	8,3	176	4,3	3,8	0,6
13,0	985	29,8	22,4	8,4	179	5,8	4,3	0,5
14,0	988	29,4	23,0	8,2	173	10,0	5,2	1,1

TABLE A3.2 Chemical analysis of biooxidation and acid-wash liquors for the +75 micron sample

TIME	ANALYSIS OF LIQUORS +75 MICRON SAMPLE							
	BIOOXIDATION LIQUORS				HCL-WASH LIQUORS			
Days	Volume ml^{-1}	Iron g/l	Total Sulphur g/l	Arsenic g/l	Volume ml^{-1}	Iron g/l	Total Sulphur g/l	Arsenic g/l
feed					239	1,3	0,1	0,2
0,0	965	4,1	2,8	1,0	241	1,7	0,2	1,0
1,0	969	4,0	5,7	0,9	243	1,7	1,1	1,0
4,0	985	4,7	5,8	1,9	249	11,3	3,6	3,1
6,0	964	8,8	8,6	2,3	235	9,0	2,4	3,4
7,0	966	11,4	11,2	2,2	207	9,1	3,1	1,5
8,0	976	15,7	14,3	3,2	205	10,9	3,9	1,5
10,0	955	21,0	19,3	4,0	187	8,9	4,5	0,9
11,0	965	23,6	20,9	3,7	194	9,9	6,6	0,8
12,0	963	25,5	21,3	4,0	228	9,0	6,2	0,5
13,0	961	25,0	22,9	3,9	207	9,1	6,4	0,6
15,0	949	28,5	22,1	3,9	212	7,0	6,1	0,4
18,0	961	28,7	23,6	3,8	213	9,0	6,4	0,5
22,0	966	28,1	20,9	3,9	246	16,5	8,5	0,5

TABLE A3.3 Chemical analysis of biooxidation and acid-wash liquors for the -75 +53 micron sample

TIME	ANALYSIS OF LIQUORS -75 +53 MICRON SAMPLE							
	BIOOXIDATION LIQUORS				HCL-WASH LIQUORS			
Days	Volume ml^{-1}	Iron g/l	Total Sulphur g/l	Arsenic g/l	Volume ml^{-1}	Iron g/l	Total Sulphur g/l	Arsenic g/l
feed					244	1,5	0,3	0,6
0,0	961	4,0	3,7	0,1	238	1,7	0,1	0,8
3,0	968	1,9	3,3	0,2	234	2,7	0,4	2,1
6,0	990	2,8	4,3	0,5	231	2,2	0,2	1,7
10,0	968	3,9	5,7	1,3	235	1,7	0,2	1,3
13,0	973	4,5	6,0	1,6	221	2,4	0,3	2,0
17,0	974	5,1	6,1	2,1	236	3,4	0,5	3,0
21,0	996	5,7	7,0	2,6	230	3,6	0,3	3,3
26,0	973	6,7	8,0	3,2	220	5,6	0,6	5,5
33,0	965	12,4	11,9	6,7	202	1,0	0,2	0,6
34,0	969	13,7	15,2	6,9	181	1,0	0,2	0,6
38,0	969	20,3	20,0	7,8	197	1,9	4,8	0,7
39,0	966	26,9	20,8	7,8	225	1,4	4,7	0,6
40,0	957	28,5	21,9	7,5	228	2,1	5,0	0,7
43,0	961	29,6	24,9	7,3	207	2,6	5,2	0,8
46,0	955	30,9	25,8	7,4	208	2,5	5,1	0,7
51,0	956	33,0	27,4	7,5	212	3,5	5,35	0,7

TABLE A3.4 Chemical analysis of biooxidation and acid-wash liquors for the -53 +38 micron sample

TIME	ANALYSIS OF LIQUORS -53 +38 MICRON SAMPLE							
	BIOOXIDATION LIQUORS				HCL-WASH LIQUORS			
Days	Volume ml^{-1}	Iron g/l	Total Sulphur g/l	Arsenic g/l	Volume ml^{-1}	Iron g/l	Total Sulphur g/l	Arsenic g/l
feed					222	1,7	0,5	0,2
0,0	974	3,4	3,5	0,6	200	3,2	0,6	1,0
1,0	968	2,1	3,9	0,4	203	13,3	0,8	3,0
4,0	973	3,2	4,1	1,3	210	14,0	1,0	3,9
5,0	973	5,9	4,3	2,0	210	6,8	1,1	4,4
6,0	976	5,0	5,1	2,8	217	17,8	2,8	7,3
7,0	973	6,1	6,4	2,9	206	13,5	2,9	9,2
8,0	976	8,2	10,3	3,5	208	14,4	5,9	7,2
11,0	975	16,5	14,1	6,4	187	5,1	2,4	1,5
12,0	970	19,0	10,3	7,4	181	5,0	6,2	1,0
13,0	983	23,0	16,6	8,0	178	7,9	6,2	1,4
14,0	968	23,9	16,6	7,8	197	10,3	6,3	2,3
15,0	964	24,5	18,3	8,4	200	11,8	6,9	1,3
18,0	960	27,8	20,0	8,7	192	9,9	8,0	1,0
20,0	953	27,9	18,9	8,4	208	9,8	7,6	0,9
22,0	961	31,0	19,0	9,1	181	9,9	6,8	0,8

TABLE A3.5 Chemical analysis of biooxidation and acid-wash liquors for the -38 +25 micron sample

TIME	ANALYSIS OF LIQUORS -38 +25 MICRON SAMPLE							
	BIOOXIDATION LIQUORS				HCL-WASH LIQUORS			
Days	Volume ml^{-1}	Iron g/l	Total Sulphur g/l	Arsenic g/l	Volume ml^{-1}	Iron g/l	Total Sulphur g/l	Arsenic g/l
feed					225	1,44	0,4	0,3
0,0	978	3,0	6,2	1,5	223	0,77	0,2	0,2
1,0	991	3,7	6,1	1,5	222	1,19	0,2	0,7
2,0	986	3,7	6,0	1,4	209	1,34	0,3	1,0
4,0	965	4,7	6,6	1,6	206	2,58	0,6	1,8
6,0	957	4,7	6,6	1,7	215	3,66	1,0	2,6
7,0	958	5,2	6,9	2,2	223	4,38	0,5	3,1
10,0	970	8,5	8,6	5,1	196	4,33	0,4	2,6
11,0	971	9,8	9,9	5,4	205	5,82	0,6	4,9
12,0	974	12,4	12,0	7,3	189	2,83	0,3	1,8
13,0	961	11,9	11,1	5,4	224	16,12	5,4	12,0
14,0	968	16,6	13,5	8,0	190	7,06	4,7	6,6
17,0	956	16,5	12,7	5,4	240	22,75	6,5	18,0
18,0	965	27,0	19,6	1,1	163	6,91	5,6	5,2
19,0	975	29,6	24,0	1,2	146	1,81	5,0	0,4
20,0	961	32,7	23,2	1,2	188	2,31	5,5	0,5
21,0	964	33,5	24,6	1,1	175	2,06	5,2	0,4
24,0	958	32,0	23,9	1,1	189	6,80	5,9	1,0
27,0	958	31,3	23,9	1,1	174	3,50	4,6	0,4

TABLE A3.6 Chemical analysis of biooxidation and acid-wash liquors for the -25 micron sample

TIME	ANALYSIS OF LIQUORS -25 MICRON SAMPLE							
	BIOOXIDATION LIQUORS				HCL-WASH LIQUORS			
Days	Volume ml^{-1}	Iron g/l	Total Sulphur g/l	Arsenic g/l	Volume ml^{-1}	Iron g/l	Total Sulphur g/l	Arsenic g/l
feed					199	8,0	1,3	2,9
0,0	967	4,8	4,1	1,7	186	4,6	0,8	1,6
1,0	970	5,2	4,2	1,2	186	6,2	0,9	3,1
4,0	968	9,6	5,5	4,8	154	8,1	1,1	5,7
5,0	969	12,0	6,6	6,0	141	7,1	1,0	4,4
6,0	972	15,2	8,0	6,9	131	4,7	0,6	1,6
7,0	973	19,2	9,8	7,4	165	2,4	0,4	0,8
8,0	960	22,4	9,9	7,6	141	3,5	5,0	1,1
9,0	967	25,0	10,7	8,0	138	3,6	5,0	1,0
10,0	968	27,0	11,2	7,9	143	3,1	5,0	1,0
11,0	966	27,6	11,5	7,6	137	3,1	4,8	1,0
12,0	964	27,7	11,0	7,4	151	3,6	5,0	1,0

APPENDIX 4

BASIC LISTING OF THE NELDER-MEAD OPTIMISATION ROUTINE

```
1000 REM ************************************************
1010 REM *                                              *
1020 REM *          NONLINEAR OPTIMIZATION              *
1030 REM *  using the Sequential Search Method of        *
1040 REM *  Spendley W., Hext G.R. and Himsworth F.R.    *
1050 REM *  Technometrics 4,1962 and extended by         *
1060 REM *  Nelder J.A. and Mead R.,Comp.J.,7,308,1965   *
1070 REM *                                              *
1080 REM ************************************************
1090 CLEAR
1100 CLS
1105 DEFDBL S
1106 DEFDBL A-F
1107 DEFDBL X
1108 DEFDBL G
1109 DEFDBL S
1110 DEFINT I-N
1120 KEY OFF
1121 DIM Y1(20),Y2(20),Y3(20),Y4(20), FV(20)
1122 DIM SIMPLEX(6,6),X(6),FVAL(6),TEMP(3,2)
1130 FM$ = "##.######^^^^"
1140 GOSUB 2890
1150 ALPHA = .995:BETA=.495:GAMMA=1.995
1160 ITERATION = 0:NFUNC=0!:INDEX=1!
1170 LENG=LEN(TITLE$):LP=40-LENG/2
1180 LOCATE 3,LP:PRINT TITLE$
1190 LOCATE 4,LP:PRINT STRING$(LENG,"=")
1200 LOCATE 6,27:PRINT "Iteration # : "
1210 LOCATE 8,24:PRINT "Function Value : "
1220 FOR I=1 TO NVAR
1230 LOCATE 9+I,32:PRINT "X("; I; ") :"
1240 NEXT I
1250 LOCATE 11+NVAR,29:PRINT "Step Size :"
1260 LOCATE 13+NVAR,12:PRINT "No of Function Evaluations : "
1270 LOCATE 16,16:PRINT "Current Function Value : "
1280 NVP1 = NVAR+1
1290 NVP2 = NVAR+2
1300 NVP3 = NVAR+3
1310 REM Sets up Initial values of simplex
1320 S1 = SIZE/(NVAR*SQR(2))*(SQR(NVAR+1!)+NVAR-1!)
1330 S2 = SIZE/(NVAR*SQR(2))*(SQR(NVAR+1!)-1!)
1340 FOR J = 1 TO NVAR
1350   TEMP(1,J) = 0!
1360 NEXT J
1370 FOR I = 2 TO NVP1
1380   FOR J = 1 TO NVAR
1390     TEMP(I,J) = S2
1400     L = I-1
1410     TEMP(I,L) = S1
1420   NEXT J
1430 NEXT I
1440 FOR I = 1 TO NVP1
1450   FOR J = 1 TO NVAR
1460   SIMPLEX(I,J) = X(J)+TEMP(I,J)
1470   NEXT J
1480 NEXT I
```

```
1490 FOR INDEX = 1 TO NVP1
1500   GOSUB 2680: REM FUNCTION EVALUATION
1510 NEXT INDEX
1520 FMIN = FVAL(1)
1530 KMIN = 1
1540 GOSUB 2420
1550 ITERATION = ITERATION+1
1560 FMAX = FVAL(1)
1570 KMAX = 1
1580 FMIN = FVAL(1)
1590 KMIN = 1
1600 REM Searches for largest amd smallest function values
1610 FOR I = 2 TO NVP1
1620   IF FVAL(I) > FMAX THEN FMAX = FVAL(I): KMAX = I
1630   IF FVAL(I) < FMIN THEN FMIN = FVAL(I): KMIN = I
1640 NEXT I
1650 :
1660 REM Program reflects around smallest function values
1670 FOR J = 1 TO NVAR
1680   S2 = 0!
1690   FOR I = 1 TO NVP1
1700     S2 = S2+SIMPLEX(I,J)
1710   NEXT I
1720   SIMPLEX(NVP2,J) = 1!/NVAR*(S2-SIMPLEX(KMAX,J))
1730   SIMPLEX(NVP3,J) = (1!+ALPHA)*SIMPLEX(NVP2,J)-ALPHA*SIMPLEX(KMAX,J)
1740 NEXT J
1750 INDEX = NVP3
1760 GOSUB 2680
1770 IF FVAL(NVP3) > FMIN THEN GOTO 1880
1780 :
1790 REM Program assumes unsuccessful reflection so contracts
1800   FOR J = 1 TO NVAR
1810     SIMPLEX(NVP4,J) = (1-GAMMA)*SIMPLEX(NVP2,J)+GAMMA*SIMPLEX(NVP3,J)
1820   NEXT J
1830   INDEX = NVP4
1840   GOSUB 2680
1850   IF FVAL(NVP4) < FMIN THEN IACCEPT = NVP4 ELSE IACCEPT = NVP3
1860   GOSUB 2560: REM ACCEPT NEW POINT
1870   GOTO 2170
1880 IF KMAX <> 1 THEN FSECOND = FVAL(1) ELSE FSECOND = FVAL(2)
1890 FOR I = 1 TO NVP1
1900   IF ((KMAX <> I) AND (FVAL(I) > FSECOND)) THEN FSECOND = FVAL(I)
1910 NEXT I
1920 IF FVAL(NVP3) > FSECOND THEN GOTO 1960
1930   IACCEPT = NVP3
1940   GOSUB 2560
1950   GOTO 2170
1960 IF FVAL(NVP3) < FMAX THEN IACCEPT = NVP3: GOSUB 2560
1970 :
1980 REM Programs finds successful reflection so expands
1990 FOR J = 1 TO NVAR
2000   SIMPLEX(NVP4,J) = BETA*SIMPLEX(KMAX,J)+(1!-BETA)*SIMPLEX(NVP2,J)
2010 NEXT J
2020 INDEX = NVP4
2030 GOSUB 2680
2040 IF FVAL(NVP4) >= FMAX THEN GOTO 2080
```

```
2040 IF FVAL(NVP4) >= FMAX THEN GOTO 2080
2050   IACCEPT = NVP4
2060   GOSUB 2560
2070   GOTO 2170
2080 FOR J = 1 TO NVAR
2090   FOR I=1 TO NVP1
2100     IF I=KMIN THEN 2120
2110     SIMPLEX(I,J) = .5*(SIMPLEX(I,J)+SIMPLEX(KMIN,J))
2120   NEXT I
2130 NEXT J
2140 FOR INDEX = 1 TO NVP1
2150   GOSUB 2680
2160 NEXT INDEX
2170 INDEX = NVP2
2180 GOSUB 2680
2190 DELTAF=0!
2200 FOR I = 1 TO NVP1
2210   DELTAF = DELTAF+(FVAL(I)-FVAL(NVP2))*(FVAL(I)-FVAL(NVP2))
2220 NEXT I
2230 DELTAF = (1!/NVAR)*SQR(DELTAF)
2240 IF DELTAF > STOPCRITER THEN ICONVERGE = 0 ELSE ICONVERGE = 1
2250 IF (ITERATION MOD ITERPRINT = 0) THEN GOSUB 2420: REM PRINT
2260 IF NOT ((ICONVERGE = 1) OR (ITERATION > MAXITER)) THEN GOTO 1550
2270 LOCATE 16,1:PRINT STRING$(80," ")
2280 IF ICONVERGE <> 1 THEN 2300
2290 LOCATE 16,17: PRINT "***** CONVERGENCE ACHIEVED! *****"
2291 REM GOSUB 3270
2300 IF ITERATION < MAXITER THEN 2320
2310 LOCATE 16,15: PRINT "***** MAXIMUM NUMBER OF ITERATIONS EXCEEDED! *****"
2320 GOSUB 2420: REM PRINT
2325 GOSUB 3270
2330 LOCATE 25,1:PRINT "End of Program":BEEP
2340 END
2350 REM ------------------------------------------------------------------
2360 REM ** SUBROUTINE TO PRINT OUT ITERATIONS **
2370 REM ** INPUT VARIABLES: DELTAF, FM$, FMIN, ITERATION
2380 REM ** INPUT VARIABLES: KMIN, NFUNC, NVAR, SIMPLEX()
2390 REM ** INPUT/OUTPUT VARIABLES: **
2400 REM ** OUTPUT VARIABLES: **
2410 REM ** SUBROUTINES: **
2420 LOCATE 6,41: PRINT ITERATION
2430 LOCATE 8,41: PRINT USING FM$; FMIN
2440 FOR I = 1 TO NVAR
2450   LOCATE 9+I,41: PRINT USING FM$; SIMPLEX(KMIN,I)
2460 NEXT I
2470 LOCATE 11+NVAR,41: PRINT USING FM$; DELTAF
2480 LOCATE 13+NVAR,41: PRINT NFUNC
2490 RETURN
2500 REM ------------------------------------------------------------------
2510 REM ** SUBROUTINE TO ACCEPT NEW POINT **
2520 REM ** INPUT VARIABLES: IACCEPT, KMAX, NVAR **
2530 REM ** INPUT/OUTPUT VARIABLES: SIMPLEX() **
2540 REM ** OUTPUT VARIABLES: INDEX **
2550 REM ** SUBROUTINES: EVALUATE FUNCTION **
2560 FOR J = 1 TO NVAR
2570   SIMPLEX(KMAX,J) = SIMPLEX(IACCEPT,J)
2580 NEXT J
```

```
2590 INDEX = KMAX
2600 GOSUB 2680
2610 RETURN
2620 REM ------------------------------------------------------------------
2630 REM ** SUBROUTINE TO ESTABLISH FUNCTION EVALUATION **
2640 REM ** INPUT VARIABLES: INDEX, NVAR, SIMPLEX() **
2650 REM ** INPUT/OUTPUT VARIABLES: FVAL(), NFUNC **
2660 REM ** OUTPUT VARIABLES: **
2670 REM ** SUBROUTINES: USER FUNCTION **
2680 NFUNC = NFUNC+1
2690 FOR I = 1 TO NVAR
2700   X(I) = SIMPLEX(INDEX,I)
2710 NEXT I
2720 GOSUB 2750: REM USER FUNCTION
2730 FVAL(INDEX) = FVALUE
2740 RETURN
2750 REM ------------------------------------------------------------------
2760 REM ** SUBROUTINE FOR USER TO INSERT FUNCTION **
2770 REM ** INPUT VARIABLES: X() **
2780 REM ** INPUT/OUTPUT VARIABLES: **
2790 REM ** OUTPUT VARIABLES: FVALUE **
2800 REM ** SUBROUTINES: **
2810 LOCATE 16,40:PRINT STRING$(40," ")
2815  REM INPUT " NUMBER OF DATA POINTS " , NDAT
2820 FVALUE = 0
2830 FOR I = 1 TO NDAT
2840 FV(I)=Y2(I)-(SQR((X(1)/(2*X(2)*Y1(I))-X(1)/2)^2+Y3(I)*X(1)/X(2)/Y1(I))-X
/2/X(2)/Y1(I)+X(1)/2)
2850 REM FV(I)=Y2(I)-(X(1)*(1-1/(X(2)*Y1(I))))
2859 REM F1=.96746*(1-.4933/Y1(5))
2860 FVALUE = FVALUE + (FV(I)/Y2(I))^2
2870 NEXT I
2880 LOCATE 16,41:PRINT FVALUE:RETURN
2890 REM ------------------------------------------------------------------
2900 REM                      ** DATA ENTRY **
2910 REM    1)Enter rate concentration data
2920 REM    2)Enter Title of Search
2930 REM    3)Enter # of X Variables, Iteration interval, Max Iterations
2940 REM    4)Enter Initial Step Size, Stopping Criterion
2950 REM ------------------------------------------------------------------
2960 :
2970 DATA 5, 15
3000 REM DATA 1.610, .515, 2.415, .599, 3.221, .659, 4.026, .702, 4.831, .762
3010 REM DATA .805, .649, .4751, 1.208, .76, .6101, 1.61,  .858, .6776, 2.013
884, .718, 2.415, .905, .7451              :REM TANK 2
3020 REM DATA .805, .8071, .6465, 1.208, .896, .7892, 1.61, .95, .851, 2.013,
63, .8844, 2.415, .973, .9048             :REM TANK 3
3090 DATA .805, .815, .803, 1.208, .927, .908, 1.61, .967, .944, 2.013, .974,
61, 2.415, .9797, .970                 :REM TANK 4
3100 READ NDAT, NVAR
3120 FOR I = 1 TO NDAT
3130 READ Y1(I), Y2(I), Y3(I)
3140 NEXT I
3150 :
3160 DATA "TANK 4 : LOGISTIC MODEL"
3170 DATA 2, 10, 500
3180 DATA 1, 1.E-15, 0, .01
```

```
3190 READ TITLE$
3200 READ NVAR, ITERPRINT, MAXITER
3210 READ SIZE, STOPCRITER, CARB, SCALE1
3230 DATA 1.2, 0.85
3240 FOR I = 1 TO NVAR
3250   READ X(I)
3260 NEXT I
3265 RETURN
3270 REM This section calculates the predicted values of Fn from the
3280 REM      constants optimised for
3290 REM ..........................................................
3300 :
3310 DIM YY2(20)
3320 FOR I=1 TO NDAT
3330 REM YY2(I)=((X(1)/(2*X(2)*Y1(I))-X(1)/2)^2+Y3(I)*X(1)/X(2)/Y1(I))-X(1)/2
2)/Y1(I)+X(1)/2
3331 YY2(I)=SQR((X(1)/(2*X(2)*Y1(I))-X(1)/2)^2+Y3(I)*X(1)/X(2)/Y1(I))-X(1)/2/
)/Y1(I)+X(1)/2
3332 REM YY2(I)=(X(1)*(1-1/(X(2)*Y1(I))))
3340 NEXT I
3350 LOCATE 18,10 :PRINT "TIME (DAYS)": LOCATE 18,25 :PRINT "F(n-1)" : LOCATE
,40 :PRINT "F(n)" : LOCATE 18,55 :PRINT "PREDICTED F(n)"
3660 FOR J=1 TO NDAT
3670 LOCATE 18+J,10:PRINT Y1(J)
3680 LOCATE 18+J,25:PRINT Y3(J)
3690 LOCATE 18+J,40:PRINT Y2(J)
3700 LOCATE 18+J,55:PRINT YY2(J)
3710 NEXT J
3720 RETURN
```